Optimal Placement of Dispersed Generators for Practical Distribution Network

A Thesis submitted in fulfillment of the requirements for the award of the degree of

Doctor of Philosophy

Submitted By

Navdeep Kaur

(Reg. No. 950904019)

Under the supervision of

Dr. Sanjay K. Jain

Electrical & Instrumentation Engineering Department

Thapar Institute of Engineering & Technology

PATIALA–147004

August, 2019

CERTIFICATE

I hereby certify that the work which is being presented in the Thesis entitled, ***"Optimal Placement of Dispersed Generators for Practical Distribution Network"*** in fulfilment of the requirement for the award of the Degree of ***Doctor of Philosophy*** submitted in the ***Electrical & Instrumentation Engineering Department*** of the **Thapar Institute of Engineering & Technology** is an authentic record of my own work carried out under the supervision of **Dr. Sanjay K. Jain** and refers other researcher's work, which are duly listed in the reference section.

The matter presented in this Thesis has not been submitted for the award of any other degree of this or any other University.

Navdeep Kaur
950904019

This is to certify that the above statement made by the candidate is correct and true to best of my knowledge.

Dr. Sanjay K. Jain
Associate Professor

Date: 26 Aug 2019

Abstract

The usage of dispersed generators (DGs) are proving a promising and environmental friendly sources to supply electrical energy near to load centers. The interest in assimilation of DGs in distribution networks (DN) is because of increasing load demand and availability of renewable generation. However, the concept of integrating DGs to low voltage DN is a paradigm that differs from conventional central generation based paradigm. The integration of dispersed generation is directed to complement the efforts in improving the energy efficiency and reliability of power systems. With the usage of DGs, the increasing load demand can be met without expanding the existing transmission systems.

The DNs are characterized by large number of buses and lines with a high *R/X* ratio and the power flow from the higher to lower voltage levels to supply loads. In radial distribution network (RDN), the voltage of buses drop when moved away from the source and results into high losses. Moreover, the DNs are mostly subjected to growing or varying load demand. The integration of DGs benefits the DNs by diminishing losses and enhancing the voltage of all buses while meeting the load demand. Such integration is beneficial only, if DGs of appropriate sizes are placed at suitable locations. The use of shunt capacitors in DNs is expected to reduce losses and yield lower reactive burden. The optimal placement of DG and capacitor simultaneously can be investigated to supply load demand. For the practical DNs, the load cannot be assumed simply as constant power (CP) load. The bus voltage has strong influence on load associated with that bus. The prevalent practical loads can be voltage dependent as found in commercial, residential and industrial loads. Further, the inherent uncertainty in practical DNs shall be analyzed by some probabilistic approach in modeling and analysis.

In this research work, the effectiveness of DG integration is investigated for diminution of losses in DNs using analytical expressions based approach and Particle Swarm Optimization (PSO) for practical voltage-dependent loads. Based on the characteristics, four types of DGs are considered for integration. The analytical expressions based on equivalent current injection are derived by utilizing topological structure of RDN to obtain optimal size of DG for minimum loss. In the presented formulation, the optimal DG placement is obtained without repeatedly

computing the load flow. The proposed formulation finds the optimal size of all types of DGs. The optimal size and site of DGs are also determined by PSO. The potential candidate buses for allocation of DGs are obtained through sensitivity factors. It limits the search space without compromising on the quality of the solution. The allocation obtained from analytical expressions and PSO are compared. The investigations are carried out on 33-bus and 69-bus RDNs.

The Type-I and Type-III DGs are allocated optimally at multiple locations in DNs for optimization of a multi-objective function (MOF). The MOF is derived by combining indices of active power loss, reactive power loss, voltage deviation and overall economy with fuzzy decision approach. This MOF is optimized using PSO to find the optimal sizes and sites of DGs for voltage dependent practical loads. The objective function is optimized under operating constraints of bus voltage and MVA limit. Using base case power flow solution, the clusters of buses are formulated to limit the search space. The true Pareto based multi-objective optimization is also analyzed for VDI and PLI. Theses approaches are tested on a 69-bus RDN.

The optimal allocation of DG and capacitor is determined through single and multi-objective optimization of power loss index and voltage deviation index. The placement of DG and capacitor is attempted separately and concurrently. The fuzzy decision approach is implemented to solve multi-objective optimization by assigning fuzzy memberships to the objective indices and optimizing the MOF. This formulation is implemented under PSO to attain the optimal sizes and locations of DG and capacitor for voltage-dependent practical loads. The multi-objective allocation of DG and capacitor is attained through true Pareto based approach. The proposed approaches are tested on 33-bus and 69-bus RDNs.

The uncertainty in loads present in practical DN is expressed through probabilistic measures and analysis is carried out through Latin Hypercube Sampling and Monte Carlo Simulation techniques. The probable size of DG and capacitor are obtained through probabilistic approach. In this probabilistic approach, the size of DG and capacitor for a pre-defined optimal location is computed corresponding to each load sample obtained by two techniques. The optimization is achieved through PSO for minimizing power loss and voltage deviation indices individually. Moreover, these indices are combined to form a MOF, to be optimized by multi-objective PSO. This probabilistic approach is employed for single and multi-objective optimization problem on 33-bus RDN. The results obtained through two sampling techniques and results between the deterministic and probabilistic allocation of DG and capacitor are compared.

Acknowledgements

This study was an elaborate mission and it would have been unachievable without the help and gratitude of many people. I honestly feel short of words to acknowledge all those who helped me directly and indirectly during this mission.

With due regards and great delight, I convey my heartful gratitude and indebtedness to my research supervisor **Dr. Sanjay K. Jain**, Associate Professor, Electrical & Instrumentation Engineering Department, Thapar Institute of Engineering & Technology, Patiala for his skillful guidance, proficient evaluation, persistent encouragement, and conscientious supervision throughout this academic endeavor. He was always available to help me with utmost care, kind attention, and prudent suggestions. His vibrant persona, hard-working nature, and methodical suggestions were a constant source of encouragement for me. It is owing to his able guidance, expertise, inquisitive attitude, and tireless efforts that I find my vision even more broadened. I earnestly thank him from the core of my heart for being a consistent source of inspiration right through the beginning till the end.

I am very thankful to **Dr. Ajay Batish**, Professor & Deputy Director, **Dr. Ravinder Agarwal**, Professor, Electrical & Instrumentation Engineering Department and **Dr. Sunil Kumar Singla**, Associate Professor, Electrical & Instrumentation Engineering Department for being the members of Doctoral Committee and spending their valuable time in reviewing and critically examining the work.

I am also thankful to present Chairman of the Doctoral Committee **Dr. R.S. Kaler**, Senior Professor & Head, Electrical and Instrumentation Engineering Department for the much-needed support throughout the work. My heart felt gratitude is due to **Dr. Rafat Siddique**, Senior Professor & Dean, Research and Sponsored Projects and Honourable Director **Dr. Prakash Gopalan** for the encouragement, support and providing the necessary facilities to carry out and complete this work on steady course.

I also wish to express my deep sense of gratitude to all the faculty and staff members, particularly **Dr. Mukesh Singh**, **Dr. Nitin Narang**, **Dr. Shakti Singh**, and **Mr. Souvik Ganguli** of Electrical & Instrumentation Engineering Department and all the persons who with their encouraging and caring words, constructive criticism and suggestions or by smile have contributed directly or indirectly in a significant way towards completion of this work.

Special and sincere heartfelt gratitude to **Dr. Sushma Jain**, Assistant Professor, Computer Science & Engineering Department and **Ms. Manbir Kaur**, Associate Professor, Electrical & Instrumentation Engineering for their continuous support and motivation provided to me throughout my research and who have always stood by me in all the times.

I appreciate the support provided by my friend **Dr. Neeraj Gupta**, Assistant Professor, Department of Electrical Engineering, National Institute of Technology, Srinagar, for realization of work. My deepest appreciations are due to my friends particularly **Dr. Gurbir Kaur, Dr. Sangeeta Kamboj** and **Dr. Navneet Seth**. They always stood by me in all difficult times and reinforced my confidence. Their never-ending support is a constant source of motivation and always keeps me going.

My sincere thanks to **Ms. Akanksha Sharma** and **Mr. Nagendra Singh** for their support in providing long working hours during the final stage of Thesis.

I bow with gratitude for my parents, who are the most precious persons in my life and without whose efforts I would have not achieved this mission. I feel honored in recognizing the love and affection of Preet.

I express my gratitude to all those, with whom I have worked, interacted, and whose thoughts have helped me in furthering my grasp and understanding of the subject.

Last but not least, I bow in reverence to Almighty God who has always showered blessings on me at each and every step to complete this thesis.

Navdeep Kaur

(950904019)

Contents

List of Figures

List of Tables

Symbols and Acronyms

List of Symbols

β_k	Cardinal priority rank of k^{th} pareto solution
c_1, c_2	Acceleration constants
C^{DG}	Cost of power supplied by DG
CE, CE^{DG}	Cost of losses and energy purchased before and after DG integration respectively
C_{PT}	Power tariff
$c(X)$	Inequality constraint
ϵ_i	maximum limit of i^{th} objective
$f_i(X)$	i^{th} objective function
f_i^{max}, f_i^{min}	maximum and minimum limits of i^{th} objective function respectively
$h(X)$	Equality constraint
I	Bus current matrix
$Iter, Iter_{max}$	Iteration count and maximum iteration count respectively
M	Sample size
μ_i^k	Normalized membership for i^{th} objective function and k^{th} solution
μ_{OEI}	Membership assigned to OEI
μ_{PLI}	Membership assigned to PLI
μ_{QLI}	Membership assigned to QLI

μ_{VDI}	Membership assigned to VDI
$\mu(x)$	Mean of variable x
n	Number of buses
nb	Number of branches
np, nq	Active and reactive power exponents respectively
OEI	Overall economy index
P	Active power matrix
P_{DGi}	Active power generation by DG at i^{th} bus
P_{Di}	Active power load demand at i^{th} bus
pf	Power factor
pf_{DG}	Power factor of DG
P_i	Voltage-dependent active power load demand at i^{th} bus
P_{io}	Base active power load demand at i^{th} bus
P_{Loss}	Active power loss in distribution network before DG integration
PLI	Active power loss in distribution network before DG integration
P_{Loss}^{DG}	Active power loss in distribution network after DG integration
Q	Reactive power matrix
Q_{DGi}	Reactive power generation by DG at i^{th} bus
Q_{Di}	Reactive power load demand at i^{th} bus
Q_i	Voltage-dependent reactive power load demand at i^{th} bus
Q_{io}	Base reactive power load demand at i^{th} bus
QLI	Reactive power loss index
Q_L	Reactive power loss in distribution network before DG integration
Q_L^{DG}	Reactive power loss in distribution network after DG integration

R	Branch resistance matrix
r_1, r_2	Random numbers between 0 and 1
S	Solution space
$\sigma(x)$	Standard deviation of variable x
S_{ij}	MVA flow between bus i and j
S_{ij}^{max}	Maximum limit of S_{ij}
V	Bus voltage before DG integration
VD	Voltage deviation before DG integration
VD^{DG}	Voltage deviation after DG integration
V^{DG}	Bus voltage after DG integration
VDI	Voltage deviation index
v_i^k	Current velocity of i^{th} particle for k^{th} solution
V_{max}, V_{min}	Minimum and maximum limits of bus voltage respectively
VD_{nom}	Nominal bus voltage
V_p	Velocity vector of particles
w_i	Weight assigned to i^{th} objective function
w_{iner}	Inertia weight for i^{th} iteration
w_{max}, w_{min}	Maximum and minimum inertia weights
X	Solution vector
x_i^k	Current position of i^{th} particle for k^{th} solution
X_p	Position vector of particles
y_j	Value of j^{th} performance index
y_{max}, y_{min}	Maximum and minimum limits of y_j

List of Acronyms

ABC	Artifical bee colony
BCBV	Branch-current to bus-voltage
BIBC	Bus-injection to branch-current
CP	Constant power
DG	Dispersed generator
DN	Distribution network
GA	Genetic algorithm
LHS	Latin hyper-cube sampling
LSF	Loss senstivity factor
MCS	Monte carlo simulation
MOF	Multi-objective function
OPDG	Optimal placement of DG
PSO	Particle swarm optimization
RDN	Radial distribution network

Chapter–1

Introduction

1.1 OVERVIEW

The large generators are mostly used in the conventional power systems, where the generated electricity is transmitted through high voltage transmission networks to low voltage distribution networks (DNs) to end consumers. In such conventional arrangements, large generators are located mostly away from the load centers. The concept of integrating dispersed generations to low voltage DN is a paradigm that differs from central generation based paradigm used in conventional power systems.

The integration of dispersed generation is complementing the efforts in improving the energy efficiency and reliability of power systems. Further, it is poised to address the concerns of gaseous emissions and techno-economical difficulties in implementing large power plants. With the usage of dispersed generators (DGs), the increasing load demand can be met without much expanding the existing transmission systems. The dispersed generation refers to use the non-dispatchable resources for electric power generation. These resources may be renewable, non-renewable or combined reheat plants. The technical benefits of integrating DGs include diminution of losses, enhancement in the voltage profile, improvement in power quality, reliability *etc.* (Pepermans *et al.*, 2005). The Indian perspective of different dispersed generation technology was summarized (Banerjee, 2006; Mukhopadhyay and Singh, 2009).

The DN is a passive network where power flows through higher to lower voltage levels. Such networks are characterized by large number of buses and lines with a high *R/X* ratio. In radial distribution network (RDN), the voltage of buses drops when moved away from the source

and results into high losses. Moreover, the DNs experience stress due to constantly growing or varying load demand.

It is important to minimize the losses and enhance the voltage profile of buses to improve the overall performance of the DN. The integration of DGs is an attractive alternative to overcome these issues. Such integration is more beneficial, if DGs of appropriate sizes are placed at suitable locations. Therefore, the optimal placement of DGs (OPDG) is an important area for investigation. The OPDG depends on the choice of objectives, which can be based on power losses, voltage profile, DG cost, energy losses cost, DG capacity, profit, system average interruptions duration index *etc.* The use of shunt capacitors in DNs is expected to reduce the losses and yield lower reactive power burden. The optimal placement of DG and shunt capacitor simultaneously, can be a better proposition.

For the practical DNs, the load cannot always be constant power (CP) load. The bus voltage has strong influence on load associated with that bus. The prevalent voltage-dependent practical loads are found in commercial, residential and industrial sectors. Further, the inherent uncertainty in practical DNs shall be analyzed by some probabilistic approach in modeling and analysis.

There are wide range of analytical and heuristic methods to analyze the optimum allocation of DGs, which differs on the basis of objectives, type of DGs, nature of loads and the constraints. The problem formulation gets complicated with the consideration of practical probabilistic loads. The placement of multi-types of DGs, and DG and capacitor becomes important to meet ever changing practical loads. The multi-objective optimization to decide the allocation considering the above mentioned aspects of different types of DGs, DG and capacitor, and practical probabilistic loads shall be investigated. The true multi-objective optimization shall be giving a set of Pareto-optimal solutions. To help decision maker, it is important to select a solution from the Pareto solutions.

1.2 DISTRIBUTION NETWORK

The DN is an interface between the bulk power system and the consumers. These networks typically include medium and low-voltage power lines and carry electricity from the transmission system to be delivered to the end users. The DNs have typical features such as large number

of buses and branches, falling voltage from source to load side, stress of ever increasing load demand, high *R/X* ratio, which differentiate them from transmission networks (Kersting, 2002). Also, the presence of different types of consumers in DNs may lead to unbalanced operation of DN.

The DNs can be classified on the basis of voltage level and connection scheme. Based on the voltage level, DNs are categorized as primary and secondary DNs. The primary DNs supply large consumers at medium voltage levels. The typical voltage levels for primary DNs are 3.3 kV, 6.6 kV and 11 kV. In addition to large consumers, substations at secondary DNs are also fed from primary DNs. The three-phase three-wire system is employed for primary DNs. The secondary DNs supplies the end users at low voltage usually employing three-phase four wire system. Usually, single-phase supply is utilized by domestic users and three-phase supply is utilized by commercial and industrial users.

Based on the topology of feeders, DNs are classified as radial, open loop, link arrangement, interconnected and mesh connected DNs. The single line diagram of a these DNs are shown in Figure 1.1 (a), (b), (c), (d) and (e) respectively (Lakervi and Holmes, 2003). The RDN as shown in Figure 1.1 (a), is a simple and most economical from the perspective of both construction and protection system. In RDNs, different feeders come out radially from the generating station. The distributors also come out radially from secondary of distribution transformer. Hence, the power flow in RDNs is in one direction only. The main drawback of RDNs is that the voltage level falls significantly to the customers, which are at the far end to the main feeder. Also, the RDNs are not reliable; as the failure of a feeder results in failure of supply to the consumers connected to that feeder.

The reliability of RDN can be improved by the open-loop arrangement of DN, as shown in Figure 1.1 (b). In this configuration, the network operates as RDN under normal operating conditions. The open disconnector can be closed at fault occurrence busbar and open point to provide back-up supply. In link arrangement of DNs shown in Figure 1.1 (c), the open points can be closed if supply from one sub-station is interrupted and network behaves as RDN. These DNs are commonly employed in urban and industrial environments. The reliability of DN can also be improved by using meshed DNs. In such networks a few interconnecting loops are present. Meshed networks, as shown in Figure 1.1 (d), can work as RDNs if the interconnectors fail.

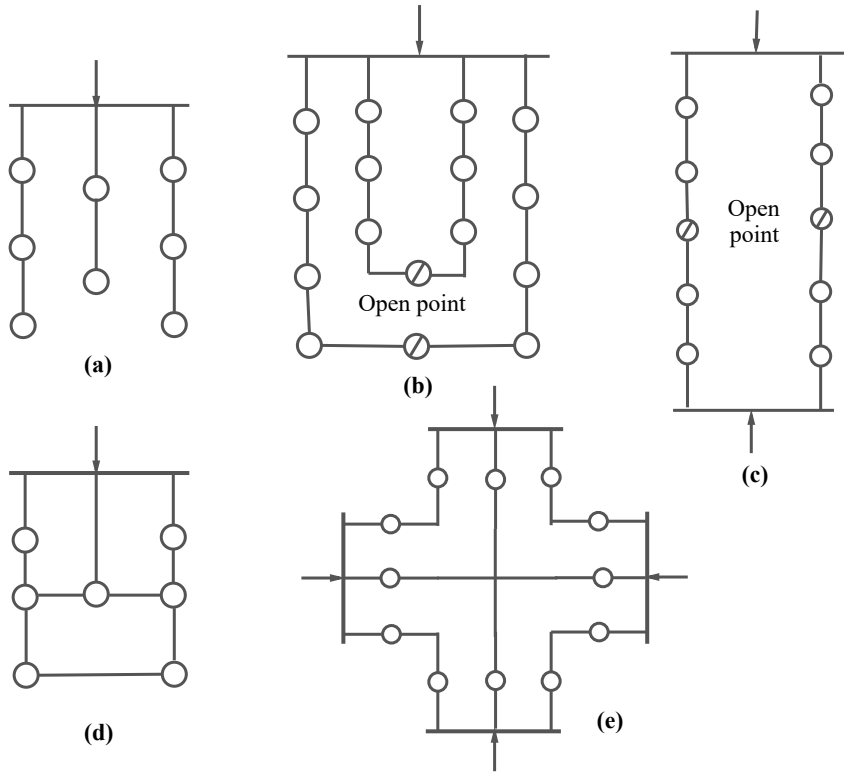

Fig. 1.1: Types of DNs (a) Radial (b) Open loop (c) Link (d) Mesh (e) Interconnected

These networks are usually employed in medium and low voltage DNs. Further improvement in reliability of DN can be achieved by using interconnected DN. In this DN, the distribution transformers are fed from a number of feeders but in different paths.

1.3 DISPERSED GENERATION

The structure of conventional electric systems is based on central generation. The power from large generators is transported over considerable distances through high voltage transmission network. This power is then supplied to the end users through distribution transformers. This conventional arrangement of an interconnected power system is advantageous as it allows minimal reserve requirements, dispatching of the most efficient generating plant at any time, and limited losses during bulk power transfer. However, the factors such as concern to gaseous emissions, techno-economical difficulties in implementing large power plants, rational use and diversification of energy resources to meet the national requirement, deregulation and competition policy *etc*. have resulted in the increased interest in connecting the generation into DNs referred as *dispersed generation*. The dispersed generation often offers a valuable alternative to traditional

sources and arrangement for electric power generation. The dispersed generation has technical as well as environmental benefits as most of the dispersed generation is based on renewable sources. The comparison of the central generation with dispersed generation is depicted in Figure 1.2 (Viral and Khatod, 2012).

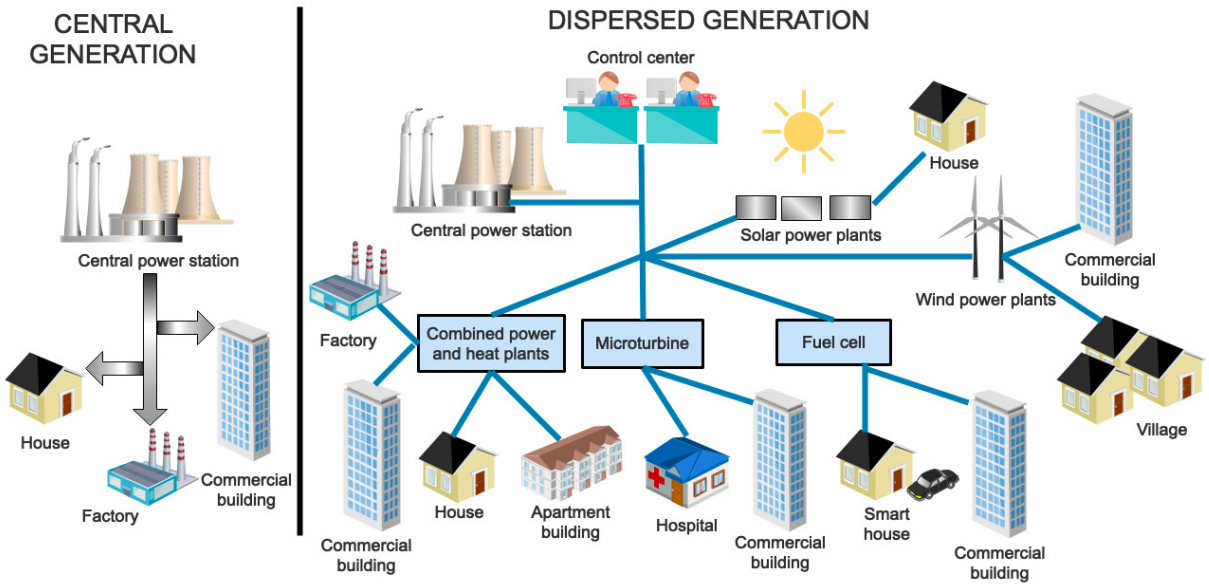

Fig. 1.2: Central Generation versus Dispersed Generation

In the central generation, the DN behaves as a passive network as power is supplied from a bus and the power flows from the higher to the lower voltage levels. In such networks, the bus voltage drops when moved away from the source. With significant dispersed generation, the system behaves like an active network where the power flows and voltages are determined by both main and DGs.

Generally, the term dispersed or distributed generation refers to generation technology that is integrated close to the point of use within the DN. DGs are small generators with typical generation ranging from few kW to 100 MW connected directly to the medium or low voltage grid/DNs. The problem of constantly growing load demand in DNs can be conquered with the dispersed generation. The dispersed generation is being contemplated as an attractive option to defer transmission and distribution upgrading and to support reliability and system performance. The increased interest on the dispersed generation can be further attributed to availability of modular plants, ease of finding sites, short construction times and lower capital costs, and the government support for renewable technology. Even, the cost of renewable energy technologies

is decreasing with increasing demand and production. The usage of DGs are likely to increase due to deregulation and open access.

Various definitions of dispersed generation are based on the related issues such as location, rating, purpose, environmental impacts, technology, power delivery area, mode of operation, ownership, and penetration. The *Electric Power Research Institute* defines DG range from a few kW up to 50 MW (Ackermann *et al.*, 2001). The DG technologies, DG types and benefits of DGs are summarized in the following sub sections.

1.3.1 DG Technologies

The environmental concerns like gaseous emission from fossil fuels led to the exploitation of renewable resources. These resources possess lower energy density and therefore used in smaller plants spread widely. The DGs may be based on-

- **Fuel Cell:** It converts chemical energy of a fuel to electrical energy. They operate like a battery. As the output of the fuel cell is DC, so the fuel cell based DGs are connected to the grid through power electronics interface. The fuel cells have a quieter operation, and due to the absence of a mechanical process, the efficiency of these is higher in comparison to other thermo-mechanical processes.

- **Photovoltaic Cell:** The energy contained in sunlight can be converted into electricity. The photovoltaic (PV) system consists of series/ parallel connected multiple cells depending on the ratings. As the output of PV cell is DC, so like the fuel cell based DGs, PV cell-based DGs are also connected to the grid via power electronics interface. PV cells do not emit any emission and have lower maintenance.

- **Wind Turbines:** The fixed speed wind turbine drives the cage induction generator directly connected to grid. Whereas, variable speed wind turbine uses synchronous generator or doubly fed induction generator. Although the output of a wind turbine based DGs is AC but still a power electronic interface is required because the output voltage and frequency are variable.

- **Internal Combustion Engine:** It converts chemical energy from gaseous or liquid fuels into mechanical energy, which drives the synchronous or induction generator. Its size ranges from less than 5kW to over 5,000 kW.
- **Gas Turbines:** The chemical energy of fossil fuels is converted to heat to drive the gas turbines and consequently the AC generator. The capacity of these turbines ranges typically between 1-5 MW. They are characterized with low capital cost, low emission and low electric efficiency. The gas turbines are used primarily to supply peak demand in co-generation.
- **Micro-Turbines:** The working of micro-turbines is same as gas turbines, but they drive high-speed permanent magnet synchronous generator. The power electronic interface is used for grid connection.

The energy of DGs may be injected to the grid via AC generators connected directly to the grid, or via power electronic interface depending on the technology. The DG technologies and interface methodologies to grid are summarized in Table 1.1.

Table 1.1: DG Technologies Summary

Technology	**Output Type**	**Methodology for Grid Connection**
Fuel Cell	DC	Power electronic interface
Photovoltaic Cell		
Wind Turbine	AC	Directly or through power electronic interface
Micro Hydro		
Internal Combustion Engine		
Gas Turbine		
Micro-Turbine		Power electronic interface

1.3.2 DG Types

The DGs are based on different DG technologies as described in section 1.3.1. Depending on the characteristics of various technologies, output and the methodology of interconnection to

grid; the active power is either injected by the DG or it may be zero, but reactive power can be injected, absorbed or zero. The DGs are classified into four types (Hung *et al.*, 2010) as:

- The **Type-I** DGs can inject only active power e.g. generation based on fuel cells and photovoltaic systems.
- The **Type-II** DGs can inject reactive power only e.g. synchronous compensator, capacitor etc.
- The **Type-III** DGs can inject both active and reactive power e.g. synchronous generator operating at lagging power factor.
- The **Type-IV** DGs can inject real power but absorb reactive power e.g. wind turbines driven induction generators. These generators have leading power factor.

1.3.3 Benefits of DGs

The dispersed generation is being contemplated as an attractive option to defer transmission and distribution upgrading and to support reliability and system performance (Pepermans *et al.*, 2005). The economic and environmental aspects are the main drivers for the development of DGs. The DGs have an impact on the grid voltage quality, safety and protection (Driesen and Belmans, 2006).

The integration of DGs has technical, economical as well as environmental benefits, as shown in Figure 1.3. The technical benefits include diminution of losses, enhancement in the voltage level of all buses, improvement in power quality *etc.* of DN. These benefits are accomplished only if DGs are allocated properly. The diminution of losses further leads to saving in the cost of energy loss making DGs integration economically favorable. The integration of DGs, might change the characteristics of DN and therefore there are associated challenges. There are power quality issues with the integration of DGs in DNs (Carvalho *et al.*, 2008; Pradhan *et al.*, 2018).

- ***Loss Diminution :*** As DNs are characterized by high *R/X* ratio, lower voltage level and higher current level; the losses are highest in DNs when compared to generation

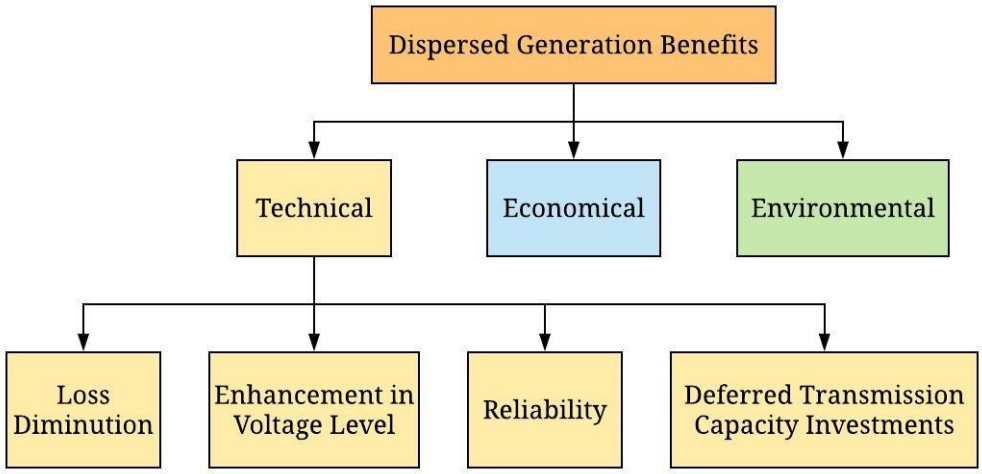

Fig. 1.3: Dispersed Generation Benefits

or transmission systems. Moreover, the DNs are always under stress due to constantly growing load demand. Due to heavy loads, the voltage level of all buses falls and causes the increase in real power losses. The major benefit of DGs integration in DN is the diminution in real power losses, which reduces the cost of energy lost.

- ***Enhancement in Voltage Level :*** The decreasing voltage profile of all buses is concern in DNs, which may lead to voltage instability. This is due to the shortage of reactive support at the distribution level. In past capacitors were employed for the support of reactive power and hence enhancing the voltage profile. The integration of DGs in DN is expected to enhance the voltage level of all buses by locally meeting the demand and reducing the burden on substation.

- ***Reliability :*** The reliability is associated with interruptions in power supply due to fall of voltage or voltage collapse or outages. As the assimilation of DGs enhances the voltage level of all buses, hence the reliability of power supply gets improved with the integration of DGs.

- ***Deferred Transmission Capacity Investments :*** As the load is continuously increasing due to increasing dependency on the electricity, there is a need to expand and reform the transmission systems. The investment to enhance transmission capacity can be deferred by assimilation of DGs as the increased load demand can be met by DGs.

- ***Economical Benefits :*** The economical benefits of DGs assimilation in DN are linked to technical benefits. The lower power loss reduces the cost of power lost and also reduces the cost of transmission system expansion.

- ***Environmental Benefits :*** The fossil fuel based conventional power plants have three major emissions *i.e.* carbon dioxide, sulphur dioxide, and nitrogen oxide. These emissions should be minimized as per the agreements of global climate change. These environmental concerns are major forces for the deployment of renewable based DGs such as photovoltaic cells, wind turbines, and hydro turbines.

1.4 SINGLE AND MULTI-OBJECTIVE OPTIMIZATION

The optimization is an act of attaining best solution by achieving specific goals under some given constraints. The optimization is done either to minimize or to maximize the objective/cost function. When the optimization is performed to achieve a single goal, it is termed as the *single objective optimization*; while when considered objectives are more than one, it is termed as the *multi-objective optimization*.

Various types of objectives and there solutions are shown in Figure 1.4 for a typical two variable problem. As shown in Figure 1.4 (a) and Figure 1.4 (b), there is only one solution if the objective is concave or convex. For the non-concave or non-convex objective, as shown in Figure 1.4 (c), number of local optimal solutions exist and it is difficult to find global optimal solutions.

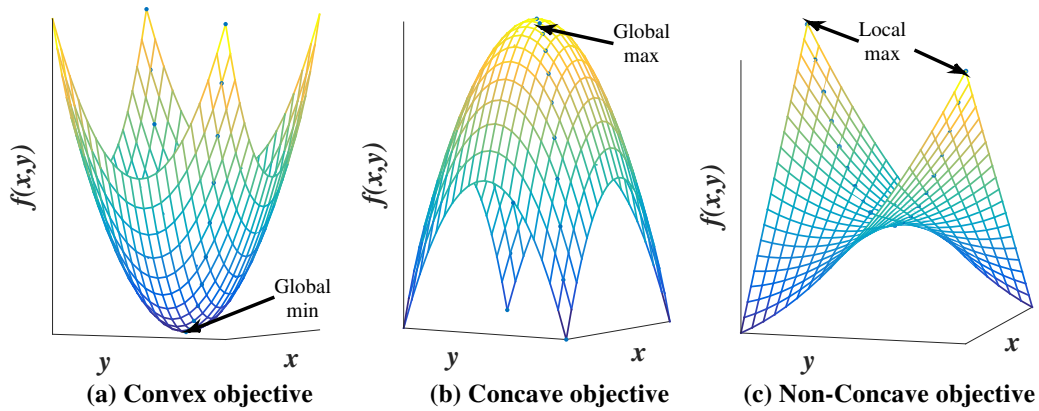

Fig. 1.4: Objective Types and Solutions for Two Variable Problem

Although, single objective problems are simple, but most of the practical problems are multi-objective in nature. The general single objective optimization and multi-objective optimization problems are expressed as equation (1.1) and equation (1.2), respectively.

Single objective optimization problem structure:

$$\begin{aligned} \min_{\mathbf{X}} \quad & f(\mathbf{X}) \\ \text{s.t.} \quad & \mathbf{h}(\mathbf{X}) = \mathbf{0} \\ & \mathbf{C}(\mathbf{X}) \leq \mathbf{0} \\ \text{such} \quad & \mathbf{X^{min}} \leq \mathbf{X} \leq \mathbf{X^{max}} \end{aligned} \tag{1.1}$$

Multi-objective optimization problem structure:

$$\begin{aligned} \min_{\mathbf{X}} \quad & \mathbf{f}(\mathbf{X}) = min(f_1(\mathbf{X}), f_2(\mathbf{X}), \dots f_n(\mathbf{X})) \\ \text{s.t.} \quad & \mathbf{h}(\mathbf{X}) = \mathbf{0} \\ & \mathbf{C}(\mathbf{X}) \leq \mathbf{0} \\ \text{such} \quad & \mathbf{X^{min}} \leq \mathbf{X} \leq \mathbf{X^{max}} \end{aligned} \tag{1.2}$$

where in equation (1.1) and equation (1.2), $\mathbf{X}$ represents solution vector, the solution is bounded by $\mathbf{X^{min}}$ and $\mathbf{X^{max}}$, $f(\mathbf{X})$ is an objective function, **h(X)** is equality constraints set and **C(X)** is inequality constraints set.

The single as well as multi-objective optimization problem can be solved by different optimization methods. The multi-objective problems are complicated, and their solution is difficult as compared to a single objective problem. This is because usually, the objectives are conflicting in nature. Typically, there is no single solution to multi-objective problems which can optimize all objectives concurrently. The concept of dominance is applied in multi-objective optimization. The set of non-dominated solutions is achieved after the convergence of multi-objective problem. These non-dominated solutions are known as *Pareto optimal solutions*, which are set of equally good solutions.

The non-dominated solution is a solution which can not improve an objective without degrading the other one. The set of Pareto optimal solutions is termed as *Pareto optimal set*

and the corresponding values of objective functions are referred as *Pareto optimal front*. A typical Pareto optimal front for a problem with minimization of two objectives problem is shown in Figure 1.5. From the Pareto optimal solutions, one solution is selected for realization or implementation.

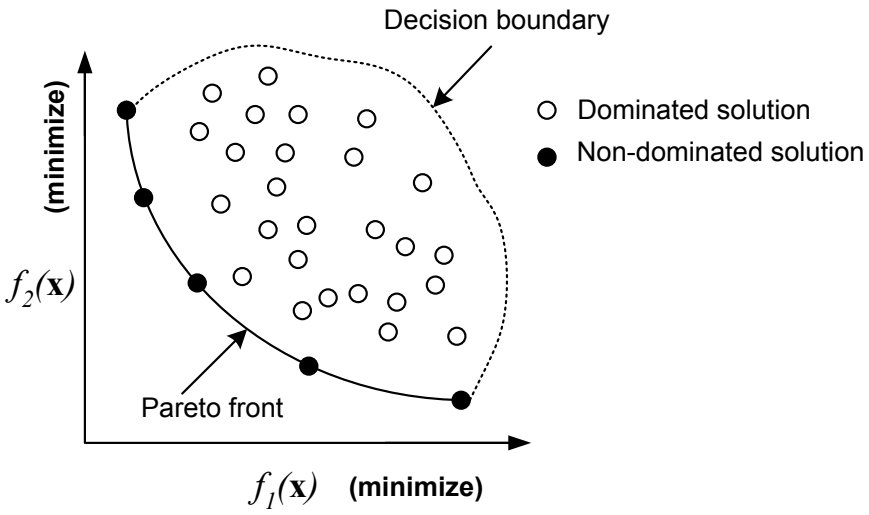

Fig. 1.5: Pareto Front of Min-Min Problem

1.5 PRACTICAL LOADS

In conventional power flow analysis, the load is considered as CP load. In practical DNs, the loads such as industrial, commercial, and residential are prevalent. These loads are significantly affected by the bus voltages. Therefore, it is appropriate to model these loads as voltage-dependent with varying degree of influence of bus voltage. These loads are modeled as:

$$P_i = P_{i0} V_i^{np} \tag{1.3}$$

$$Q_i = Q_{i0} V_i^{nq} \tag{1.4}$$

where P_i and Q_i is voltage-dependent active and reactive load respectively at i^{th} bus; P_{i0} and Q_{i0} is base active and reactive load respectively at i^{th} bus; *np* and *nq* are the active and reactive power exponents. These exponents are considered as zero for CP load.

The consideration of ZIP load model is another approximation of voltage-dependent loads. The values of power exponents np and nq for various types of loads are tabulated in Table 1.2 (Singh and Misra, 2007).

Table 1.2: Load Models and Exponents

Load Model	***np***	***nq***
Constant Power	0	0
Constant Current	1	1
Constant Impedance	2	2
Commercial	1.51	3.40
Residential	0.92	4.04
Industrial	0.18	6.00

In addition to voltage-dependent loads, the load in DNs are also dependent on frequency, time and weather conditions. The load in practical DNs is uncertain due to different types and number of consumers. The uncertainty in load can be modeled using probabilistic models. These practical loads has significant effect on optimal allocation of DGs in RDN.

1.6 MOTIVATION AND RESEARCH OBJECTIVES

1.6.1 Motivation of Work

The integration of dispersed generation offers a valuable alternative to cater the ever increasing load demand and improve the performance of DN. Its usage can significantly affect the power flow pattern, losses, and the bus voltages. Thus, it is felt that there is a scope to investigate the allocation of DGs making a positive impact on the performance of the network. When considering the allocation of DGs, the attention should be paid on the type, siting and sizing of DGs. The allocation is dependent on the objective function and solution methodology. Therefore, there is a need to investigate the allocation with different methods and objectives.

The losses and bus voltages in a DN can be managed by the shunt capacitors also. However, there is a paucity of literature on optimal allocation of DGs and shunt capacitors simultaneously. Therefore, it is felt that there is a scope to investigate the allocation of both DGs

and shunt capacitors making positive impact on the performance of DN. From the view point of optimization, the multi-objective optimization is a different paradigm from single objective, where the conflicting objectives are optimized simultaneously. These conflicting objectives may alter the allocation obtained from single objective optimization. Therefore, there is a need to investigate the allocation of DGs from the viewpoint of multi-objective optimization.

For deciding the allocation of DGs in the practical DNs, the loads shall be treated as realistic as possible. These realistic loads can be voltage-dependent such as residential, commercial and industrial or having some random uncertainty. There is a paucity of literature on the optimal placement of DG for such practical and uncertain loads. Therefore, it is felt to investigate the DG and capacitor allocation in presence of practical voltage-dependent and uncertain loads.

1.6.2 Research Objectives

In view of the above-identified scope, the research work entitled ***Optimal Placement of Dispersed Generators for Practical Distribution Network*** is carried out to achieve the following objectives:

- Investigate the effectiveness of distributed generators in distribution system.
- Develop the algorithm for the optimal allocation of DGs for optimizing various performance parameters.
- Develop the algorithm for optimal allocation of DGs and shunt capacitors for optimizing various performance parameters.
- Develop the algorithm to obtain optimal allocation of DG and shunt capacitors for varying load conditions.

1.7 RESEARCH CONTRIBUTIONS

The contributions of work reported in this Thesis are as follows:

- A state-of-art review has been conducted to study various existing classical optimization techniques for optimal placement of DGs. Along with that, various bio-inspired and nature

inspired meta-heuristic techniques have also been explored for optimal allocation of DGs. Moreover, the techniques have also been explored for deterministic and probabilistic allocation of DG and capacitor. For the allocation, it is assumed that the locations are available for placement of limited number of moderate size (commercial/industrial) DGs instead of placing modular size (household) DGs at many locations.

- The investigations have been carried out for analyzing the effectiveness of four different types of DGs. These investigations are carried out by proposed analytical expressions, which are capable of attaining the optimal size and site of four types of DGs. In addition to analytical expressions, the optimal allocation of distinct types of DGs is also achieved through PSO for voltage-dependent practical loads.

- A multi-objective approach realized by PSO is proposed for optimal placement of multiple DGs to optimize various performance indices. The multi-objective optimization is investigated through Pareto based formulation and combining the objectives through fuzzy decision based approach. The effect of practical voltage-dependent loads is also considered for multi-objective allocation of DGs.

- The single and multi-objective approach is employed for individual and simultaneous allocation of DG and capacitor in RDN in presence of voltage-dependent loads. The multi-objective allocation of DG and capacitor is also attained through true Pareto based approach.

- The effect of uncertainty in load is investigated for optimal allocation of DG and capacitor using a probabilistic approach. The probabilistic nature of load is catered by having mean and standard variation. The probabilistic allocation of DG and capacitor is attempted to optimize performance indices on single objective as well as multi-objective optimization approach.

1.8 ORGANIZATION OF THESIS

To achieve the research objectives, the optimal placement (sizing and siting) of DGs, the DG and capacitor concurrently have been investigated on the basis of single-objective and multi-objective optimization for practical DNs comprising of voltage-dependent loads and uncertain loads. This

work has been presented in seven Chapters in the Thesis. The composition of these Chapters is briefed herewith.

Chapter 1 Introduction

A brief introduction of dispersed generation, summarizing various DG technologies and their characteristics, is presented in this Chapter. The impacts of integrating DGs with DNs and the concept of multi-objective optimization are briefed. The chapter also enlists the research motivation, research objectives and describe the organization of Thesis.

Chapter 2 Literature Review

This Chapter presents the comprehensive review on load flow under DG and on the analytical, numerical and meta-heuristic approaches used for the optimal placement of DGs. The review is carried out on the usage of various types of generators, techniques adopted for DG placement through single and multi-objective optimization. The research challenges being addressed in this research work are also summarized.

Chapter 3 Optimal Allocation of DGs for Diminution of Losses

In this Chapter, the effectiveness of DG integration is investigated for diminution of losses in DNs. Two approaches have been used for the allocation of all types of DGs using the loss formulation. Firstly, an analytical method is used to find the optimal size and site of DGs without repeatedly computing the load flow. Secondly, the loss minimization is carried out through an algorithm based on PSO. The effectiveness of these methods is tested on 33-bus and 69-bus RDNs for constant and practical voltage-dependent loads.

Chapter 4 Multi-Objective Optimal Allocation of DGs

In this Chapter, the performance indices based on active power loss, reactive power loss, voltage deviation, and the overall economy are used as objectives for optimal placement of Type-I and Type-III DGs. These indices are optimized individually as well as simultaneously for multi-objective optimization. The multi-objective optimization is investigated through Pareto-front based optimization and Multi-objective function (MOF) formulation obtained by combining objectives using fuzzy memberships. The optimization is carried out through PSO for practical voltage-dependent loads. The search space for the selection of optimal sites has

been reduced by forming the clusters of buses. The effectiveness of the proposed approach is tested on 69-bus RDN.

Chapter 5 Optimal DG and Capacitor Placement

The optimal allocation of DG, capacitor, DG and capacitor simultaneously is determined using both single and multi-objective optimization in this Chapter. The active power loss index and voltage deviation index are considered as objectives for optimization. The optimization is investigated through Pareto-based and non Pareto MOF based optimization using PSO. The formulation is tested on 33- bus RDN and 69-bus RDN for practical voltage-dependent loads.

Chapter 6 Probabilistic Allocation of DG and Capacitor for Uncertainty in Load

This Chapter presents the optimal allocation of DG, DG and capacitor simultaneously under uncertain, randomly varying loads. The loads are sampled through well-known Monte Carlo Simulation (MCS) and Latin Hypercube Sampling (LHS). The optimal probabilistic allocationof DG , DG and capacitor are decided at candidate bus for single and multi-objective formulation. The probabilistic allocation is presented in form of probability density function (PDF). The performance is tested on 33-bus RDN.

Chapter 7 Conclusions and Future Scope

The conclusions of the work carried out for the thesis preparation are summarized in this Chapter. The scope for further research is also presented.

Chapter–2

Literature Review

The term dispersed generation was introduced in the eighties by the interconnection of wind turbine and micro-turbine based generators. Since then, it is preferred due to sustained growth in liberalized power sector. Conventionally, the DGs are considered as passive negative loads producing power and not perturbing the DN operation. However, their usage will be advantageous only if the allocation is optimal. The load flow analysis is paramount to investigate the effect of DG integration in DNs. However, the load flow analysis of DNs is distinct from the transmission systems due to their different characteristics and has been investigated by many researchers. The optimal allocation of DGs was investigated through different methods and with the consideration of different objectives or set of objectives. Herewith, the brief literature review is presented on load flow and allocation methods from the view-point of optimal allocation of DGs, which mainly includes:

- Load Flow with DG
- Optimal DG Allocation
- Optimal DG and Capacitor Allocation
- Probabilistic Allocation of DGs

2.1 LOAD FLOW WITH DG

The load flow analysis providing the steady-state solution is essential to express various performance parameters for operation and planning studies. The load flow methods used in transmission systems, are not suitable for DNs because these networks are characterized by lines of high *R/X* ratio (Kersting, 2002). The load flow methods are classified as illustrated in Figure 2.1.

The load flow of RDN was carried out using ladder network formulation using Kirchhoff's laws (KCL and KVL) (Baran and Wu, 1989*b*; Ghosh and Das, 1999; Haque, 2000; Ranjan and Das, 2003). The methods used unique path information between the source and a given bus and employed forward/backward sweep. In the forward sweep, the bus voltages were calculated from the sending end to the far end; whereas in the backward sweep, the injected bus currents were calculated from the far end to the sending end on the basis of updated voltages. A direct method of load flow utilized topological bus-injection to branch-current (BIBC) and branch-current to bus-voltage (BCBV) matrices (Teng, 2003).

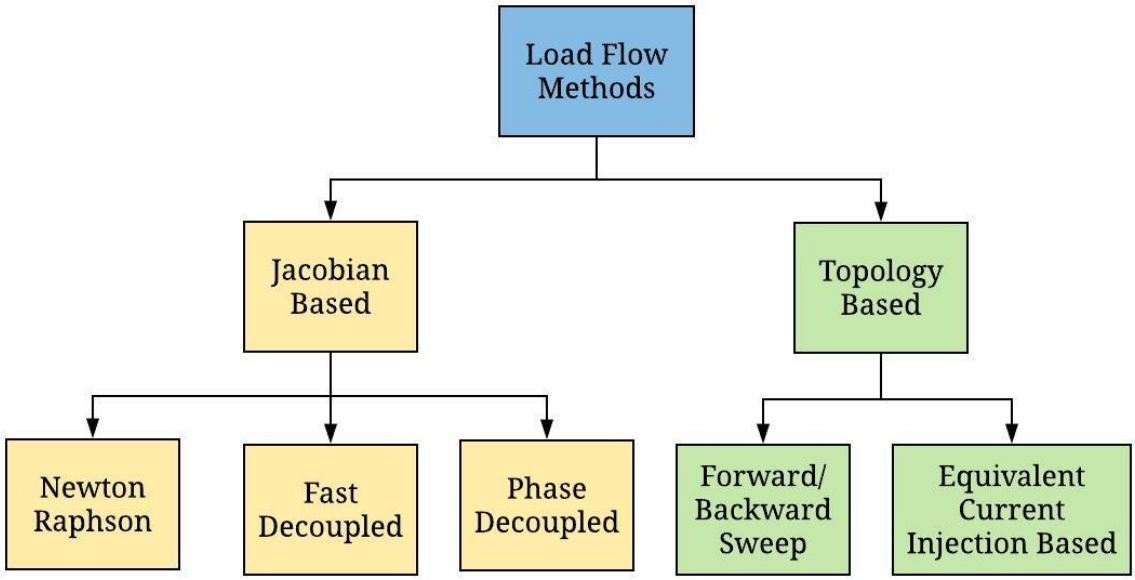

Fig. 2.1: Classification of Load Flow Methods

The load flow of weakly meshed networks was carried out using compensation method (Shirmohammadi *et al.*, 1988; Luo and Semlyen, 1990; Haque, 2000). The interconnection points were broken to change the meshed structure into the radial. Thereafter, traditional ladder network method was applied to obtain load flow of the equivalent radial system. The direct method using BIBC and BCBV matrices was formed for weakly meshed networks (Teng, 2003).

The operation of DN can be unbalanced due to a large number of single phase loads and unsymmetrical conductor spacing of three-phase underground and overhead lines. For such cases, the load flow was carried out on three-phase basis (Zimmerman and Chiang, 1995; Lin and Teng, 2000; Garcia *et al.*, 2000; Vieira *et al.*, 2004). The three-phase Fast Decoupled power flow algorithm (Zimmerman and Chiang, 1995) is identical to the forward/backward sweep algorithm.

The rectangular Newton-Raphson (NR) method was suited more for practical high voltage DNs (Lin and Teng, 2000). The Jacobian matrix had the same structure as the admittance matrix, thereby suited for unbalanced DNs (Garcia *et al.*, 2000). The forward/backward sweep method was modified to compute three-phase power flow algorithm for unbalanced RDNs (Thukaram *et al.*, 1999; Ranjan *et al.*, 2004).

Various researchers presented the models of DGs suited for load flow. The wind farms had been modeled as PQ and RX buses utilizing the steady-state behavior of induction generators (Feijoo and Cidras, 2000). The models of wind DG was developed to calculate the power output of wind turbine at given wind speed and terminal voltage (Divya and Rao, 2006). Three classes of mathematical models of DGs were developed on the basis of electrical machine and the type of interface between DG and DN (Losi and Russo, 2005; Moghaddas-Tafreshi and Mashhour, 2009). The DGs had been modeled as PQ and PV nodes based on control of excitation (Khushalani *et al.*, 2007). The output power characteristics were utilized in developing the model of DG for load flow analysis (Teng, 2008). The various DG models are summarized in Table 2.1.

Table 2.1: DG Models Summary

Reference	**DG Model (bus type)**	**Major Finding**
Feijoo and Cidras (2000)	PQ and RX	Wind turbines are modeled based on characteristics of induction generators
Losi and Russo (2005)	PQ and PV	Models are based on the electrical machines and power electronic interface
Divya and Rao (2006)	————	Mathematical models for obtaining power output of wind turbine based DGs
Khushalani *et al.* (2007)	PQ and PV	Small output DGs are considered as PQ modes while large output DGs as PV nodes
Teng (2008)	Constant *pf*, constant voltage or variable reactive power	DG models are based on output power characteristics
Moghaddas-Tafreshi and Mashhour (2009)	PQ, PV and static voltage characteristic model	DGs are modeled based on grid interface and control of excitation

Compensation based method (Shirmohammadi *et al.*, 1988) had been extended for three-phase power flow; capable of handling DGs, voltage regulators, shunt capacitors and unbalanced and distributed loads (Cheng and Shirmohammadi, 1995). The DGs had been considered as PV node. The voltage mismatches of PV nodes were eliminated by use of PV node sensitivity matrix. The adaptive compensation method (Zhu and Tomsovic, 2002) supported the

load flow of radial and weakly meshed networks, balanced and unbalanced networks considering DGs as PQ and PV nodes. The DGs integration with the three-phase load flow was presented using BIBC and BVBC matrices (Teng, 2008) by accounting their integration as a modification in equivalent current injections. An algorithm based on ladder iterative method had been presented by incorporating DG as PV or PQ model in unbalanced three-phase load flow, capable of handling multiple sources (Khushalani *et al.*, 2007). The power flow of unbalanced DNs with low losses had been solved by the power summation method of forward/backward sweep algorithm contemplating the DGs (Moghaddas-Tafreshi and Mashhour, 2009).

2.2 CLASSIFICATION OF DG ALLOCATION TECHNIQUES

The foreseeable large use of dispersed generation requires, the engineers to take its impact into account properly. For this, the attention should be paid not only to the siting and sizing of DGs but on power factor of DG, optimal number of DGs, and type of DG. The OPDG starts with the selection of objective(s), which have a strong influence on the optimal solution. These objectives are either considered individually or concurrently, consequently categorizing the OPDG problem as *single objective* or *multi-objective* optimization problem.

The optimal allocation had been handled by many techniques such as classical analytical approaches, numerical techniques, and meta-heuristic techniques. The classification of optimization techniques adopted for OPDG is shown as Figure 2.2.

The analytical approaches are based on loss formulas. Being non-iterative techniques, minimum time is expended during computation. The numerical techniques approach to solution either in defined steps or converges iteratively. The Simplex Algorithm designed for Linear Programming (LP) is an example of the numerical technique with defined steps while Newton's Method, Sequential Quadratic Programming (SQP), Non-linear Programming (NLP), Mixed Integer Non-linear Programming (MINLP) *etc.* are examples of iterative methods.

The meta-heuristic techniques are high level computational procedures employed to generate sufficiently good solutions for problems. These techniques do not guarantee the optimal solution but, provide satisfactory solutions that are close to optimal. These techniques are not

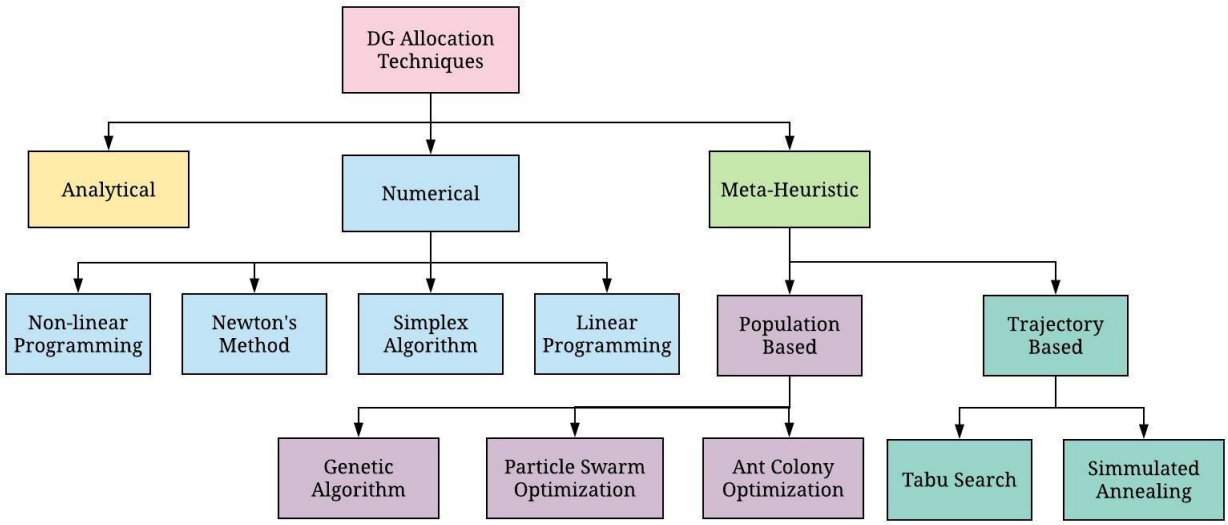

Fig. 2.2: Classification of Optimization Techniques for DG Allocation

problem specific and are independent of objectives and constraints. These techniques are further classified as population-based and trajectory based algorithms.

The population based algorithms generally start with random solutions to the problem and search for feasible solutions in search space. These algorithms are popular mainly due to their flexibility and ease of adaptation to different and complex optimization problems. Genetic Algorithm (GA), Particle Swarm Optimization (PSO), and Ant Colony Optimization (ACO) are some examples of population based optimization techniques. The trajectory based algorithms involve the designing of a trajectory, which optimizes some performance parameters while satisfying a set of constraints. Variable Neighbourhood Search, Iterated Local Search, Tabu Search (TS) and Simulated Annealing (SA) are examples of trajectory based optimization algorithms. Some researchers considers TS and SA as population based algorithms.

2.3 ANALYTICAL APPROACHES

The optimal location of DGs had been obtained by an analytical approach considering time-invariant and variant loads (Wang and Nehrir, 2004). Although the optimal size of DG had not been found, but DG size had been increased in steps to satisfy the voltage regulation. The suggested approach was applied to both radial and meshed networks. Another analytical approach had been applied to accomplish the optimal size and location of Type-I DG (Acharya

et al., 2006). This approach was based on exact loss formula, and an analytical expression had been obtained to find the optimal size corresponding to each bus. These analytical expressions had been extended to achieve the optimal size, location and *pf* of four types of DGs (Hung *et al.*, 2010). Further improvement in these analytical expressions had been done to handle multiple DGs (Hung and Mithulananthan, 2013). The major disadvantage of these analytical expression based approaches is the requirement of Z_{bus} (Gözel and Hocaoglu, 2009). However, this problem had been eliminated by another analytical approach based on the equivalent current injection (Gözel and Hocaoglu, 2009). The topological structure of DNs was exploited to obtain BIBC and BCBV matrices. An analytical expression had been developed in terms of these matrices for calculation of the optimal size of DG at each bus. In all these analytical approaches, the DGs of optimal size were placed at respective buses, one at a time and the bus corresponding to minimum losses was chosen as the optimum location.

A power stability index based on analytical expressions had been derived for identification of the optimum location of DG while the optimum capacity of DG had been varied in the step of one percent (Aman *et al.*, 2012). Three different analytical approaches had been presented to evaluate the optimum size of DG using same methodology to evaluate the optimum site and optimal power factor (Hung *et al.*, 2013). The analytical approach based on multi-objective index had been proposed to evaluate the optimal size, location, and *pf* of DG to diminish the losses and enhance loadability (Hung and Mithulananthan, 2014). The multi-objective index is the weighted sum of active and reactive power losses indices. It had been extended to select the optimal size, site, and number of DGs for industrial DNs (Hung *et al.*, 2014).

An analytical method based on non-iterative power flow of DNs was presented for a system with high *R/X* ratio branches (Elsaiah *et al.*, 2014). In this approach, the optimal locations of DGs had been selected from the priority list of loss sensitivity factors (LSFs) while the optimal size and *pf* had been evaluated from the developed analytical expressions. Naik *et al.* (2015) had considered the real and reactive power losses as objectives for determining the optimal size and location of DG for known *pf*. The analytical approach capable of handling multiple DG had been proposed for diminishing the losses (Viral and Khatod, 2015). The summary of significant findings of analytical approaches is presented in Table 2.2.

Table 2.2: Summary of Analytical Approaches

Reference	DG Type	Objective(s)	DG Variables
Single Objective DG Placement			
Single DG Placement			
Wang and Nehrir (2004); Acharya *et al.* (2006); Gözel and Hocaoglu (2009); Aman *et al.* (2012)	Type-I	Loss	Size and site
Hung *et al.* (2010)	Type-III		Size, site and *pf*
Hung *et al.* (2013)	Renewable DG units		Size, site and *pf*
Multiple DG Placement			
Hung and Mithulananthan (2013)	Type-I, III	Loss	Size and site
Elsaiah *et al.* (2014)	Type-III, IV		Size, site and *pf*
Viral and Khatod (2015)	Type-III		Size and site
Multi-objective DG Placement			
Single DG Placement			
Hung and Mithulananthan (2014); Hung *et al.* (2014)	Type-III	Loss and loadability	Size, site and *pf*
Multiple DG Placement			
Naik *et al.* (2015)	Type-I, III	Active and reactive loss	Size and site

2.4 NUMERICAL TECHNIQUES

An optimal power flow (OPF) based approach had been employed to maximize the capacity of DG with fixed power factor at pre-defined location in DN (Harrison and Wallace, 2005). The OPDG problem was solved to minimize the planning cost by MINLP (El-Khattam *et al.*, 2005). In addition to the optimal size and site of DG, the approach could decide facilities and amount of power required from the main grid. LP had been employed for DG capacity maximization in DN (Keane and O'Malley, 2005). The OPDG had been planned from investment view, hence it is inadequate to handle the operational issues like losses. The OPDG had been solved in the deregulated electricity market by considering two different objectives individually by OPF (Gautam and Mithulananthan, 2007). The effect of voltage-dependent loads on OPDG had been investigated by exhaustive load flow (Singh and Misra, 2007). Hedayati *et al.* (2008) attained

the optimal site of DG by continuation power flow to minimize the losses. The buses had been loaded to maximum capacity, and the most sensitive bus for voltage collapse had been selected as an optimal site for DG.

The classical Kalman Filter Algorithm had been employed to attain the optimal size of DGs while the optimal location had been selected as per load connected to buses (Lee and Park, 2009). Jabr and Pal (2009) evaluated the OPDG by Ordinal Optimization (OO) in three phases, *i.e.*, reduction of search space to select alternatives, evaluation of objective by LP for selected alternatives and selection of the top alternative from second phase and determination of optimal size and site of DG using NLP based OPF. Exhaustive load flow was employed for the attainment of OPDG for various objectives individually (Singh *et al.*, 2009*a*).

MINLP had been employed for determining the optimal location and number of DGs in hybrid electricity market (Kumar and Gao, 2010). The zones in DNs had been identified on the basis of price and loss sensitivity. The best location of DG had been selected as the zone with the highest nodal price and loss sensitivity. Ghosh *et al.* (2010) employed NR method based load flow for OPDG to reduce the weighted sum of losses and cost of DG.

The optimal size of wind generation based DG had been obtained by OPF in presence of variable load and generation (Ochoa and Harrison, 2011). Dynamic Programming (DP) was employed to obtain optimal DG site for profit maximization by considering time-varying nature of load (Khalesi *et al.*, 2011). The optimal sites of DGs had been attained by continuation power flow algorithm for the predefined capacity of DGs in medium voltage DN (Hemdan and Kurrat, 2011). A two-step procedure was proposed for OPDG in which optimal locations and size were identified by normalized LSFs and predefined DG size alternatives, respectively (Rotaru *et al.*, 2012).

Combined heat and power based DGs were placed optimally in urban DN for maximization of DG output by non-linear mathematical programming (Zhang *et al.*, 2014). The DP was applied to attain the solution of OPDG considering enhancement of voltage stability and loss minimization as objectives which were amalgamated together by weighted sum method (Esmaili *et al.*, 2014). Kaur *et al.* (2014) employed MINLP in two phases to reduce computational time for optimal placement of multiple DGs in presence of the uncertain load and generation. The

solutions for multi-objective OPDG problem had been obtained by SQP and the compromised solution had been selected by fuzzy decision making (Darfoun and El-Hawary, 2015). MINLP had been employed for the solution of multi-objective OPDG by changing the multi-objective problem to a single objective problem (Zheng *et al.*, 2017). Vita (2017) had utilized exhaustive load flow for OPDG to minimize losses. The summary of numerical techniques is presented in Table 2.3.

Table 2.3: Summary of Numerical Techniques

Reference	DG Type	Load Model	Objective(s)	Technique
Single Objective DG Placement				
Single DG Placement				
Singh and Misra (2007)	Type-I	Voltage-dependent	Loss	Exhaustive load flow
Ochoa and Harrison (2011)	Type-IV	Variable	Energy loss	OPF
Multiple DG Placement				
El-Khattam *et al.* (2005)	Type-I	CP	Planning cost	MINLP
Keane and O'Malley (2005)			DG Generation	LP
Lee and Park (2009)		Variable	Loss	Kalman filter algorithm
Khalesi *et al.* (2011)			Profit	DP
Hedayati *et al.* (2008)	Type-III	CP	Loss	Continuation power flow
Kaur *et al.* (2014)			Loss	MINLP
Hemdan and Kurrat (2011)	Type-I, III		Voltage limit loadability	Continuation power flow
Harrison and Wallace (2005)	Type-I, II, III		DG capacity	OPF
Vita (2017)	Type-I, IV		Loss	Exhaustive load flow
Zhang *et al.* (2014)	CHP		DG output	Mathematical programming
Multi-objective DG Placement				
Single DG Placement				
Gautam and Mithulananthan (2007)	Type-I	CP	Social welfare Profit	OPF
Ghosh *et al.* (2010)			DG cost Loss	NR method
Multiple DG Placement				
Singh *et al.* (2009*a*)	Type-I	Voltage-dependent	Power loss MVA intake Cost Energy loss	Exhaustive load flow

Table 2.3 continued .....

Table 2.3 – Continued from previous page

Reference	DG Type	Load Model	Objective(s)	Technique
Kumar and Gao (2010)	Type-I	CP	Cost Loss	MINLP
Rotaru *et al.* (2012)			Loss Voltage profile	Exhaustive search
Esmaili *et al.* (2014)			Voltage stability Loss	DP
Darfoun and El-Hawary (2015)			Loss DG cost	SQP
Jabr and Pal (2009)	Type-III		Loss DG capacity	OO
Zheng *et al.* (2017)	Type-IV		Voltage stability System reliability Phase unbalance	MINLP

2.5 META-HEURISTIC TECHNIQUES

2.5.1 *Genetic Algorithm (GA)*

GA is a nature-inspired optimization algorithm frequently applied to attain the optimization problem solutions. It has three major operators namely selection, crossover and mutation. GA can be applied to optimize both single and multi-objective problems.

GA had been utilized for maximization of benefits to DN by OPDG (Borges and Falcão, 2006). It had also been employed for OPDG in radial as well as mesh connected DNs targeting the minimization of losses (Singh and Goswami, 2009). The OPDG had been attained for maximization of profit, which is evaluated by cost of losses and electricity (Singh and Goswami, 2010). The optimal locations and size of multiple DGs had been obtained by loss sensitivity and GA respectively, for minimization of cost (Shukla *et al.*, 2010). The DGs had been placed optimally in DN so that the protection system remains unaltered even after integration of DG by maximizing its capacity (Zhan *et al.*, 2016).

GA had been combined with ε-constrained technique to obtain the optimal location of DG with predefined size (Celli *et al.*, 2005; Carpinelli *et al.*, 2005; Singh and Goswami, 2011). The solutions of a multi-objective OPDG problem had been yielded with GA, whereas ε-constrained

technique had been employed to select the compromised solution from the set of alternatives provided by GA. A multi-objective index formulated by weighted sum of different indices was optimized by GA for OPDG (Singh *et al.*, 2009*b*). Abou El-Ela *et al.* (2010) and Akorede *et al.* (2011) had employed weighted sum approach to amalgamate different objectives considered for OPDG. GA was employed to optimize a weighted MOF formulated by assignment of fuzzy membership to each objective (Vinothkumar and Selvan, 2011).

The OPDG was achieved by optimization of weighted MOF (Biswas *et al.*, 2012; Hosseini *et al.*, 2013; Gampa and Das, 2015). Non-dominating sorting GA-II (NSGA-II) had been employed for OPDG, while the compromised solution had been identified by fuzzy decision making from the Pareto front (Liu *et al.*, 2015). An NSGA-II was presented for OPDG for maximization of voltage stability margin, minimization of line losses and voltage deviation (Sheng *et al.*, 2015).

An amalgamation of NSGA and LSFs had been proposed for OPDG in which the search space for GA had been reduced by obtaining the potential buses for DG placement using LSF (Zhang *et al.*, 2015). A MOF was formulated by the weighted sum approach in which active power loss reduction was considered with the highest weight followed by reactive power loss reduction (Bohre *et al.*, 2016).

The comprehensive summary of OPDG using GA is tabulated in Table 2.4 highlighting the significant findings related to considered objectives, load models and DG types for OPDG.

Table 2.4: Summary of OPDG using GA

Reference	**DG Type**	**Load Model**	**Objective(s)**
Single Objective DG Placement			
Single DG Placement			
Borges and Falcão (2006)	Type-I	CP	Benefit
Multiple DG Placement			
Singh and Goswami (2009)	Type-I	Time variant	Loss
Singh and Goswami (2010)			Profit
Shukla *et al.* (2010)		3-level load	Cost
Zhan *et al.* (2016)	Type-III	CP	DG capacity
Prenc *et al.* (2013)	Type-I, IV	Hourly (CP)	Loss

Table 2.4 continued .....

Table 2.4 – continued from previous page

Reference	DG Type	Load Model	Objective(s)
Multi-objective DG Placement			
Single DG Placement			
Celli *et al.* (2005)	Type-I	CP	Cost of energy losses Service interruptions Network upgrading Energy purchased
Singh *et al.* (2009*b*)		Voltage-dependent	Multi-objective index
Zhang *et al.* (2015)	Type-I, III	CP	Benefits to DG owners Benefits to distribution companies
Abou El-Ela *et al.* (2010)	—		Voltage profile Total spinning reserve Power flow in critical lines Total line loss
Singh and Goswami (2011)	—	Voltage-dependent	Customers interruptions Cost of real power loss Cost of purchased energy Bus voltage deviation Security margin
Multiple DG Placement			
Biswas *et al.* (2012)	Type-I	CP	Active power loss Load disturbance Total cost of DGs
Akorede *et al.* (2011)		3-level load	Loading margin Profit
Sheng *et al.* (2015)		CP	Line losses Voltage deviation Voltage stability margin
Hosseini *et al.* (2013)	Type-III		Loss DG capacity Short circuit current Voltage profile
Carpinelli *et al.* (2005)	Type-IV		Cost of energy losses Voltage regulation Total harmonic distortion
Vinothkumar and Selvan (2011)	Type-I and IV		Voltage deviation Real power loss Reactive power loss Line loading Short-circuit index

Table 2.4 continued .....

Table 2.4 – continued from previous page

Reference	DG Type	Load Model	Objective(s)
Gampa and Das (2015)	Type-I, III and IV	Hourly (CP)	Real power loss Branch current capacity Voltage deviation Cost factor index
Bohre *et al.* (2016)	Type-I, II, III and IV	Voltage-dependent	Active power loss Reactive power loss Voltage deviation Reliability Sensitivity factor
Liu *et al.* (2015)	——	Hourly (CP)	DG investment cost DG operational cost Cost of purchasing electricity Voltage deviation

2.5.2 *Particle Swarm Optimization (PSO)*

PSO is another important meta-heuristic technique widely used as an optimization algorithm. It is also a nature-inspired algorithm based on the flocking behavior of birds. PSO has good exploration characteristics. Similar to GA, PSO also does not require the objective function to be differentiable. The implementation of PSO is simple compared to GA due to absence of crossover and mutation operators.

The optimal allocation of Type-I and Type-II DGs (Karimyan *et al.*, 2014) and Type-I, II and III DGs (Kansal *et al.*, 2013) had been attained for diminution of losses. The optimal location of biomass-based DG had been decided by binary PSO (BPSO) for maximization of profitability index (Lopez *et al.*, 2008). PSO with constriction factor approach had been employed for OPDG without violating constraints for growing load demand (Mistry and Roy, 2014). Gomez-Gonzalez *et al.* (2012) employed a hybrid approach for allocation of multiple DGs in which optimal size and location were provided by OPF and PSO respectively. The optimal site, size, and type of DG had been identified to maximize the DG penetration in DN (Ravikumar Pandi *et al.*, 2013). A combination of PSO and maximum power stability index, which identifies the most weak buses for DG placement, was proposed for OPDG (Ishak *et al.*, 2014). BPSO had been utilized for OPDG while constructing virtual power plants with the aim of minimizing total cost during

long-term planning (Bahrami and Imari, 2014). The OPDG was carried out for loss minimization through different variants of PSO (Jamian *et al.*, 2015) and a combination of PSO and analytical expressions (Kansal *et al.*, 2016). The OPDG had been attained by considering time-varying loads to cater the more realistic picture of DN (Kumawat *et al.*, 2017). The variation in load had been assumed to be the same throughout the year.

Weighted sum approach had been utilized for formulation of a multi-objective index, which is optimized by PSO by considering non-linear current as harmonic constraint (El-Zonkoly, 2011). Aman *et al.* (2013), Kayal and Chanda (2013), Musa and Adamu (2013) and Zongo and Oonsivilai (2017) also formulated a weighted MOF, which was optimized through PSO. A voltage stability factor was proposed to identify the weak buses for DG placement (Kayal and Chanda, 2013). Musa and Adamu (2013) combined PSO with Evolutionary Programming (EP) while Zongo and Oonsivilai (2017) combined it with NR method of load flow for OPDG.

The Pareto-front non-dominated sorting Multi-objective PSO (MOPSO) was employed for optimal allocation of different types of DGs and the compromised solution was selected with fuzzy decision making (Mahesh *et al.*, 2016). DG had been placed optimally in DN to maximize the load pickup after natural disasters and reliability under normal conditions using PSO (Reddy *et al.*, 2017).

The comprehensive summary of OPDG using PSO is presented in Table 2.5 highlighting the various considered objectives for OPDG, types of DG and load models.

Table 2.5: Summary of OPDG using PSO

Reference	DG Type	Load Model	Objective(s)
Single Objective DG Placement			
Single DG Placement			
Karimyan *et al.* (2014)	Type-I, II	CP	Loss
Kansal *et al.* (2013)	Type-I, II, III		
Lopez *et al.* (2008)	Biomass-fuelled systems	———	Profitability index
Multiple DG Placement			
Mistry and Roy (2014)	Type-I	CP	Loss
Ishak *et al.* (2014)			
Jamian *et al.* (2015)			
Kansal *et al.* (2016)	Type-I, II and III		

Table 2.5 continued .....

Table 2.5 – continued from previous page

Reference	DG Type	Load Model	Objective(s)
Kumawat *et al.* (2017)	Type-I, III	CP (Time variant)	Energy loss
Gomez-Gonzalez *et al.* (2012)	Type-I	CP	Cost
Bahrami and Imari (2014)	Micro and combustion turbine based DG		
Ravikumar Pandi *et al.* (2013)	Inverter and synchronous based DG		DG penetration
Multi-objective DG Placement			
Single DG Placement			
Aman *et al.* (2013)	Type-I	CP	Power loss Voltage stability
Zongo and Oonsivilai (2017)			Active power loss Reactive power loss Reactive power generation Voltage deviation
Multiple DG Placement			
Musa and Adamu (2013)	Type-I	CP	Power loss Voltage stability
Reddy *et al.* (2017)			Load pickup Reliability
Kayal and Chanda (2013)	Type-I, IV		Power loss Voltage stability
Mahesh *et al.* (2016)	Type-I, II, III		
El-Zonkoly (2011)	——-	Voltage-dependent	Real power loss Reactive power loss Voltage profile MVA capacity Short-circuit index

2.5.3 *Other Population Based Techniques*

- **Ant Colony Optimization (ACO):** ACO is inspired by the behavior of ants for the selection of the optimal path between food and their colony and is suited for discrete optimization problems. ACO had been utilized to attain the optimal site of DGs in the presence of reclosers to enhance the reliability of distribution system (Wang and Singh, 2008; Farhat, 2013).

- **Bacterial Foraging Algorithm (BFA):** The distinct objectives had been amalgamated using penalty factors for OPDG (Rashtchi and Darabian, 2012). A weighted MOF had been optimized by BFA to obtain optimal DG size and site by LSF (Mohamed and Kowsalya, 2014). The slow convergence of BFA is eliminated by the modification for the OPDG (Devi and Geethanjali, 2014).

- **Artificial Bee Colony (ABC):** This algorithm has the benefit that, it has the minimum number of parameters for tuning and suited for optimization (Abu-Mouti and El-Hawary, 2011). The OPDG had been optimized by ABC algorithm for diminution of power losses considering two load levels (Abu-Mouti and El-Hawary, 2011). The large number of iterations required by ABC had been taken care by using Chaotic ABC, which was employed to optimize weighted MOF (Mohandas *et al.*, 2015).

- **Bat Algorithm (BA):** It is a real-coded population-based algorithm and implemented for optimization of weighted MOF (Yammani *et al.*, 2014). In this methodology, priority was given to active power loss index by assigning maximum weight among all indices. Various improvement in BA had been suggested and applied for OPDG (Kanwar *et al.*, 2015*b*).

- **Cuckoo Search (CS):** It is inspired by the reproduction of cuckoos. The optimal locations of DGs with pre-defined sizes had been obtained by CS employed to optimize weighted MOF (Moravej and Akhlaghi, 2013). CS had also been employed for OPDG and reconfiguration of DNs individually as well as simultaneously (Nguyen *et al.*, 2016).

- **Harmony Search Algorithm (HSA):** This algorithm is based on the natural phenomena of harmony among musicians to produce pleasant music. The DGs along with reconfiguration were allocated optimally for mitigation of losses employing HSA (Rao *et al.*, 2013). It had also been employed for multi-objective OPDG problem (Nekooei *et al.*, 2013).

- **Teaching Learning Based Optimization (TLBO):** TLBO is a nature inspired optimization algorithm, which is based on the effect of teacher's influence on the results of a learner. OPDG had been attained by a discrete version of TLBO for diminution of losses (Martín García and Gil Mena, 2013). This technique was also employed for OPDG to optimize weighted MOF (Fathy, 2015) and to enhance the voltage stability (Mohanty and Tripathy, 2016).

- **Ant Lion Optimization Algorithm (ALOA):** It is also a nature-inspired algorithm, which resembles with hunting movement of ant lions. ALOA is adopted for OPDG along with LSF to optimize weighted MOF (Ali *et al.*, 2017). ALOA and IVM had been amalgamated for OPDG, where the optimal locations had been determined by IVM and the optimal size by ALOA (Dinakara Prasasd Reddy *et al.*, 2017).

- **Miscellaneous Techniques:** A nature-inspired algorithm based on the flow of water in the river known as *Intelligent Water Drop Algorithm (IWDA)*, had also been adopted for OPDG along with LSF (Rama Prabha *et al.*, 2015). *Backtracking Search Optimization Algorithm (BSOA)*, which is a single parameter controlled optimization algorithm was implemented for OPDG to optimize weighted MOF (El-Fergany, 2015). *Quasi-Oppositional Swine Influenza Model based Optimization with Quarantine (QOSIMBO-Q)* was applied to optimize weighted MOF within the specified constraints (Sharma *et al.*, 2016). *Firefly Algorithm (FA)* (Abdelaziz *et al.*, 2015), *Chaotic Symbiotic Organisms Search (CSOS)* algorithm (Saha and Mukherjee, 2016) and *Imperialistic Competitive Algorithm (ICA)* (Poornazaryan *et al.*, 2016) are other nature inspired algorithms utilized for OPDG.

- **Hybrid Algorithms:** Hybrid algorithms are the amalgamation of two or more evolutionary techniques to retain the advantages of individual algorithms. *Goal Programming (GP)* had been combined with GA (Vinothkumar and Selvan, 2012) and fuzzy (Kim *et al.*, 2008) for OPDG. GA had also been combined with PSO for OPDG (Moradi and Abedini, 2012). A hybrid algorithm was used for OPDG after modifying *Shuffled Frog Learning* (SFL) and combining it with *Differential Evolution (DE)* (Doagou-Mojarrad *et al.*, 2013). An amalgamation of LSF and *Simulated Annealing (SA)* had been employed for OPDG in which the optimal sites of multiple DGs had been identified by LSF while the optimal sizes had been identified by SA (Injeti and Kumar, 2013). In another hybrid technique, SFL had been combined with BA for OPDG (Yammani *et al.*, 2016). The exploration and exploitation abilities of ABC and ACO algorithm had been utilized for the attainment of best site and size of DG by their hybridization for uncertainties in load and generation (Kefayat *et al.*, 2015). An amalgam of fuzzy and GA was proposed by Nayanatara *et al.* (2016) in which fuzzy logic and GA were utilized as a global and local optimizers, respectively. *Invasive Weed Optimization (IWO) Algorithm* was combined with LSF considering different objectives to achieve optimal size and location, respectively (Rama

Prabha and Jayabarathi, 2016). The *Grey Wolf Optimizer (GWO)* had been hybridized with *Evolutionary Algorithms (EA)* for OPDG (Mithulananthan, 2017). The exploration ability of PSO had been combined with exploitation capability of *Gravitation Search Algorithm (GSA)* for OPDG (Rajendran and Narayanan, 2017). Another combination of PSO and GSA had been implemented for OPDG along with LSF and voltage sensitivity factor (VSF) (Tolba *et al.*, 2018).

The detail of the major finding of techniques mentioned above is summarized in Table 2.6 indicating the various considered objectives, DG types, and load models *etc*.

Table 2.6: Summary of Other Evolutionary Techniques

Reference	DG Type	Load Model	Objective(s)	Technique
Single Objective DG Placement				
Single DG Placement				
Devi and Geethanjali (2014)	Type-I	CP	Loss	Modified BFA
Dinakara Prasasd Reddy *et al.* (2017)	Type-I, II, III			ALOA and IVM
Multiple DG Placement				
Wang and Singh (2008)	Type-I	CP	Reliability	ACO
Martín García and Gil Mena (2013)			Loss	TLBO
Rama Prabha *et al.* (2015)				IWDA and LSF
Mohanty and Tripathy (2016)			Voltage stability	TLBO
Rao *et al.* (2013)		3-level	Loss	HSA
Farhat (2013)	Type-III	CP		Improved ACO
Abu-Mouti and El-Hawary (2011)				ABC
Abdelaziz *et al.* (2015)				Modified FA
Kanwar *et al.* (2015*b*)	Type-III	Voltage-dependent	Annual energy loss	IBA
Injeti and Kumar (2013)	Type-I, III	CP	Loss	SA and LSF
Mithulananthan (2017)	Type-I, II, III			GWO and EA
Rajendran and Narayanan (2017)				PSO and GSA
Multi-objective DG Placement				
Single DG Placement				
Poornazaryan *et al.* (2016)	Type-I	Linearly increasing	Power loss Voltage stability	ICA

Table 2.6 continued .....

Table 2.6 – Continued from previous page

Reference	DG Type	Load Model	Objective(s)	Technique
Tolba *et al.* (2018)	Type-I, II, III	CP	Power loss Voltage deviation Operating cost	PSO and GSA
Nayanatara *et al.* (2016)	Type-I, II, III	CP	Social welfare Loss Congestion	Fuzzy and GA
Multiple DG Placement				
Kim *et al.* (2008)	Type-I	CP	Voltage deviation Active power loss Reactive power loss Short circuit index MVA capacity	GP and GA
Rashtchi and Darabian (2012)			Loss Voltage profile Stability	BFA
Moradi and Abedini (2012)			Power loss Voltage profile	GA and PSO
Moravej and Akhlaghi (2013)			Loss Voltage deviation Voltage profile	CS
Nekooei *et al.* (2013)			Power loss Voltage deviation	IHSA
Fathy (2015)			Loss Voltage deviation	TLBO
Nguyen *et al.* (2016)			Loss Voltage stability	CS
Kefayat *et al.* (2015)			Voltage stability Loss Cost Emission	ABC and ACO
Saha and Mukherjee (2016)			Loss Voltage profile Voltage stability	CSOS
Mohandas *et al.* (2015)		Voltage-dependent	Voltage stability Voltage deviation Active power loss Reactive power loss MVA capacity	Chaotic ABC
El-Fergany (2015)	Type-I, III	CP	Loss Voltage profile	BSOA

Table 2.6 continued .....

Table 2.6 – Continued from previous page

Reference	DG Type	Load Model	Objective(s)	Technique
Sharma *et al.* (2016)	Type-I, III		Loss Voltage stability Voltage profile	QOSIMBO-Q
Mohamed and Kowsalya (2014)		Voltage-dependent	Loss Voltage deviation Operational cost	BFA and LSF
Rama Prabha and Jayabarathi (2016)			Loss Voltage deviation Operational cost	IWO and LSF
Yammani *et al.* (2016)			Power loss Cost Voltage deviation	SFL and BA
Vinothkumar and Selvan (2012)	Micro-turbine and PV based	3-level (CP)	Power loss Voltage profile	Fuzzy, GP and GA
Doagou-Mojarrad *et al.* (2013)	Renewable based	CP	Pollutant emissions Energy loss Cost	Modified SFL and DE
Ali *et al.* (2017)	PV and wind based	3-level (CP)	Loss Voltage profile Voltage stability	ALOA ans LSF

2.6 OPTIMAL DG AND CAPACITOR ALLOCATION

The capacitors had been employed extensively in DNs for minimization of losses from decades. The allocation of DGs has the added advantages of supplying additional load demand and improvement in voltage profile. The concurrent allocation of DG and capacitor has attracted researchers in the recent times.

The optimal site and size of DG and capacitors were achieved respectively by LSF and a heuristic curve fitting technique in which, the size is varied in small steps to satisfy constraints (Gopiya Naik *et al.*, 2013). An analytical approach had been presented for concurrent allocation of DG and capacitor in RDNs using PSO (Kansal *et al.*, 2015). GA had been utilized to identify the optimal locations of DGs and capacitors for minimization of cost for the planning of DNs (Rahmani-Andebili, 2016). The Intersect Mutation Differential Evolution (IMDE) was employed for the determination of sizes and sites of DGs and capacitors concurrently (Khodabakhshian and

Andishgar, 2016). A hybrid algorithm, which is a combination of HSA and particle ABC (PABC) was used for determination of optimal size and site of DGs and capacitors simultaneously (Muthukumar and Jayalalitha, 2016). ABC algorithm was modified to Gbest-guided ABC (GABC) for the improvement of exploitation characteristics (Dixit *et al.*, 2017).

The weighted sum approach had been applied to change the multi-objective problem to a single objective and optimal placement of capacitor and DG was attained by fuzzy and GA (Chandrashekhar Reddy *et al.*, 2013). GA had been implemented for optimal placement of capacitors and various DG types individually as well as concurrently (Esmaeilian *et al.*, 2012). A combination of GA and local initiative search, which is known as *Memetic Algorithm* had been employed for allocation of DGs and capacitors (Sajjadi *et al.*, 2013). The combination of ICA with GA had been used for improved convergence speed and better exploration capability (Moradi *et al.*, 2014). The initial set of solutions had been provided by ICA while the GA had been employed for generation of a new set of solutions. Zeinalzadeh *et al.* (2015) applied MOPSO for optimal DG and capacitor allotment to handle multiple objectives and obtained the Pareto front. The PSO, GA and Cat Swarm Optimization (CSO) were modified and applied for optimal allocation of both DGs and capacitors simultaneously (Kanwar *et al.*, 2015*a*). For faster convergence and to avoid the trapping in local optima, Binary Collective Animal Behaviour Algorithm (BCABA) had been implemented for simultaneous placement of DGs and capacitors (Khan *et al.*, 2015). A Biogeography-based Optimization (BBO) algorithm had been employed by Ghaffarzadeh and Sadeghi (2016) for maximization of benefits by integrating DGs and capacitors. The summary of various techniques adopted for allocation of DG and capacitors and considered objectives is presented in Table 2.7.

Table 2.7: Summary of DG and Capacitor Placement

Reference	DG Type	Objective(s)	Technique
Single Objective DG and Capacitor Placement			
Single DG and Capacitor Placement			
Kansal *et al.* (2015)	CP	Loss	Analytical and PSO
Multiple DG and Capacitor Placement			
Gopiya Naik *et al.* (2013)	CP	Loss	LSF and heuristic curve fitting
Khodabakhshian and Andishgar (2016)		Loss cost	IMDE
Rahmani-Andebili (2016)	Voltage-dependent	Total cost	GA

Table 2.7 continued .....

Table 2.7 – Continued from previous page

Reference	DG Type	Objective(s)	Technique
Muthukumar and Jayalalitha (2016)	3-level (CP)	Loss	HSA and PABC
Dixit *et al.* (2017)	2-level (CP)		GABC
Multi-objective DG and Capacitor Placement			
Single DG and Capacitor Placement			
Chandrashekhar Reddy *et al.* (2013)	CP	Energy loss cost Line voltage drop Power transfer capability	Fuzzy and GA
Multiple DG and Capacitor Placement			
Esmaeilian *et al.* (2012)	CP	Loss Voltage stability Cost of DG and capacitors	GA
Moradi *et al.* (2014)		Loss Load balancing Voltage profile Voltage stability	ICA and GA
Zeinalzadeh *et al.* (2015)		Power loss Voltage stability Balancing of sections current	MOPSO
Kanwar *et al.* (2015*a*)		Annual energy loss Voltage profile	Improved GA, PSO and CSO
Khan *et al.* (2015)		Loss Voltage deviation	BCABA
Sajjadi *et al.* (2013)	3-level	Voltage profile Energy loss Active power loss Reactive power loss	Memetic algorithm
Ghaffarzadeh and Sadeghi (2016)	3-level (CP)	Benefit Cost	BBO

2.7 PROBABILISTIC ALLOCATION OF DGS

The optimal placement of DGs was extensively explored for specified load using deterministic approach. However, the load is inherently uncertain in DN. Moreover, the inputs to DGs based on wind and solar are also uncertain as the wind speed and solar radiance are variable. Thus, it is required to model these uncertainties, and decide the optimal allocation.

MCS had been applied for OPDG to capture the probabilistic nature of load and wind generation with a target of loss diminution in DN by optimal integration of DG (Rao and Abhyankar, 2014). The combination with maximum probability had been identified as the best size and location of DG. Abd-El-Motaleb and Bekdach (2016) had modeled the load and generation uncertainties with 'autoregressive moving average technique', and employed MCS for the sampling of load and wind speed. Self-Adapted Evolutionary Strategy (SAES) had been adopted for the attainment of optimum capacity of wind-based DG for minimization of cost. El-Saadany and Abdelsalam (2013) contemplated the allocation of both renewable and non-renewable DGs for optimal allocation in DN with harmonics. The optimum sites had been selected based on voltage profile and total harmonic distortion, while GA had been implemented for selection of optimum size.

The renewable generation based DGs had been placed optimally under the uncertainties in load and generation, and OPDG had been attained by point estimation method (PEM) embedded GA (Evangelopoulos and Georgilakis, 2014). The renewable generation based DGs had been optimally allocated considering generation and load uncertainties by MINLP (Atwa *et al.*, 2010; Atwa and El-Saadany, 2011). Abri *et al.* (2013) considered voltage stability margin as a goal for selection of best size and site of DG. The stochastic nature of load and generation had been handled by MINLP for the attainment of best DG size.

The optimal size of DGs based on wind and solar had been attained by a Pattern Search based algorithm for optimization along with MCS (Arabali *et al.*, 2014). The PSO and OO had been combined by Zou *et al.* (2012) for the planning of DN under uncertainties. The OPDG problem under the uncertainty in load had been solved by Artificial Neural Network (Ugranli and Karatepe, 2013). The uncertainties in generation and load were considered in OPDG using a three-step methodology (Carpinelli *et al.*, 2003) involving characterizing the renewable generation with probability; applying GA for optimization and using decision theory to choose the best alternative. NSGA-II was employed to handle multi-objective OPDG in presence of uncertain load (Haghifam *et al.*, 2008).

MCS embedded GA was implemented for allocation of DGs in the presence of uncertain loads (Liu *et al.*, 2011). In addition to load uncertainty, the stochastic nature of generation was also contemplated. The uncertainties in power system had been modeled with PEM for OPDG

(Dehghanian *et al.*, 2013). The optimum locations of DGs had been identified by NSGA-II and fuzzy decision making by optimizing three different objectives simultaneously. A detailed summary of the probabilistic allocation of DGs is presented in Table 2.8.

Table 2.8: Summary of Probabilistic Allocation of DGs

Reference	DG Type	Objective(s)	Technique
Single Objective DG Placement			
Single DG Placement			
Abd-El-Motaleb and Bekdach (2016)	Type-IV	Cost	SAES
Rao and Abhyankar (2014)	Type-I, IV	Loss	MCS embedded GA
Multiple DG Placement			
El-Saadany and Abdelsalam (2013)	Type-I	Annual energy loss	GA
Ugranli and Karatepe (2013)	Type-III	Loss	Neural network
Arabali *et al.* (2014)	Type-I, III	Cost	Pattern search and MCS
Atwa *et al.* (2010); Atwa and El-Saadany (2011)	Renewable DG units	Annual energy loss	MINLP
Abri *et al.* (2013)		Voltage stability margin	MINLP
Zou *et al.* (2012)		Cost	PSO and OO
Evangelopoulos and Georgilakis (2014)			PEM embedded GA
Multi-objective DG Placement			
Multiple DG Placement			
Haghifam *et al.* (2008)	Type-III	Monetary cost Overload in the line segments Under/over-voltage Economic risk	NSGA-II
Carpinelli *et al.* (2003)	Wind and hydro turbine based	Cost of losses Cost of harmonic distortion	GA
Dehghanian *et al.* (2013)	Renewable DG units	Reliability Cost Loss	NSGA-II and PEM
Liu *et al.* (2011)	Renewable DG units	DGs investment cost Operational cost Maintenance cost Loss Capacity adequacy	MCS and GA

2.8 RESEARCH CHALLENGES

After the literature review, the following challenges are identified for the research work :

- **Optimal Siting and Sizing**: The main issue of integration of DGs in a DN is their optimal allocation i.e. to identify optimal location and size. The basis for allocation is to be formulated. Further the effect on these allocations with change in objective needs to be investigated.

- **Selection of Optimization Technique**: The choice of optimization technique is an area of investigation. The optimization technique must be capable of allocating multiple DGs, multi-type DGs and be able to handle both single objective multi-objective optimization. The limiting search space is important for faster convergence and the method must be sensitive to both exploration and exploitation capabilities.

- **Practical Loads**: The load in practical DN can be varying or voltage sensitive due to number of consumers. Further, the uncertain load variation may make the optimal placement complicated. These issues are significant for practical DNs and need to be investigated.

- **Simultaneous Allocation of DG and Capacitor**: The shunt capacitors are usually used for power factor improvement. With the DG and capacitors, the significant improvement in network performance is expected as both real and reactive demands can be served and losses can be minimized. Therefore, the issue of optimal allocation of DG and capacitor simultaneously to optimize various performance parameters in presence of practical load needs to be investigated.

2.9 CONCLUDING REMARKS

A comprehensive review on the allocation techniques of DGs has been presented in this Chapter. The allocation methods ranges from analytical, numerical and meta-heuristic techniques for different types of DGs through both single and multi-objective optimization. The research challenges were also identified to complement the research objectives.

In Chapter 3, the optimal allocation of DG is attempted for minimization of losses. The optimization is realized through classical analytical expressions based approach and PSO. Also, different types of DGs, based on their characteristics, are considered for optimal placement in RDN. The practical nature of the load is also considered by catering the effect of bus voltage on the load.

Chapter–3

Optimal Allocation of DGs for Diminution of Losses

3.1 OVERVIEW

As discussed in Chapter 2, the losses in DNs are one of the major concerns due to their impact on the revenue of utilities. The loss diminution can reduce power flows on distribution feeders, thereby making a positive impact on voltage profiles. The losses in DNs can be diminished with the integration of DGs. In addition to the diminution of losses, DGs are capable of supplying additional load demand and reduce the burden on substations. It has been found from the published literature discussed in Chapter 2 that the integration of DG is advantageous to the system only if it is allocated optimally.

This Chapter presents two techniques for allocation of DGs in RDN. The first technique is based on a classical technique, which includes analytical expressions for the determination of optimum size and a methodology for identification of the optimum site of DGs. The analytical expressions are based on equivalent current injection; derived by utilizing the topological structure of RDNs. The formulation yields optimal allocation of DG without repeatedly computing the load flow. The literature, as summarized in Chapter 2, suggested the analytical expressions based allocation for Type-I and Type-III DGs. The proposed formulation can be used to find the optimal size of all types of DGs, *i.e.*, Type-I, Type-II, Type-III and Type-IV. The second technique utilizes well developed PSO algorithm for finding the optimal size and location of different types of DG. The search space for PSO is reduced with the help of sensitivity factors. The investigations are carried out on 33-bus RDN (Kashem *et al.*, 2000) and 69-bus RDN (Baran and Wu, 1989*a*). The effect of DG placement on reduction in active and reactive power losses

and improvement in the voltage profile of the buses has been investigated. The effect of practical voltage-dependent loads on optimal DG size is also investigated using PSO.

3.2 LOSS FORMULATION

The primary motive of this work is to integrate the DGs in RDN for diminution of losses. The optimum size and location of DG are the main decision variables for the optimization problem. This section presents the objective function, development of analytical expressions for the optimal sizing of DGs and methodology for optimal siting of DGs. This analytical formulation is based on the equivalent current injection method that exploits the topological structure of RDN. The formulation utilizes $BIBC$ and $BCBV$ matrices (Teng, 2003)(Appendix A). The optimum size and site of DGs are determined for minimizing total power loss (P_{loss}). The total power loss is formulated as a function of the power injections based on the equivalent current injection (Gözel and Hocaoglu, 2009). The power loss (P_{loss}) is the objective to be minimized and it is expressed as:

$$P_{loss} = [R]^T \left([BIBC] \left[\frac{P\cos\theta + Q\sin\theta}{|V|} \right] \right)^2 + [R]^T \left([BIBC] \left[\frac{P\sin\theta - Q\cos\theta}{|V|} \right] \right)^2 \quad (3.1)$$

where P_{loss} is active power loss, P active power matrix, Q reactive power matrix,$|V|$ is bus voltage magnitude matrix, θ is bus voltage angle matrix and R is branch resistance matrix.

The equation (3.1) can be re-written into expanded form as:

$$\begin{aligned} P_{loss} = &\sum_{i=1}^{nb} R_i \left(\sum_{j=2}^{n} BIBC_{i,j-1} \left[\frac{P_j\cos\theta_j + Q_j\sin\theta_j}{|V_j|} \right] \right)^2 \\ &+ \sum_{i=1}^{nb} R_i \left(\sum_{j=2}^{n} BIBC_{i,j-1} \left[\frac{P_j\sin\theta_j - Q_j\cos\theta_j}{|V_j|} \right] \right)^2 \end{aligned} \quad (3.2)$$

where n and nb are the number of buses and branches respectively.

The reactive power at j^{th} bus can be expressed in terms of active power as:

$$Q_j = (sign)\tan(\cos^{-1}(pf))P_j = aP_j \quad (3.3)$$

where P_j and Q_j are active and reactive power at j^{th} bus respectively, pf is power factor and $sign$ is $+1$ when reactive power is supplied and -1 when reactive power is absorbed. The equation

(3.2) gets modified by using the relationship of active and reactive power given by equation (3.3) as follows:

$$\begin{aligned} P_{loss} = &\sum_{i=1}^{nb} R_i \left(\sum_{j=2}^{n} BIBC_{i,j-1} \left[\frac{P_j \cos\theta_j + aP_j \sin\theta_j}{|V_j|} \right] \right)^2 \\ &+ \sum_{i=1}^{nb} R_i \left(\sum_{j=2}^{n} BIBC_{i,j-1} \left[\frac{P_j \sin\theta_j - aP_j \cos\theta_j}{|V_j|} \right] \right)^2 \end{aligned} \tag{3.4}$$

3.3 OPTIMAL ALLOCATION OF DG USING ANALYTICAL APPROACH

In this analytical approach, the optimal allocation of different types of DG is decided in two steps by identifying the optimal size of DG at each bus and then identifying the optimal site. These are described in following subsections.

3.3.1 Optimal Sizing of DG

The optimal size of four types of DG at each bus is obtained by expressing the reactive power output of DG (Q_{DG}) in terms of its active power output (P_{DG}) as:

$$Q_{DG} = aP_{DG} \tag{3.5}$$

where, $a = (sign)\tan(\cos^{-1}(pf_{DG}))$

Here pf_{DG} is the power factor of DG, the *sign* value is taken as +1 for Type-III DG and -1 for Type-IV DG. . The optimal power factor of DG for minimum loss is equal to the power factor of load (Hung *et al.*, 2010). It is expressed as:

$$pf_{DG} = pf_D = \frac{\sum_{i=1}^{n} P_{Di}}{\sqrt{\left(\sum_{i=1}^{n} P_{Di}\right)^2 + \left(\sum_{i=1}^{n} Q_{Di}\right)^2}} \tag{3.6}$$

where P_{Di} is active power load demand and Q_{Di} is reactive power load demand at i^{th} bus.

The objective to find the optimum size of DG at a bus can be achieved by considering that the total power loss will be minimum if the partial derivative of total power loss *w.r.t.* injected

real power becomes zero *i.e.* $\partial P_{loss}/\partial P_k = 0$. The power can be injected at any bus except the reference bus. Now differentiating P_{loss} given by equation (3.4) *w.r.t.* injected power at k^{th} bus, $\partial P_{loss}/\partial P_k = 0$ as:

$$\frac{\partial P_{loss}}{\partial P_k} = \sum_{i=1}^{nb} 2R_i \left(\sum_{j=2}^{n} BIBC_{i,j-1} \left[\frac{P_j \cos\theta_j + aP_j \sin\theta_j}{|V_j|} \right] BIBC_{i,k-1} \left[\frac{\cos\theta_k + a\sin\theta_k}{|V_k|} \right] \right) + \sum_{i=1}^{nb} R_i \left(\sum_{j=2}^{n} BIBC_{i,j-1} \left[\frac{P_j \sin\theta_j - aP_j \cos\theta_j}{|V_j|} \right] BIBC_{i,k-1} \left[\frac{\sin\theta_k - a\cos\theta_k}{|V_k|} \right] \right) \quad (3.7)$$

$$\begin{aligned} \frac{\partial P_{loss}}{\partial P_k} &= \sum_{i=1}^{nb} 2R_i \left(\sum_{j=2}^{n} BIBC_{i,j-1} re(I_j) \times BIBC_{i,k-1} \left[\frac{\cos\theta_k + a\sin\theta_k}{|V_k|} \right] \right) \\ &+ \sum_{i=1}^{nb} 2R_i \left(\sum_{j=2}^{n} BIBC_{i,j-1} im(I_j) \times BIBC_{i,k-1} \left[\frac{\sin\theta_k - a\cos\theta_k}{|V_k|} \right] \right) \end{aligned} \quad (3.8)$$

here

$$re(I_j) = \frac{P_j \cos\theta_j + aP_j \sin\theta_j}{|V_j|} \quad (3.9)$$

$$im(I_j) = \frac{P_j \sin\theta_j - aP_j \cos\theta_j}{|V_j|} \quad (3.10)$$

The elements of the $BIBC$ matrix are zero ($BIBC_{j,k-1} = 0$), if the k^{th} bus is not connected the j^{th} branch, and the derivative of the corresponding element is equated to zero ($\partial P_{loss}/\partial P_k = 0$). The derivative of the total power loss *w.r.t.* k^{th} bus injected real power gives the sensitivity factor, which can be expressed as:

$$\frac{\partial P_{loss}}{\partial P_k} = \sum_{i=1}^{nb} 2R_i \sum_{j=2}^{n} dBIBC_{i,j-1} \left(re(I_j) \left[\frac{\cos\theta_k + a\sin\theta_k}{|V_k|} \right] + im(I_j) \left[\frac{\sin\theta_k - a\cos\theta_k}{|V_k|} \right] \right) \quad (3.11)$$

The matrix $dBIBC$ can be obtained by a simple algorithm given by Gözel and Hocaoglu (2009).

Expanding equation (3.11)

$$\begin{aligned} \frac{\partial P_{loss}}{\partial P_k} &= \sum_{i=1}^{nb} 2R_i \sum_{j=2 \neq k}^{n} dBIBC_{i,j-1} \left(re(I_j) \left[\frac{\cos\theta_k + a\sin\theta_k}{|V_k|} \right] + im(I_j) \left[\frac{\sin\theta_k - a\cos\theta_k}{|V_k|} \right] \right) \\ &+ \sum_{i=1}^{nb} 2R_i dBIBC_{i,k-1} \left(re(I_k) \left[\frac{\cos\theta_k + a\sin\theta_k}{|V_k|} \right] + im(I_k) \left[\frac{\sin\theta_k - a\cos\theta_k}{|V_k|} \right] \right) \end{aligned} \quad (3.12)$$

substituting the value of $re(I_k)$ and $im(I_k)$ equation (3.12) becomes:

$$\frac{\partial P_{loss}}{\partial P_k} = \sum_{i=1}^{nb} 2R_i \sum_{j=2j\neq k}^{n} dBIBC_{i,j-1}\left(re(I_j)\left[\frac{\cos\theta_k + a\sin\theta_k}{|V_k|}\right] + im(I_j)\left[\frac{\sin\theta_k - a\cos\theta_k}{|V_k|}\right]\right) + \sum_{i=1}^{nb} 2R_i dBIBC_{i,k-1}\left(\left[\frac{P_k\cos\theta_k + aP_k\sin\theta_k}{|V_k|}\right]\left[\frac{\cos\theta_k + a\sin\theta_k}{|V_k|}\right]\right) + \sum_{i=1}^{nb} 2R_i dBIBC_{i,k-1}\left(\left[\frac{P_k\sin\theta_k - aP_k\cos\theta_k}{|V_k|}\right]\left[\frac{\sin\theta_k - a\cos\theta_k}{|V_k|}\right]\right) \tag{3.13}$$

on solving equation (3.13), it becomes:

$$\frac{\partial P_{loss}}{\partial P_k} = \sum_{i=1}^{nb} 2R_i \sum_{j=2j\neq k}^{n} dBIBC_{i,j-1}\left(re(I_j)\left[\frac{\cos\theta_k + a\sin\theta_k}{|V_k|}\right]\right) + \sum_{i=1}^{nb} 2R_i \sum_{j=2j\neq k}^{n} dBIBC_{i,j-1}\left(im(I_j)\left[\frac{\sin\theta_k - a\cos\theta_k}{|V_k|}\right]\right) + \sum_{i=1}^{nb} 2R_i dBIBC_{i,k-1}\frac{P_k(1+a^2)}{|V_k|^2} \tag{3.14}$$

As $\partial P_{loss}/\partial P_k = 0$; so

$$\sum_{i=1}^{nb} 2R_i \sum_{j=2j\neq k}^{n} dBIBC_{i,j-1}\left(re(I_j)\left[\frac{\cos\theta_k + a\sin\theta_k}{|V_k|}\right] + im(I_j)\left[\frac{\sin\theta_k - a\cos\theta_k}{|V_k|}\right]\right) + \sum_{i=1}^{nb} 2R_i dBIBC_{i,k-1}\frac{P_k(1+a^2)}{|V_k|^2} = 0 \tag{3.15}$$

by solving this equation P_k becomes:

$$P_k = \frac{-|V_k|\sum_{i=1}^{nb} R_i \sum_{j=2j\neq k}^{n} dBIBC_{i,j-1}(re(I_j)(\cos\theta_k + a\sin\theta_k) + im(I_j)(\sin\theta_k - a\cos\theta_k))}{(1+a^2)\sum_{i=1}^{nb} R_i dBIBC_{i,k-1}} \tag{3.16}$$

So, with the consideration of $\partial P_{loss}/\partial P_k = 0$, the optimal size of injected power at k^{th} bus can be expressed as:

$$P_k = \frac{-|V_k|\sum_{i=1}^{nb} R_i \sum_{j=2j\neq k}^{n} dBIBC_{i,j-1}(Re(I_j) + Im(I_j))}{(1+a^2)\sum_{i=1}^{nb} R_i dBIBC_{i,k-1}} \tag{3.17}$$

where,

$$Re(I_j) = (\cos\theta_k + a\sin\theta_k) \cdot re(I_j)$$

$$Im(I_j) = (\sin\theta_k - a\cos\theta_k) \cdot im(I_j)$$

The negative sign in the above equation indicates that P_k should be injected to the system. With this, the optimal size of DG can be obtained as:

$$P_{DGk} = P_k + P_{Dk} \tag{3.18}$$

where P_{DGk} is the active power supplied by DG at k^{th} bus.

Therefore the reactive power can be obtained as:

$$Q_{DGk} = Q_k + Q_{Dk} \tag{3.19}$$

where Q_{DGk} is the reactive power supplied by DG at k^{th} bus.

The optimal power factor depends on type of DG. The optimal size for each type of DG can be obtained as:

1. **Type-I DG:** For Type-I DG, power factor is unity, $a = 0$. Combining equations (3.17) and (3.18) yields P_{DGk} as:

$$P_{DGk} = \frac{-|V_k|\sum_{i=1}^{nb} R_i \sum_{j=2j\neq k}^{n} dBIBC_{i,j-1} I_j}{\sum_{i=1}^{nb} R_i dBIBC_{i,k-1}} + P_{Dk} \tag{3.20}$$

   where

$$I_j = \cos\theta_k re(I_j) + \sin\theta_k im(I_j) \tag{3.21}$$

2. **Type-II DG:** For Type-II DG, power factor is zero and $a = \infty$. Rearranging the equations (3.5) to (3.14) the optimal size of Type-II DG is given as:

$$Q_{DGk} = \frac{-|V_k|\sum_{i=1}^{nb} R_i \sum_{j=2j\neq k}^{n} dBIBC_{i,j-1} I_j}{\sum_{i=1}^{nb} R_i dBIBC_{i,k-1}} + Q_{Dk} \tag{3.22}$$

   where

$$I_j = \sin\theta_k re(I_j) - \cos\theta_k im(I_j) \tag{3.23}$$

3. **Type-III DG:** For Type-III DG, power factor of DG is found by equation (3.6), the *sign* value is taken as $+1$ and the optimal size of DG at bus k is computed using equations (3.17) to (3.19).

4. **Type-IV DG:** For Type-IV DG, power factor of DG is found by equation (3.6)), the *sign* value is taken as -1 and the optimal size of DG at bus k is computed using equations (3.17) to (3.19).

3.3.2 Optimal Siting of DG

The DG of optimal size attained through analytical expressions need to be placed at an optimal location. The DGs of optimal size are placed one by one on each bus and corresponding losses are computed. The bus yielding minimum losses with integration of optimal sized DG is selected as optimal location. To avoid running load flow each time, the losses are calculated approximately by expressing them in terms of bus current injections (Gözel and Hocaoglu, 2009) as:

$$P_{loss} = [R]^T |[BIBC][I]|^2 \tag{3.24}$$

where I is injected current matrix.

This formulation reduces the computational effort and also the accuracy is not compromised as both exact losses, and approximate losses follow the same pattern. After sizing of DG, the bus corresponding to minimum losses is selected as the best location for placement of DG. Finally, the exact losses are computed by running the load flow.

3.3.3 Algorithm for DG Allocation using Analytical Approach

The computational algorithm to attain the optimal size and location of any type of DG among four distinct types of DGs can be summarized as:

Step 1: Read the line and bus data of DN.

Step 2: Formulate the $BIBC$ and $BCBV$ matrices.

Step 3: Carry-out the load flow using $BIBC$ and $BCBV$ matrices.

Step 4: Find the optimal size of DG for each bus except reference bus as discussed in section 3.3.1 while choosing the suitable value of a as per DG type.

Step 5: Calculate power losses using equation (3.24) by placing DG of optimal size at each bus.

Step 6: Choose the bus corresponding to minimum losses as best location.

Step 7: Run the load flow to calculate exact losses by placing optimal sized DG at the optimal location.

3.4 OPTIMAL ALLOCATION OF DG USING PSO

The optimum size and site of DG are also obtained by PSO for diminishing the losses in RDNs. The choice of self-adaptive PSO algorithm is due to its good exploration and exploitation characteristics and proven ability for handling combinatorial optimization problems. The PSO is briefly reviewed herewith. The effort to limit the search space for optimal allocation is presented before summarizing the optimal allocation of DG using PSO.

3.4.1 Particle Swarm Optimization Algorithm

Kennedy and Eberhart (1995) have broached an algorithm inspired by nature, based on the flocking behavior of birds in 1995, which is known as PSO. When birds are flying in flock, each bird adjust its position and velocity; using own and other birds flying experience in the flock. PSO is a population-based search and optimization procedure in which individuals (each possible solution) called particles change their position (state) with time in *N*-dimensional search space. The particles move through the search space to keep itself in the best position(*'pbest'*). The particles know the best position searched by the group particles (*i.e*) *'gbest'*. The particles change their position with the help of their current positions, their *'pbest'* and *'gbest'* and modify their velocity and position with a motivation to minimize the distance between their own best (*'pbest'*) and group best (*'pbest'*) with time.

Mathematically, in PSO the *N*-dimensional position vector (X_p) and velocity vector (V_p) are represented as:

$$X_p = (x_1, x_2, x_3, ...x_N) \tag{3.25}$$

$$V_p = (v_1, v_2, v_3, ...v_N) \tag{3.26}$$

Each particle attempts to change its velocity based on the following:

- the current position (x_i)
- the current velocity (v_i)
- the distance between current position and its own best *i.e.* ($pbest_i - x_i$)
- the distance between current position and its group best *i.e.* ($gbest_i - x_i$)

The updated velocity is given as:

$$v_i^{k+1} = w_{iner} v_i^k + c_1 r_1 (pbest_i^k - x_i^k) + c_2 r_2 (gbest_i^k - x_i^k) \tag{3.27}$$

where, c_1 and c_2 are acceleration constants; r_1 and r_2 are random numbers between 0 and 1; x_i^k and v_i^k are current position and velocity of i^{th} particle respectively; v_i^{k+1} is the modified velocity of i^{th} particle; w_{iner} is the inertia weight for velocity for i^{th} particle. This inertia weight is updated in each iteration as:

$$w_{iner} = w_{max} - \frac{w_{max} - w_{min}}{Iter_{max}} Iter \tag{3.28}$$

where, w_{max} and w_{min} are maximum and minimum inertia weights respectively, $Iter$ and $Iter_{max}$ are current iteration count and maximum iteration count, respectively.

This changing inertia weight results in self adaptive nature of PSO. The value of w_{iner} is maximum for first iteration and decreases with increase in iteration count. The maximum value of w_{iner} at the starting of iterative process results in the global search in search space. This feature of PSO is termed as *exploration*. As the iterative process proceeds, w_{iner} decreases and hence exploiting the reduced search space. This feature of PSO is termed as *exploitation*.

After velocity modification, the position of particles is modified by the following equation:

$$x_i^{k+1} = x_i^k + v_i^{k+1} \tag{3.29}$$

where x_i^k and x_i^{k+1} are current and modified positions of i^{th} particle respectively.

3.4.2 Search Space and Limits on DG

The loss sensitivity factors (LSF), expressed by equation (3.7) is used to find the potential buses for the placement of DGs. These are taken as 30% of the total buses and thus limiting the search space. Such identified potential buses although reduces the search space but always yields optimal solution and thereby does not compromise on the quality of the solution. The potential buses are identified using real power loss sensitivity to real power injection *i.e.* $\partial P_{loss}/\partial P_k = 0$ for all the buses and then selecting the potential buses on the basis of decreasing values of LSF. As an example, a 33-bus RDN consists of one reference bus and 32 buses where DG can be placed. The identification of potential buses reduces to the buses to 30% (10) where DG placement is investigated. The dimension of search space is reduced from 32 to only 10 in identifying the optimal location and size of DG. In this sense, the search space is reduced.

The upper generation limit of DG capped on the basis of DG size obtained from analytical expressions as described in section 3.3.1. The limits on DG size are expressed as:

$$0 \leq P_{DG} \leq P_{DG}^{max} \tag{3.30}$$

where, P_{DG}^{max} is the 1.5 times the DG size obtained through analytical expressions.

3.4.3 Algorithm for DG Allocation using PSO

The PSO described in section 3.4.1 has been implemented by following steps for optimal placement of DG to diminish the losses.

Step 1: Read the line and bus data of DN.

Step 2: Formulate the $BIBC$ and $BCBV$ matrices.

Step 3: Carry-out the base case load flow using $BIBC$ and $BCBV$.

Step 4: Calculate the power loss to real power injection sensitivity factors $\partial P_{loss}/\partial P_k$ using equation (3.7) for all buses and identify the potential buses for DG placement.

Step 5: Initialize the particles positions that are random DGs at random buses in the search space and set the iteration counter $k = 0$.

Step 6: For these positions, compute power loss P_{loss} and assign them as individual best positions *pbest*. Also, identify the best of the *pbest* as global best *gbest*.

Step 7: Update the particles positions by accounting their current positions, *pbest* and *gbest* and increase iterations as $k = k + 1$.

Step 8: Compute the power loss for current positions and update the particles individual best *pbest* and global best *gbest*.

Step 9: Go to step 7 until the convergence is achieved.

3.5 RESULTS AND DISCUSSIONS

The optimal site and size of DG are found to diminish active power losses by two presented approaches. The effectiveness of two proposed approaches is validated on two RDNs by optimal integration of DG. The analysis is carried out on 33-bus RDN (Kashem *et al.*, 2000) and 69-bus RDN (Baran and Wu, 1989*a*), having a total load of $3.715 + j2.300$ MVA and $3.803 + j2.694$ MVA respectively. The algorithms that have been described in section 3.3.3 and 3.4.3 are implemented under MATLAB, R2014b in MAC environment. The PSO algorithm has been executed for 100 iterations considering the swarm size as 50. The acceleration constants c_1 and c_2 are taken as 2 and 2 respectively. The maximum and minimum limits of inertia weight are considered as 0.9 and 0.4, respectively. The PSO is executed 10 times and the best results are presented.

3.5.1 DG Placement for 33-Bus RDN

The 33-bus RDN comprises 32 branches with detailed test data given as Table B.1 in Appendix B. This RDN results in active power loss of 210.988 kW and reactive power loss of 143.128 kVAr for constant load model for base case *i.e.* before the integration of DG. The summary of active and reactive power losses for all practical loads is also presented in Table 3.1. The losses for practical residential, commercial, industrial load are less due to different exponents np and nq. Due to these exponents the total load on the network is lower than the base case load. Among

all, the losses are minimum for commercial load because the net load experienced by network is also minimum.

Table 3.1: 33-Bus RDN Before Integration of DG

Load Model	Effective Load (MVA)	Active Power Loss (kW)	Reactive Power Loss (kVAr)
Constant	3.715+j2.300	210.988	143.128
Commercial	3.466+j1.940	159.501	107.708
Residential	3.559+j1.875	164.541	111.237
Industrial	3.684+j1.705	167.792	113.616

The optimal size of different types of DGs for 33-bus RDN is attained using the analytical method described in section 3.3.3 and PSO based algorithm described in section 3.4.3 to attain the optimum size and site of four types of DG. The summary of DG size and site for all types of DGs for constant base load model is presented in Table 3.2 along with the effect of DG integration on active and reactive power loss reduction. The exact losses are obtained by load flow after the integration of DGs with optimal size at the respective optimum location. In addition to loss diminution, the integration of DG has added the advantage of enhancement in the voltage profile of the DN. The Figure 3.1 shows the effect of optimal DG allocation on the voltage level of all buses for different types of DGs.

The optimum site for **Type-I DG** allocation is bus 6 attained by both analytical and PSO approaches; however, the size is different. The optimal size yielded by analytical and PSO is 2.4908 MW and 2.5919 MW, respectively. This optimal allocation is attained for the target of diminution of active power losses. It is inferred from the results that PSO outperforms the analytical approach as the active power loss reduction through PSO (47.381%) is higher as compared to the loss reduction obtained through analytical method (47.317%). The enhancement in the voltage level of all buses with Type-I DG integration is depicted by Figure 3.1 (a). It is observed that there is a significant improvement in the voltage level of all buses with the integration of optimal sized DG at optimal location attained by two approaches, but the size of Type-I DG calculated by the developed PSO based optimization is more effective in improving the voltage profile of the system buses.

The optimum allocation of **Type-II DG** by both analytical and PSO approaches also resulted in different size but the same location, *i.e.*, bus 30. The optimal size yielded by PSO

Table 3.2: Optimal DG Placement for 33-Bus RDN

DG Type	Approach	DG Size	DG Site (Bus)	Active Power Loss (kW)	% Active Power Loss Reduction	Reactive Power Loss (kVAr)	% Reactive Power Loss Reduction
Type-I	Analytical	2.4908 MW	6	111.156	47.317	81.694	42.922
	PSO	2.5919 MW	6	111.019	47.381	81.719	42.905
Type-II	Analytical	1.2298 MVAr	30	151.393	28.245	103.855	27.439
	PSO	1.2594 MVAr	30	151.365	28.259	103.893	27.413
Type-III	Analytical	3.0239 MVA @ 0.85 pf	6	68.310	67.624	55.059	61.532
	PSO	3.1029 MVA @ 0.85 pf	6	68.158	67.700	55.055	61.534
Type-IV	Analytical	0.8619 MVA @ 0.85 pf	30	114.089	45.926	79.211	44.657
	PSO	0.8679 MVA @ 0.85 pf	30	113.653	46.133	78.931	44.853

is slightly large as compared to the size yielded by the analytical approach. The optimization attained by PSO is found effective in loss reduction and improving the voltage profile of the system buses as shown in Figure 3.1 (b). With the optimal size of Type-II DG, the active power loss reduction of 28.259% is achieved using PSO while it is 28.245% with analytical method. In comparison to Type-I DG, Type-II DG is less effective for both loss diminution and voltage enhancement.

Type-III DG is operating at 0.85 lagging *pf* identified by the connected load. The optimal allocation of Type-III DG by both approaches also resulted in the same location and different size. The PSO is outperforming the analytical approach based on both loss diminution and voltage improvement. The active power loss reduction is 67.700% and 67.624% obtained by PSO and analytical approach, respectively. The improvement in voltage after the integration of

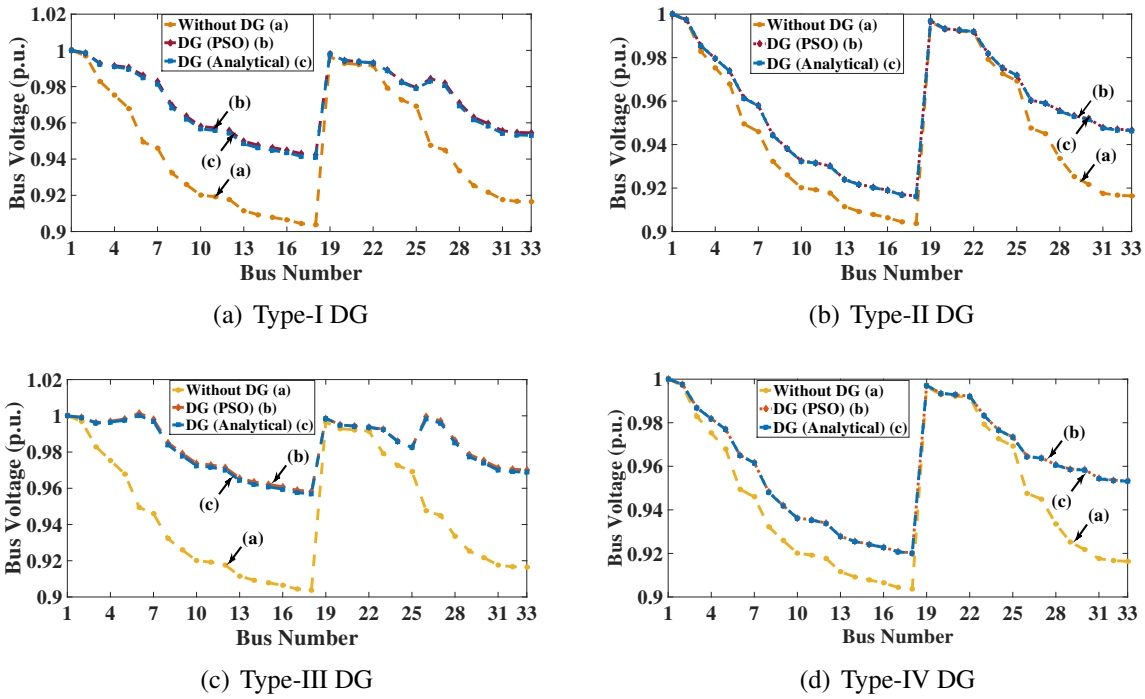

(a) Type-I DG (b) Type-II DG

(c) Type-III DG (d) Type-IV DG

Fig. 3.1: Enhancement in Voltage of 33-Bus RDN with Integration of DG

Type-III DG is depicted in Figure 3.1 (c). As compared to Type-I and Type-II DGs, Type-III DG is resulting in maximum loss reduction and voltage enhancement.

Type-IV DG is also operating at 0.85 *pf* identified by the connected load, but it is leading. The location of Type-IV DG is the same as that of Type-II DG. The size of DG is 0.8619 MVA and 0.8679 MVA, yielded by analytical and PSO approach, respectively and correspondingly resulting in 45.916% and 46.133% active power loss reduction. As compared to Type-I DG, the reduction in active power loss is less, but the reduction in reactive power loss is more. Figure 3.1 (d) represents the effect of Type-IV DG placement on the voltage level of all buses.

It is found that the Type-III DG outperforms other types of DGs as far as loss reduction is concerned. Also, the size of DGs attained by the PSO algorithm is resulting in better performance. The comparison of voltage profile improvement with the incorporation of four types of DGs individually with size yielded by PSO is presented in Figure 3.2. Although there is a significant improvement in voltage profile with the placement of all types of DGs, but Type-III is best followed by Type-I and Type-IV. Type-II DG results in the least improvement in the voltage level of all buses. As Type-III DG is resulting in the best performance among all types of DGs, the placement of Type-III DG is considered for different practical loads.

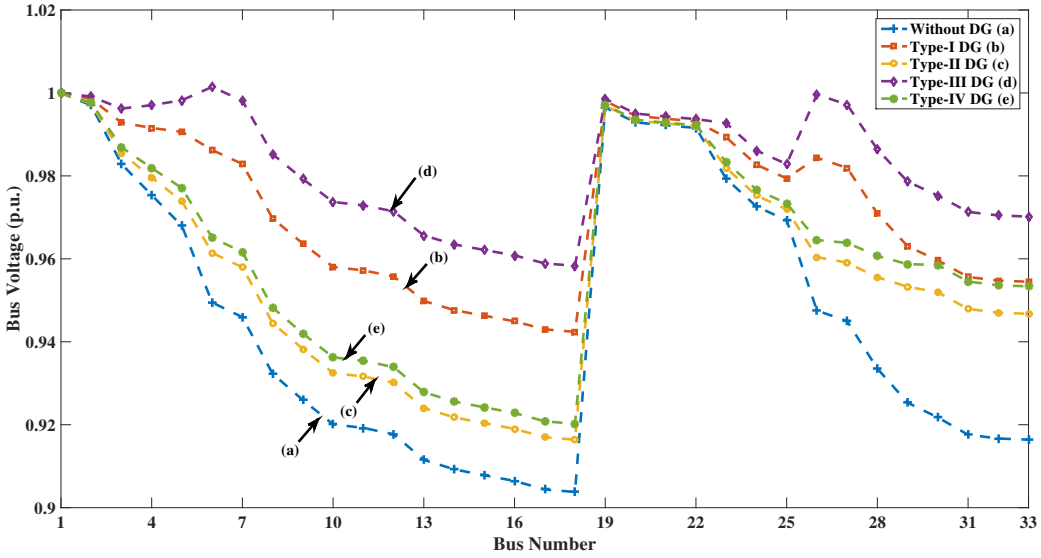

Fig. 3.2: Effect of Different Types of DG on Voltage Profile of 33-Bus RDN

Table 3.3: Effect of Load Models on Optimal Placement of Type-III DG for 33-Bus RDN

Load Model	**DG Size (MVA @ pf)**	**DG Site (Bus)**	**Active Power Loss (kW)**	**% Active Power Loss Reduction**	**Reactive Power Loss (kVAr)**	**% Reactive Power Loss Reduction**
Constant	3.1029 @ 0.85	6	68.158	67.700	55.055	61.534
Commercial	2.9043 @ 0.87	6	61.559	61.406	49.622	53.929
Residential	2.8246 @ 0.89	6	62.368	62.096	50.134	54.930
Industrial	2.8424 @ 0.91	6	62.908	62.508	50.577	55.485

Effect of Load Model on Type-III DG Placement

The load models affect the total connected load to RDN and hence on the optimal size, *pf* and location of DGs. The optimal size and location of DG are identified by the PSO algorithm described in section 3.4.3 as it is found that, PSO outperforms analytical approach. Table 3.3 presents the summary of optimal size and effect of Type-III DG integration on active and reactive power losses for different load models. The optimal location of Type-III DG is independent of load model, while the optimal size and *pf* are governed by load model. The operating *pf*

is minimum for constant load and maximum for the industrial load. The size of DG is largest for the constant load as the connected load is maximum in comparison to other load models; hence resulting in maximum loss reduction. The variation of voltage for different load models before and after placement of Type-III DG is shown in Figure 3.3 (a), (b) and (c) for commercial, residential and industrial loads respectively.

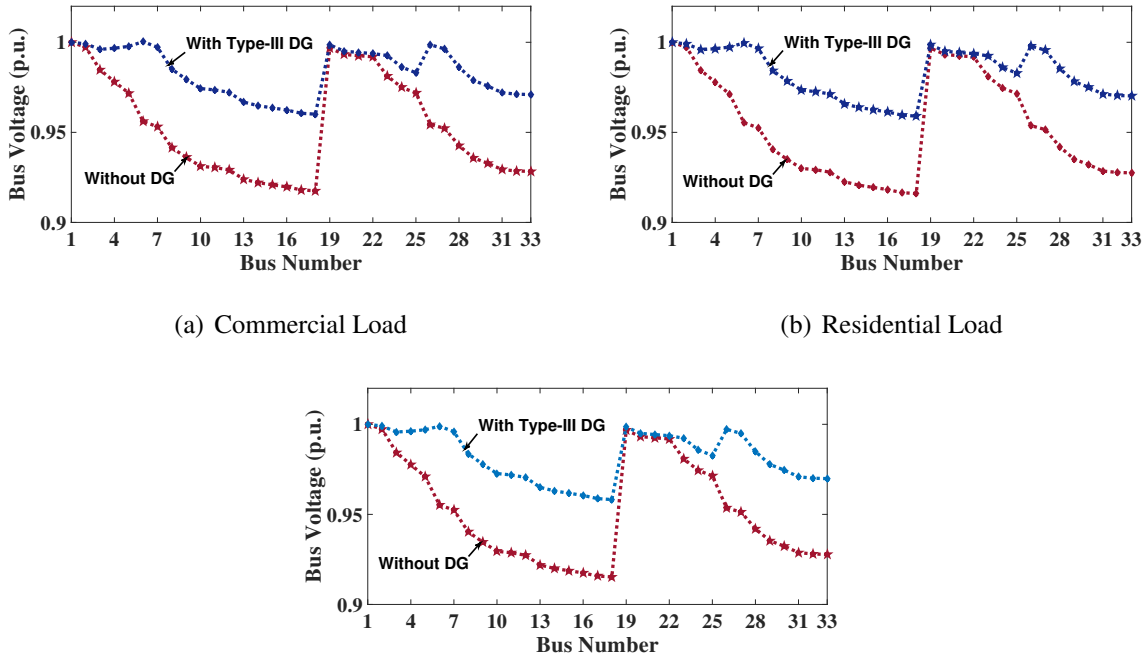

(a) Commercial Load

(b) Residential Load

(c) Industrial Load

Fig. 3.3: Variation of Bus Voltage of 33-Bus RDN for Load Models Before and After Integration of Type-III DG

3.5.2 DG Placement for 69-Bus RDN

The 69-bus RDN comprises 68 branches with detailed test data given as Table B.2 in Appendix B. For constant load model before the integration of DG, this RDN has an active power loss of 225.005 kW and reactive power loss of 102.173 kVAr. The active and reactive power losses for all practical load models are summarized in Table 3.4. The performance for 69-bus RDN is similar to that obtained for 33-bus RDN. The minimum losses are resulted for commercial load due to net reduction in the load experienced by the network. As explained, the optimal DG allocation of all types has been carried out through analytical approach and PSO based algorithm.

Correspondingly, Table 3.5 summarizes the DG size and site for constant load model along with the effect of DG integration on active and reactive power loss reduction. The additional benefit of enhancement in the voltage profile of the DN with the integration of DG is shown in Figure 3.4 for different types of DGs.

Table 3.4: 69-Bus RDN Before Integration of DG

Load Model	**Effective Load (MVA)**	**Active Power Loss (kW)**	**Reactive Power Loss (kVAr)**
Constant	3.803+j2.694	225.005	102.173
Commercial	3.568+j2.340	165.050	76.417
Residential	3.654+j2.274	170.834	78.896
Industrial	3.773+j2.099	175.104	80.687

Table 3.5: Optimal DG Placement for 69-Bus RDN

DG Type	**Approach**	**DG Size**	**DG Site (Bus)**	**Active Power Loss (kW)**	**% Active Power Loss Reduction**	**Reactive Power Loss (kVAr)**	**% Reactive Power Loss Reduction**
Type-I	Analytical	1.8082 MW	61	83.316	62.972	40.669	60.196
	PSO	1.8729 MW	61	83.168	63.037	40.510	60.352
Type-II	Analytical	1.2918 MVAr	61	152.118	32.393	70.582	30.919
	PSO	1.3317 MVAr	61	152.061	32.412	70.516	30.984
Type-III	Analytical	2.2223 MVA @ 0.82 pf	61	23.161	89.707	14.411	85.895
	PSO	2.2244 MVA @ 0.82 pf	61	23.146	89.714	14.366	85.939
Type-IV	Analytical	1.6173 MVA @ 0.82 pf	61	36.892	83.604	21.199	79.252
	PSO	1.6973 MVA @ 0.82 pf	61	34.075	84.856	19.890	80.533

Type-I DG allocation by analytical and PSO approach results in the same optimal site i.e. bus 61 and different optimal size. The optimal size is obtained as 1.8082 MW and 1.8729 MW respectively through analytical approach and PSO, which yields the active power loss

reduction of 62.97% and 63.037% correspondingly. Similar to 33-bus RDN, PSO outperforms the analytical approach in deciding the optimum size of Type-I DG for the active power loss reduction. The improvement in the voltage level of all buses with Type-I DG integration is depicted in Figure 3.4 (a). As evident from Figure 3.4 (a), the voltage with the integration of optimized DG is higher than the voltage yielded by the integration of DG calculated through the analytical method for all the buses.

The optimum allocation of **Type-II DG** by both analytical and PSO approaches also resulted in the same optimal location, *i.e.* bus 61 and different optimal size. The optimal size yielded by PSO and analytical approach is 1.3317 MVAr and 1.2918 MVAr, respectively. Figure 3.4 (b) shows the effect of Type-II DG integration on the voltage level of all buses. The active power loss reduction and improvement in the voltage profile of the system attained by PSO are more effective as compared to the analytical approach. The active power loss reduction of 32.412% is achieved using PSO, and 32.393% from the analytical method. As in the case of 33-bus RDN, Type-II DG is less effective in loss diminution and voltage enhancement as compared to Type-I DG.

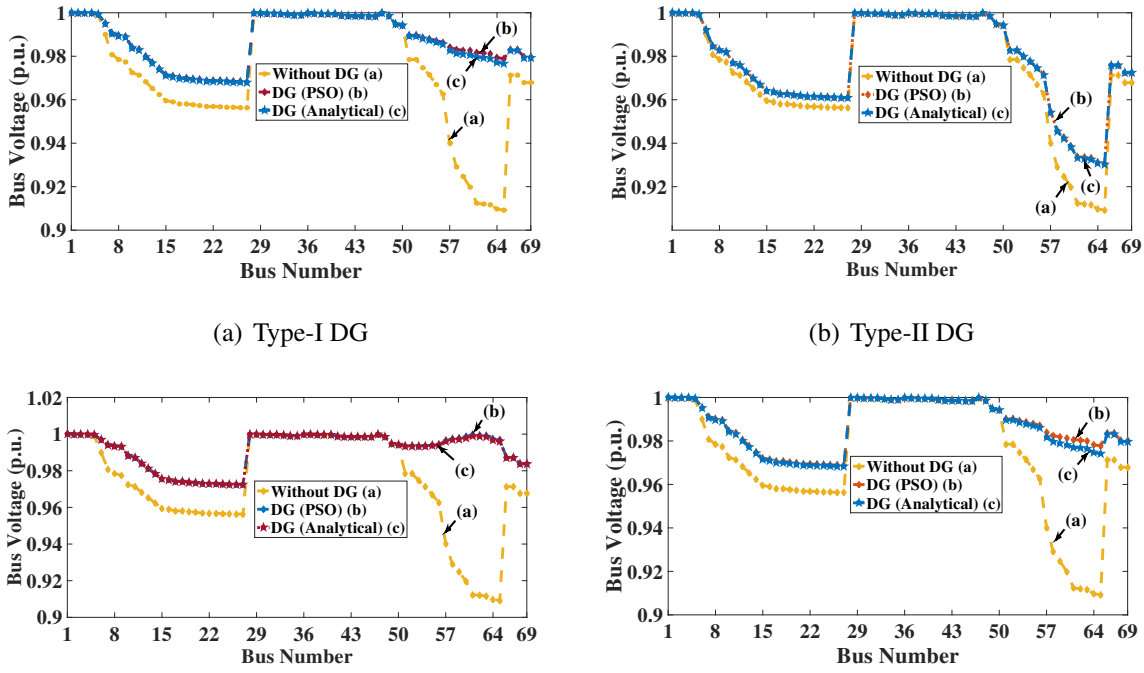

(a) Type-I DG

(b) Type-II DG

(c) Type-III DG

(d) Type-IV DG

Fig. 3.4: Enhancement in Voltage of 69-Bus RDN with Integration of DG

The operating *pf* of **Type-III DG** is identified as 0.82 lagging by the connected load. Similar to optimal placement of Type-I and Type-II DG, the optimal location of Type-III DG by both approaches is same *i.e.*, bus 61 but having different optimal sizes. The PSO is outperforming the analytical approach based on both active power loss diminution and voltage improvement. The active power loss reduction is 89.714% and 89.707% obtained by PSO and analytical approach, respectively. The enhancement in voltage after integration of Type-III DG is depicted in Figure 3.4 (c). Similar to 33-bus RDN, Type-III DG is resulting in maximum loss reduction and voltage enhancement as compared to Type-I and Type-II DGs.

Type-IV DG is operated at leading 0.82 *pf* determined by the connected load. The resulted optimal size of DG is 1.6173 MVA and 1.6973 MVA by analytical approach and PSO respectively and corresponding active power loss reduction is 83.604% and 84.856%. The optimal site of DG identified by both approaches is bus 61. Figure 3.4 (d) represents the effect of Type-IV DG placement on the voltage level of all buses.

Similar to 33-bus RDN, it is inferred from results, that Type-III DG outperforms other types of DGs for loss minimization. Also, PSO outperforms the analytical approach for all types of DGs, as the size of DGs attained by the PSO algorithm is resulting in better performance. Figure 3.5 depicts the comparison of voltage profile improvement with the incorporation of different DGs types of optimal size achieved by PSO. As evident from Figure 3.5 the performance of Type-III DG is best followed by Type-I, Type-IV and Type-II DG.

Effect of Load Model on Type-III DG Placement

The placement of Type-III DG is investigated through PSO for other voltage-dependent practical loads as maximum loss reduction is achieved using it previously. The optimal size, *pf*, and location of DG are affected by the load models as the total connected load to RDN. The summary of optimal size and effect of DG integration on active and reactive power losses for different load models is presented in Table 3.6. The optimal size and *pf* are affected by load model. However, the optimal location of DG for all practical loads is same. The operating *pf* is minimum for constant load and maximum for the industrial load. The size of DG is most substantial for the constant load as the connected load is maximum in comparison to other load models. The

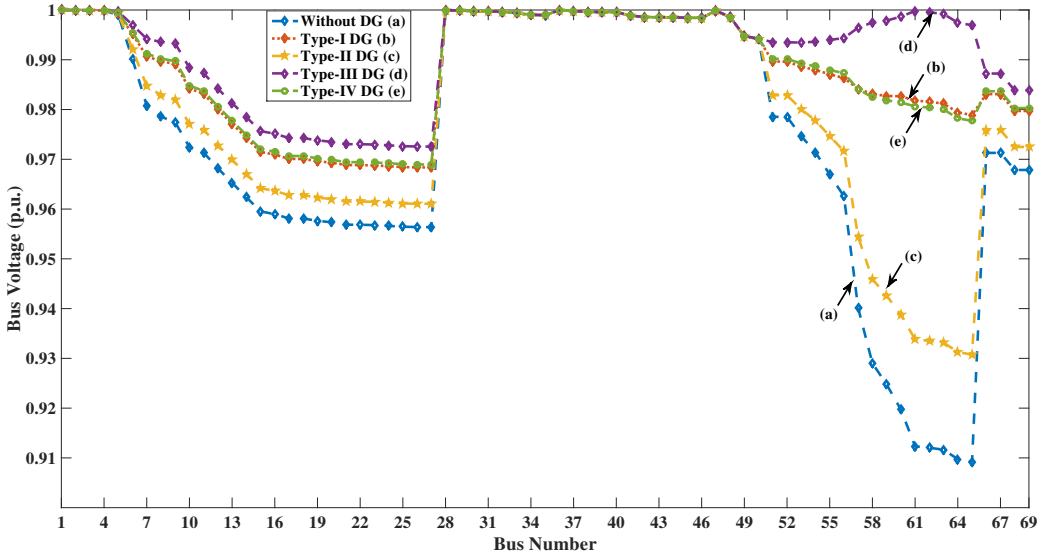

Fig. 3.5: Effect of Different Types of DG on Voltage Profile of 69-Bus RDN

variation of voltage before and after placement of Type-III DG is shown in Figure 3.6 (a), (b) and (c) for commercial, residential, and industrial loads respectively.

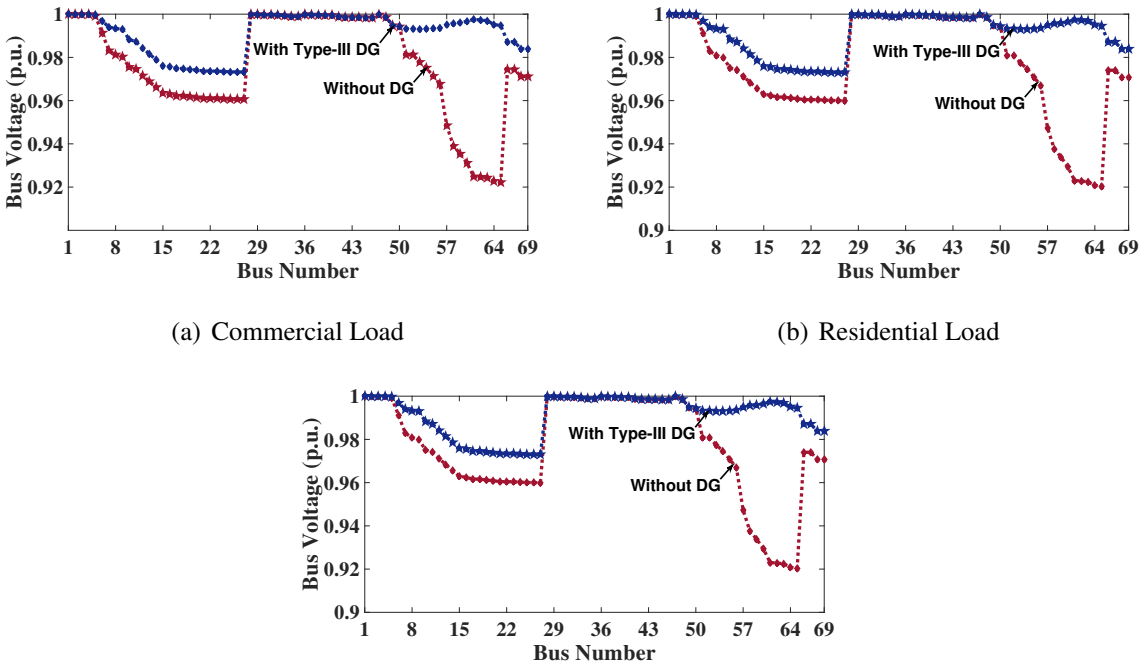

(a) Commercial Load

(b) Residential Load

(c) Industrial Load

Fig. 3.6: Variation of Bus Voltage of 69-Bus RDN for Load Models Before and After Integration of Type-III DG

Table 3.6: Effect of Load Models on Optimal Placement of Type-III DG for 69-Bus RDN

Load Model	**DG Size (MVA @ pf)**	**DG Site (Bus)**	**Active Power Loss (kW)**	**% Active Power Loss Reduction**	**Reactive Power Loss (kVAr)**	**% Reactive Power Loss Reduction**
Constant	2.2244 @ 0.82	61	23.146	89.714	14.366	85.939
Commercial	2.1486 @ 0.84	61	21.829	86.774	13.881	81.836
Residential	2.1378 @ 0.85	61	22.370	86.906	14.131	82.089
Industrial	2.1541@ 0.87	61	23.486	86.588	14.564	81.950

3.5.3 Comparative Results

The robustness of the proposed approaches is tested on two test systems, *i.e.*, 33-bus and 69-bus RDNs. The comparison of presented DG allocation results, with already reported work in the literature for 69-bus RDN is summarized in Tables 3.7, 3.8 and 3.9 for Type-I, Type-II and Type-III DGs respectively. The optimal size and site of Type-I DG have been found in the literature using analytical approach (Acharya *et al.*, 2006; Gözel and Hocaoglu, 2009), GA (Shukla *et al.*, 2010), PSO (Kansal *et al.*, 2013), and ABC (Abu-Mouti and El-Hawary, 2011) algorithms for diminution of losses, while Type-II is considered only by Kansal *et al.* (2013) and Type-III DG is considered by Hung *et al.* (2010) and Kansal *et al.* (2013).

Table 3.7: Comparison of Type-I DG Results

Approach	**Site**	**Size (MW)**	**% Active Power Loss Reduction**
Analytical (Acharya *et al.*, 2006)	61	1.8078	62.860
Analytical (Gözel and Hocaoglu, 2009)	61	1.8078	59.093
GA (Shukla *et al.*, 2010)	61	1.8100	62.950
PSO (Kansal *et al.*, 2013)	61	1.8078	62.950
ABC (Abu-Mouti and El-Hawary, 2011)	61	1.9000	62.970
Proposed Analytical	61	1.8082	62.972
Proposed PSO	61	1.8729	63.037

Table 3.8: Comparison of Type-II DG Results

Approach	Site	Size (MVAr)	% Active Power Loss Reduction
PSO (Kansal *et al.*, 2013)	61	1.2900	32.400
Proposed Analytical	61	1.2918	32.393
Proposed PSO	61	1.3317	32.412

Table 3.9: Comparison of Type-III DG Results

Approach	Site	Size (MVA @ pf)	% Active Power Loss Reduction
Analytical (Hung *et al.*, 2010)	61	2.2219 @ 0.82	89.684
PSO (Kansal *et al.*, 2013)	61	2.2430 @ 0.82	89.690
Proposed Analytical	61	2.2223 @ 0.82	89.707
Proposed PSO	61	2.2244 @ 0.82	89.714

The proposed formulation yields better results for loss minimization with Type-I and Type-III DG and it is comparable with optimal placement of Type-II DG.

3.6 CONCLUDING REMARKS

In this Chapter, two different approaches based on analytical expressions and PSO are presented for the determination of the optimal site and size of DG to diminish the active power losses for constant power and voltage-dependent practical loads. The search space for PSO is limited by sensitivity factors. The effectiveness of the proposed methodologies is tested on 33-bus and 69-bus RDNs. The commercial load model results into minimum losses because minimum load is experienced by the DN with its formulation. It is observed that PSO has better performance as compared to the analytical approach. Based on the characteristics of DGs, four different types of DGs are considered for optimal placement. Further, the optimal allocation of Type-I, Type-II, Type- III and Type-IV DG results in improved voltage profile and reduced losses; however, the Type-III DG is most effective in achieving the loss reduction as well as the voltage profile improvement. The effect of load models is also considered on Type- III DGs and it is found that the load models affects the optimal size of DGs. The formulation outperforms even the reported results for all types of DG allocation.

In this Chapter-3, the optimal allocation of DGs has been obtained for minimization of active power losses only. As reactive power losses, voltage deviation and economy are also major decision factors. In Chapter 4, the optimal allocation of DG is investigated through multi-objective perspective for the placement of single and multiple Type-I and Type-III DGs.

Chapter–4

Multi-Objective Optimal Allocation of DGs

4.1 OVERVIEW

This Chapter presents a multi-objective approach for placement of DGs in RDNs. The DG placement for active power loss minimization is presented in Chapter 3. In addition to active power losses, the reactive power losses are also significant in RDNs. Therfore, reactive power loss minimization is considered along with active power losses minimization. The voltage level of all buses falls due to heavy loads, and it increases real power losses. Thus, minimization of voltage deviation is also contemplated as objective for the optimization problem. Another objective considered for DG allocation is the overall economy of the system, as the integration of DG has an impact on the economy of the system.

In this Chapter the optimal allocation of Type-I and Type-III DG is determined using both single objective and multi-objective optimization. The multi-objective optimization, accounting conflicting objectives, is realized by forming a membership based MOF using fuzzy decision approach. This non-Pareto MOF is optimized through PSO to find the optimal size and site of single as well as multiple DGs for voltage-dependent residential, commercial and industrial loads. The search space for placement of multiple DGs is reduced by formulating different clusters of buses based on base case load flow. The true Pareto based multi-objective optimization is also carried out for minimization of active power loss and voltage deviation. The conventional PSO algorithm is modified using the concept of non-dominace to yield Pareto front and best compromised solution is selected by fuzzy decision making. The effectiveness of the optimal DG allocation is tested on 69-bus RDN.

4.2 MULTI-OBJECTIVE OPTIMIZATION

In optimization when two or more objectives are to be optimized simultaneously, it is termed as *multi-objective optimization*. A general multi-objective problem can be formulated mathematically by equation (1.2) and concept of Pareto front has been discussed in section 1.4. The multi-objective problem can be solved by four different methods:

- **Weighted Sum Method:** In this method, the multi-objective problem is changed to the single objective problem by assignment of weights to different objectives. The objective function is weighted sum of the individual objectives. The weights are assigned by the decision maker as per the priority of objectives, and combine the multiple objectives to form a single objective.

  Mathematically it is expressed as:

$$\begin{cases} min\left(\sum_{i=1}^{n} w_i f_i(\mathbf{X})\right) \\ \mathbf{X} \in \mathbf{S} \\ \mathbf{h(X)} = \mathbf{0} \\ \mathbf{C(X)} \leq \mathbf{0} \end{cases} \tag{4.1}$$

  where w_i is the weight assigned to i^{th} objective.

  This method has the advantage of simplification of a problem, but the major drawback of this method is that the weight assignment is dependent on the priority of decision maker.

- **ϵ-constrained Method:** In this method, one objective is contemplated as an objective for optimization while the other objectives are contemplated as constraints. The primary objective acts as master objective while others act as slaves.

  In this technique, if k^{th} objective is selected as master objective and others as constraints, then it represented mathematically as:

$$\begin{cases} min f_k(\mathbf{X}) \\ \mathbf{X} \in \mathbf{S} \\ \mathbf{h(X)=0} \\ \mathbf{C(X)} \leq \mathbf{0} \\ f_i(\mathbf{X}) \leq \epsilon_i \quad \text{i=1.....n and } i \neq k \end{cases} \tag{4.2}$$

where ϵ_i is the maximum limit for i^{th} objective, which can be obtained from the initial non-inferior value of i^{th} objective and the trade-off between the conflicting objectives is decided by the decision maker. In this method also, the trade-off chosen by decision maker has a significant impact on the final solution of the optimization problem.

- **Direct Non-Pareto Solution Approach:** This methodology is also termed as *Max-Min Approach*. In this method, the normalized membership is computed for each objective, and fuzzy max-min decomposition is employed to calculate the membership to be optimized. The normalized membership for i^{th} objective function and k^{th} non-dominated solution is computed as:

$$\mu_j^k = \begin{cases} 1, & \text{for } f_i \leq f_i^{min} \\ \dfrac{f_i^{max} - f_i^k}{f_i^{max} - f_i^{min}}, & \text{for } f_i^{min} < f_i < f_i^{max} \\ 0, & \text{for } f_i \geq f_i^{max} \end{cases} \tag{4.3}$$

If n is total number of objectives considered for the multi-objective problem, then membership to be optimized using max-min decomposition is calculated as:

$$\mu^k = max[min(\mu_1^k, \mu_2^k, ...\mu_n^k)] \tag{4.4}$$

The procedure of single objective optimization is utilized further to optimize μ^k.

- **True Pareto Front Approach:** In this approach, the Pareto front as shown in Figure 1.5 is obtained as solution of multi-objective problem. The concept of non-domination is utilized to get optimal Pareto front in which each solution is equally good solution. The best-compromised solution is selected from non-dominating solutions of the Pareto front by high-level fuzzy decision making. In this approach, the normalized membership function (β) is calculated, which indicate the fuzzy cardinal priority rank of the Pareto

optimal solution. For k^{th} non-dominated solution, it is computed as:

$$\beta_k = \frac{\sum_{i=1}^{n} \mu_i^k}{\sum_{i=1}^{n}\sum_{k=1}^{m} \mu_i^k} \tag{4.5}$$

where

$$\mu_i^k = \frac{f_i^{max} - f_i^k}{f_i^{max} - f_i^{min}}$$

The solution with maximum β_k is the selected as best compromised solution for the multi-objective problem.

In this chapter, the multi-objective optimization is investigated through both non-pareto and Pareto based approaches. The computational burden is more for True Pareto based approach because of applying non-dominance concept and thus slow convergence to Pareto optimal front. The time complexity, for a problem with m objectives and N population size, is $O(mN^2)$ in Pareto based approach, which is otherwise $O(N^2)$ in non-pareto approach (Li *et al.*, 2016).

4.3 OBJECTIVES FOR DG PLACEMENTS

The placement of DGs in RDNs affects active power losses, reactive power losses, voltage profile of buses and economy. If DG of appropriate size is placed at an optimum site, then the losses will decrease, and voltage profile of the buses and economy gets improved. The optimal allocation of DGs is attempted for the minimization of active and reactive power loss, voltage deviation and improvement of the overall economy. These objectives are considered individually as well as simultaneously resulting in the single objective and multi-objective problem. As the nature of these objectives is different from each other, so these are normalized as indices to formulate a multi-objective optimization problem. These indices are active power loss index (PLI), reactive power loss index (QLI), voltage deviation index (VDI) and overall economy index (OEI). The indices PLI, QLI, VDI and OEI are contemplated as objectives for DG placement. The values of indices before integration of DG is unity, and it is desired to reduce the value of these indices by placement of optimal sized DG at the optimal site. These indices are formulated as:

Active Power Loss Index (PLI)

With the integration of DG in RDNs, active power losses are expected to reduce. The PLI gives the effectiveness of DG integration on active power losses and is defined as:

$$PLI = \frac{P_{loss}^{DG}}{P_{loss}} \tag{4.6}$$

where P_{loss} and P_{loss}^{DG} are active power loss before and after integration of DG, respectively.

Reactive Power Loss Index (QLI)

The reactive power losses also vary with the integration of DG in RDNs. The effectiveness of DG integration on reactive power losses is given by QLI, which is expressed as:

$$QLI = \frac{Q_{loss}^{DG}}{Q_{loss}} \tag{4.7}$$

where Q_{loss} and Q_{loss}^{DG} are reactive power loss before and after integration of DG, respectively.

Voltage Deviation Index (VDI)

The voltage deviation is a measure of the deviation of bus voltages from reference bus. The effectiveness of improvement in voltage profile of buses after optimal placement of DG is measured by VDI. It is formulated as:

$$VDI = \frac{VD^{DG}}{VD} \tag{4.8}$$

where VD and VD^{DG} are measure of deviation in the bus voltage with respect to reference voltage before and after integration of DG respectively. These are defined as:

$$VD = \sum_{i=2}^{n} \left(\frac{V_{nom} - V_i}{V_{nom}} \right)^2 \tag{4.9}$$

$$VD^{DG} = \sum_{i=2}^{n} \left(\frac{V_{nom} - V_i^{DG}}{V_{nom}} \right)^2 \tag{4.10}$$

where V_i and V_i^{DG} is voltage of i^{th} bus before and after placement of DG respectively and V_{nom} is nominal voltage taken as 1 p.u.

Overall Economy Index (OEI)

The economy is accompanying every activity nowadays. The OEI is minimized to make DG operation economical. The OEI is expressed as:

$$OEI = \frac{CE^{DG}}{CE} \tag{4.11}$$

where CE and CE^{DG} are cost of losses and energy purchased before and after DG integration respectively. These are expressed as:

$$CE = P_{loss} C_{PT} + \sum_{i=1}^{n} (C_{PT} P_{Di}) \tag{4.12}$$

$$CE^{DG} = P_{loss}^{DG} C_{PT} + \sum_{i=1}^{n} \big(C_{PT}(P_{Di} - P_{DGi}) + C^{DG} P_{DGi}\big) \tag{4.13}$$

where in equation (4.12) and (4.13), C_{PT} is power tariff and C^{DG} is cost of power supplied by DG.

4.4 MOF FORMULATION FOR NON-PARETO MULTI-OBJECTIVE OPTIMIZATION

4.4.1 MOF Objective

The objectives are combined using the membership functions derived from the fuzzy decision approach. The fuzzy membership function values (μ) are computed for each objective and are defined as:

$$\mu_j = \begin{cases} 0, & \text{for } y_j \leq y_{min} \\ \dfrac{y_j - y_{min}}{y_{max} - y_{min}}, & \text{for } y_{min} < y_j < y_{max} \\ 1, & \text{for } y_j \geq y_{max} \end{cases} \tag{4.14}$$

where y_j is the value of performance index. In this work, the values of y_{max} and y_{min} are considered as 1.25 and 0 respectively. The MOF formulated by combining four objectives can be expressed as:

$$minMOF = min[\mu_{PLI} \times PLI + \mu_{QLI} \times QLI + \mu_{VDI} \times VDI + \mu_{OEI} \times OEI] \tag{4.15}$$

where μ_y is the fuzzy membership assigned to performance index y.

The objective function represented by equation (4.15) is subjected to inequality constraints of bus voltage limits and MVA capacity of lines.

4.4.1.1 Bus Voltage Constraints

The incorporation of DGs in RDN boosts the voltage level of all buses, which may result in over-voltage at some buses. Moreover, there are always limits on the lower level of voltage, so the bus voltage constraints are defined as:

$$V_i^{min} \leq V_i \leq V_i^{max} \tag{4.16}$$

where V_i^{min} and V_i^{max} are minimum and maximum limits for voltage of i^{th} bus respectively. The limits for V_i^{min} and V_i^{max} are taken as 0.90 and 1.05 p.u. (Hung and Mithulananthan, 2013).

4.4.1.2 MVA Capacity Constraints

The integration of DG in RDN changes the nature of RDN from passive to active, and hence the current levels change. This constraint is necessary to ensure the thermal limits of lines. MVA capacity constraint is expressed as:

$$S_{ij} \leq S_{ij}^{max} \tag{4.17}$$

where S_{ij} is MVA flow in line between bus *i* and *j* and S_{ij}^{max} is maximum limit of S_{ij}.

4.4.2 Limiting Search Space

The search space for optimal allocation of DG is limited by making the clusters of buses. Bus voltages obtained after the load flow for the base case are used to decide these clusters, which represent the group of buses having significant low voltage. The potential buses for the placement of DGs are selected from these clusters, and thus limiting the search space. Such identified clusters of buses although reduces the search space but always yield the optimal solution and thereby does not compromise on the quality of the optimal solution.

4.5 MOF OPTIMIZATION USING PSO FOR DG ALLOCATION

PSO described in section 3.4.1 is a population-based search and optimization technique, is applied to optimize the multi-objective function given by equation (4.15). Figure 4.1 shows the flowchart for implementing the multi-objective DG allocation problem using PSO, where algorithm steps are described as follows:

Step 1 Read the DN line data, bus data and the type of load.

Step 2 Carry-out the base case load flow using $BIBC$ and $BCBV$ matrices.

Step 3 Calculate the indices, i.e., PLI, QLI, VDI and OEI before placement of DG.

Step 4 Identify the cluster of buses for obtaining optimal site of DG.

Step 5 Initialize the particles positions that are random DGs at random buses in the search space and set the iteration counter $k = 0$.

Step 6 For these positions, calculate load flow and check for constraints satisfaction. Compute the performance indices and corresponding membership functions using equation (4.14).

Step 7 Obtain the objective function from equation (4.15).

Step 8 For the positions, assign them as individual best positions (*pbest*). Also identify the best of the *pbest* as global best (*gbest*).

Step 9 Update the particles positions by accounting their adaptive weight, current positions, *pbest*, *gbest* and increase iterations as $k = k + 1$.

Step 10 Go to Step 6 until the convergence is achieved.

The single objective optimization is also realized using this algorithm by selecting individual objectives.

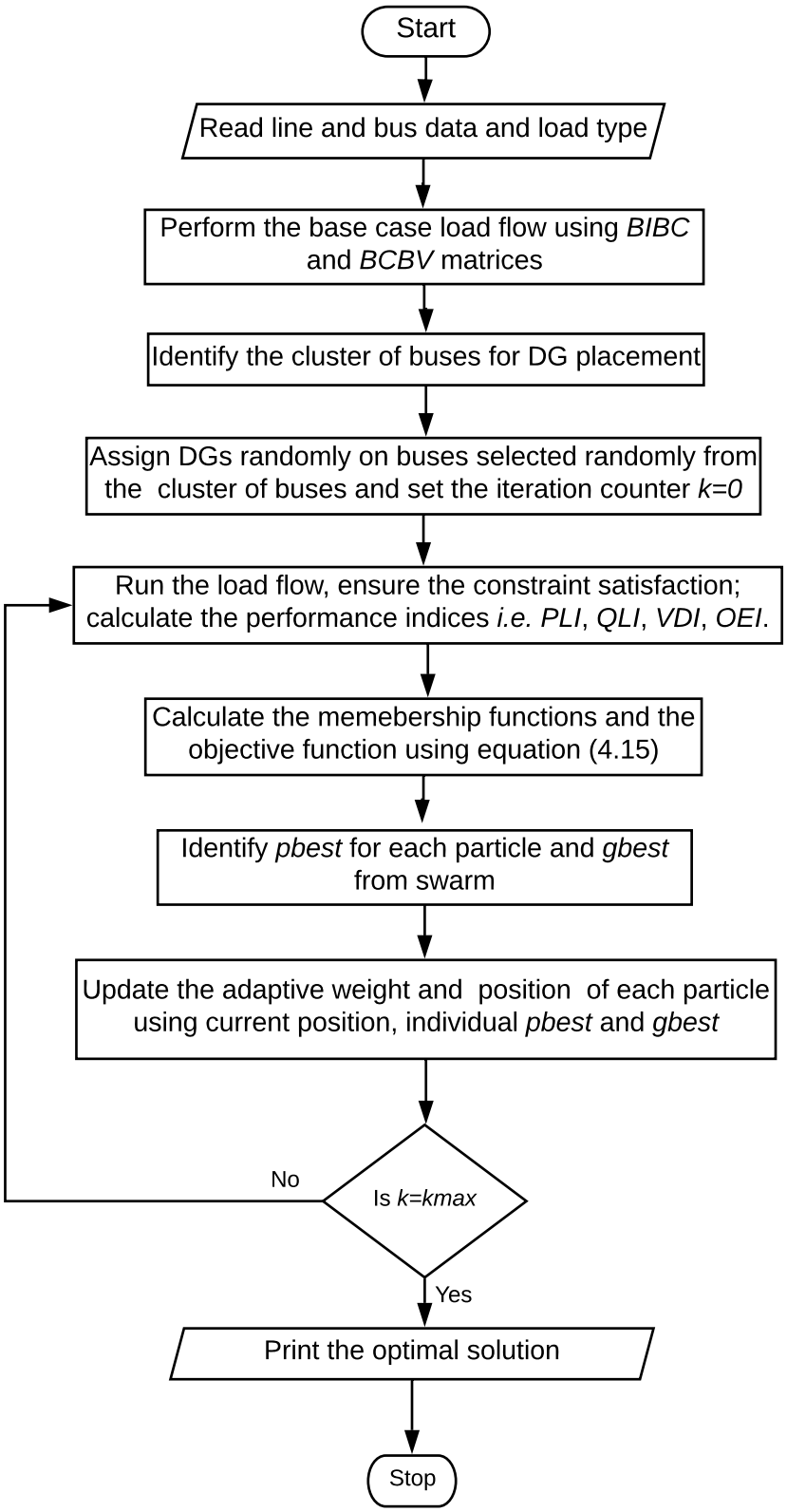

Fig. 4.1: Flowchart for Non Pareto Based DG Allocation

4.6 TRUE PARETO BASED MULTI-OBJECTIVE PSO FOR DG PLACEMENT

In the true Pareto based multi-objective optimization, the indices are used directly. The concept of non-domination is used in getting Pareto optimal front. The PSO based algorithm is modified to suit this, with the following considerations:

- In PSO, the leaders such as x^{gbest} and x_i^{pbest} are used to guide the search. The x^{gbest} is the global best position attained by entire swarm and the x_i^{pbest} is the personal best position attained by the individual particles. These leaders x^{gbest} and x_i^{pbest} are updated in each iteration.

- As truely multi-objective optimization return multiple non-dominated solutions at the convergence of optimization process; the x^{gbest} is taken as set of non dominated solutions instead of a single solutions. This set of non-dominated solutions, is updated in each iteration. As all solutions in the $\mathbf{X}^{gbest}$ are equally good, one of the non-dominated solution randomly selected will be a leader.

$$x^{gbest} = rand(\mathbf{X}^{gbest}) \tag{4.18}$$

- The solution x_i^{pbest} is taken as the non-dominated value between x_{i} and x_i^{pbest}. Instead of managing a set of non-dominated positions that the individual particles have acquired, this one solution nomenclature of x_i^{pbest} will help save the memory requirement.

$$x_i^{pbest} = \mathrm{nondominate}(x_i, x_i^{pbest}) \tag{4.19}$$

Thereafter, the particle velocity and position are updated, the velocity is expressed as equation (4.20)

$$v_i(t) = x_i(t-1) + w \times v_i(t-1) + C_1 \times r_1 \times (x_i^{pbest} - x_i) + C_2 \times r_2 \times (x^{gbest} - x_i) \tag{4.20}$$

where,

$$x_i^{pbest} = \mathrm{nondominate}(x_i, x_i^{pbest})$$
$$x^{gbest} = rand(\mathbf{X}^{gbest})$$

4.6.1 Algorithm Steps

The modified PSO described in section 4.6 is employed to obtain Pareto front and best compromised solution. Figure 4.2 shows the flowchart for implementing the multi-objective DG allocation, where algorithm steps are described as follows:

Step 1 Read the DN line data, bus data and the type of load.

Step 2 Carry-out the base case load flow using $BIBC$ and $BCBV$ matrices.

Step 3 Calculate the indices, namely PLI and VDI before placement of DG.

Step 4 Identify the cluster of buses for obtaining optimal site of DG.

Step 5 Initialize the particles positions that are random DGs at random buses in the search space and set the iteration counter $k = 0$.

Step 6 For these positions, calculate load flow and check for constraints satisfaction. Compute the PLI and VDI.

Step 7 Assign these positions as individual best x_i^{pbest}.

Step 8 Apply non-dominated sorting to $\mathbf{X}^{pbest}$ to obtain a solution vector non-dominated solutions $\mathbf{X}^{gbest}$.

Step 9 Obtain the particle positions by using current position x_i, its best x_i^{pbest} and a randomly picked solution from non-dominated set $\mathbf{X}^{gbest}$.

Step 10 Obtain x_i^{pbest} as the non-dominated value between x_i^{pbest} and x_i.

Step 11 Set iteration $k = k + 1$.

Step 12 Go to Step 6 until the convergence is achieved.

Step 13 Compute the normalized membership β for each Pareto-optimal solution. Select the solution with maximum β as best compromised solution.

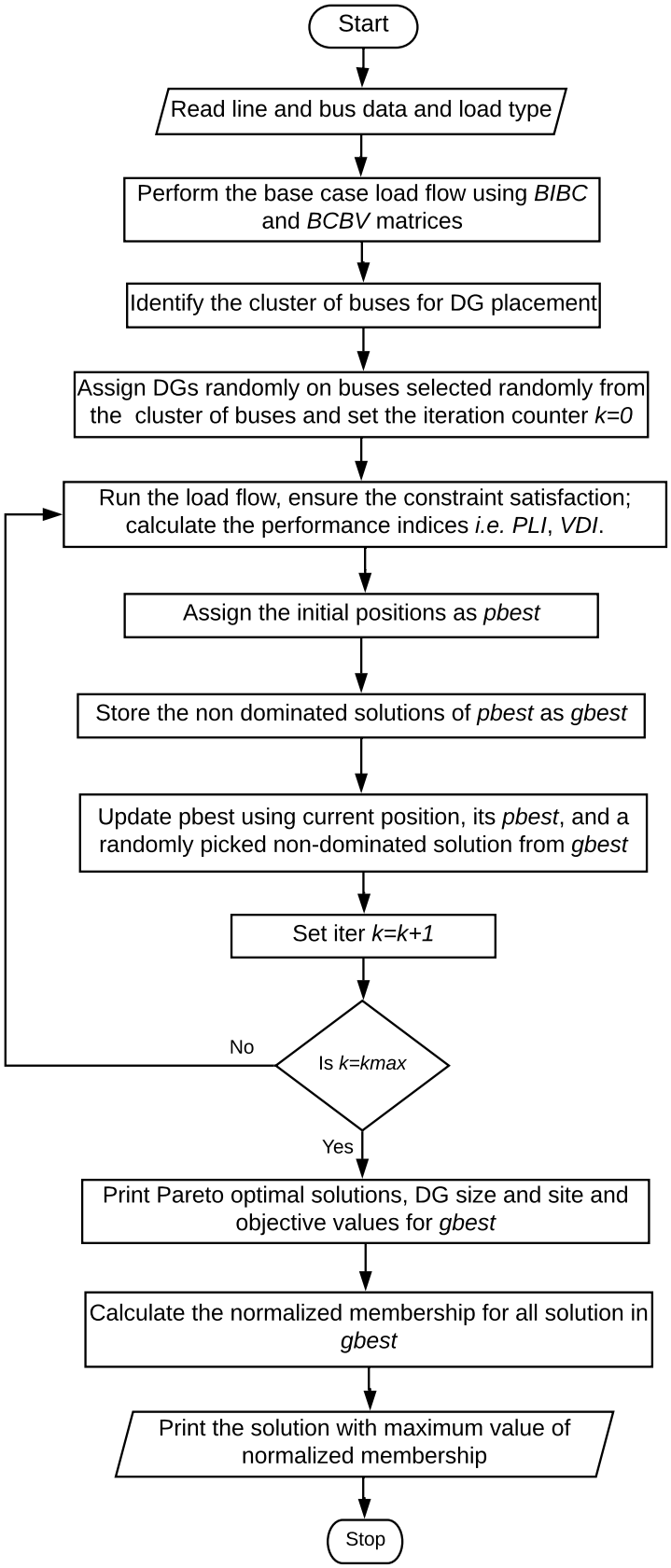

Fig. 4.2: Flowchart for True Pareto Based DG Allocation

4.7 RESULTS AND DISCUSSIONS

The methodology adopted for optimal allocation of DGs presented above is tested on 69-bus RDN. The algorithms are implemented under MATLAB R2014b in MAC environment. The algorithm parameters are considered as: swarm size as 50, maximum iterations as 100, c_1 and c_2 as 2, w_{max} as 0.9 and w_{min} as 0.4. The best results after 10 runs of PSO are presented. For multi-objective optimization, the optimal size and site of DG are found for the placement of single as well as multiple DGs. In Chapter 3, Type-I and Type-III DG are found as most effective, so these are further considered for optimization.

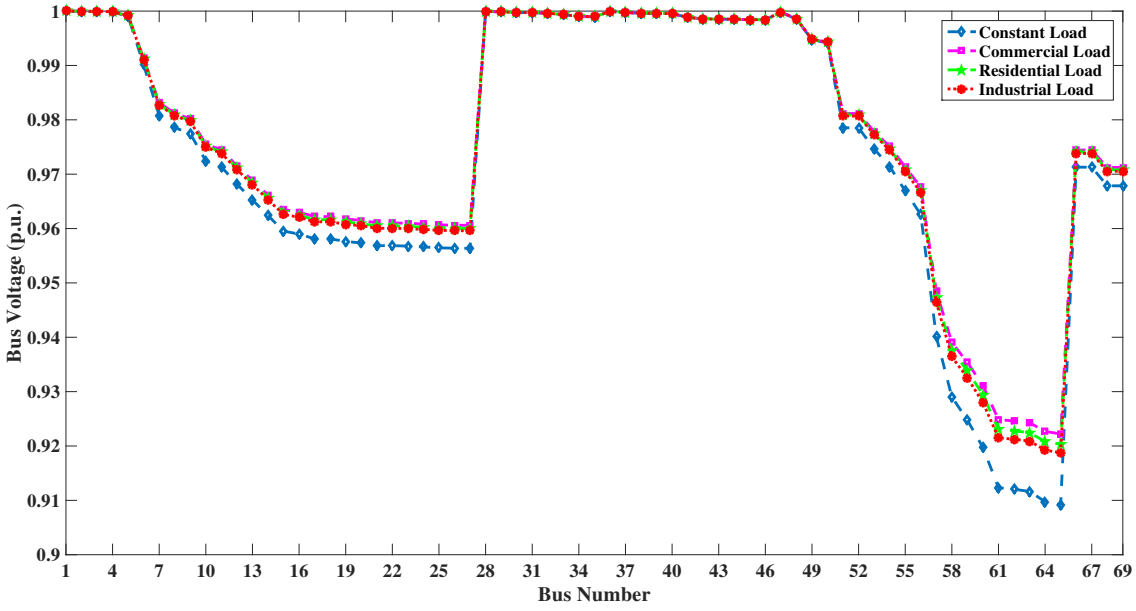

Fig. 4.3: Variation of Base-case Bus Voltage for All Loads

The search space for obtaining the optimal site of DG is obtained by forming the clusters of buses with significantly lower bus voltage from base-case load flow for all types of loads. The variation of bus voltage for base case load flow is shown in Figure 4.3. Two clusters of buses with minimum voltage are selected to obtain the optimal site of DG. The first cluster of buses consists of buses from 57 to 65 and second cluster of buses ranges from bus 16 to 28. The two cases of optimization are discussed in following section. Both single and multiple DG placement is carried out on the basis of single objective and multi-objective optimization. The multi-objective optimization is analyzed through MOF formulation and simultaneously optimizing PLI and VDI using true Pareto based approach.

4.7.1 DG Placement for Single Objective Optimization

Optimal size and site of DG are found when all four indices are considered independently for placement of single as well as multiple DGs. For placement of single DG, only first cluster of buses is considered while for placement of two DGs, one DG location is selected from each of the respective cluster. The four cases that are investigated for DG placement through single objective optimization are: Minimizing PLI, Minimizing QLI, Minimizing VDI and Optimizing OEI.

4.7.1.1 Minimizing *PLI*

With PLI as objective, the optimal size and site of DG and corresponding indices after optimal allocation of DG for all types of loads are presented in Table 4.1. The value of PLI is 1.0 before placement of DG in RDN. Its value reduces significantly after integration of optimal sized DG at the optimal site due to the reduction in active power loss. For constant load, the improvement is maximum, where its value reduces to 0.3696 and 0.3280 corresponding to the placement of single and multiple DGs, respectively. The values of all other indices also reduce after DG placement.

Table 4.1: Optimal Size and Site of Type-I DG and Indices Values for PLI as Objective

Load Model	DG Size (MW)	DG Site	*PLI*	*QLI*	*VDI*	*OEI*
Constant	1.88	61	0.3696	0.3964	0.2011	0.4946
	1.83, 0.42	61, 26	0.3280	0.3596	0.0689	0.4641
Commercial	1.63	61	0.4437	0.4763	0.2805	0.5839
	1.37, 0.46	61, 23	0.3962	0.4366	0.1527	0.5485
Residential	1.62	61	0.4217	0.4555	0.2790	0.5646
	1.51, 0.34	61, 26	0.3763	0.4166	0.1502	0.5307
Industrial	1.70	61	0.3893	0.4235	0.2533	0.5388
	1.62, 0.50	61, 21	0.3352	0.3762	0.0893	0.4985

4.7.1.2 Minimizing *QLI*

With QLI minimization, attained optimal DG size, site and corresponding values of indices are presented in Table 4.2 for placement of single as well as multiple DGs. In addition to the

reduction in QLI, all other indices are also reduced, *i.e.*, performance is improved. The reduction in QLI is almost same for both objectives PLI and QLI, as both are current dependent.

Table 4.2: Optimal Size and Site of Type-I DG and Indices Values for QLI as Objective

Load Model	**DG Size (MW)**	**DG Site**	***PLI***	***QLI***	***VDI***	***OEI***
Constant	1.93	61	0.3700	0.3961	0.1920	0.4974
	1.80, 0.57	61, 19	0.3199	0.3522	0.0519	0.4578
Commercial	1.76	61	0.4461	0.4764	0.2512	0.5864
	1.34, 0.57	62, 23	0.4054	0.4432	0.1313	0.5558
Residential	1.76	61	0.4239	0.4522	0.2473	0.5668
	1.61, 0.54	61, 22	0.3682	0.4068	0.0852	0.5256
Industrial	1.70	61	0.3891	0.4234	0.2549	0.5386
	1.64, 0.52	61, 25	0.3475	0.3849	0.0799	0.5080

4.7.1.3 Minimizing VDI

The deviation in bus voltages in RDN is a crucial factor, which can be improved by the integration of DG. The optimal size, site of DG and performance indices are summarized in Table 4.3 corresponding to a minimization of VDI for placement of single as well as multiple DGs. The size of DG for VDI optimization is higher in comparison to the sizes of DGs obtained for optimizing PLI and QLI independently. The improvement in VDI results in improvement of the voltage of all buses in RDN. The placement of multiple DGs is found more effective as the reduction in VDI is more as compared to single DG placement.

Table 4.3: Optimal Size and Site of Type-I DG and Indices Values for VDI as Objective

Load Model	**DG Size (MW)**	**DG Site**	***PLI***	***QLI***	***VDI***	***OEI***
Constant	2.98	58	0.5706	0.5622	0.1016	0.6603
	2.33, 0.69	63, 20	0.4033	0.4289	0.0057	0.5260
Commercial	2.54	59	0.6173	0.6169	0.1527	0.7177
	2.33, 0.71	62, 19	0.5273	0.5471	0.0068	0.6522
Residential	2.67	59	0.6277	0.6232	0.1376	0.7238
	2.41, 0.65	60, 21	0.5325	0.5537	0.0083	0.6528
Industrial	2.82	58	0.6523	0.6387	0.1265	0.7415
	2.35, 0.71	63, 20	0.5274	0.5495	0.0069	0.6470

4.7.1.4 Minimizing *OEI*

The optimization of OEI is a critical objective as the economy is a major deciding factor. For OEI formulation, the cost of power supplied by DG is taken as 46 US$/MWh and power tariff is taken as 44.5 US$/MWh (Singh and Goswami, 2011). Corresponding to the optimization of OEI, the optimal placement and values of the indices are summarized in Table 4.4. The reduced value of OEI results in economic operation of DG. It is observed that the placement of multiple DGs is more economical as compared to single DG. The obtained OEI for placement of two DG is always lower than its value for single DG. The reduction in OEI follows the pattern of PLI, as OEI is dependent on active power losses, given by equation (4.13).

Table 4.4: Optimal Size and Site of Type-I DG and Indices Values for OEI as Objective

Load Model	DG Size (MW)	DG Site	*PLI*	*QLI*	*VDI*	*OEI*
Constant	1.87	61	0.3696	0.3966	0.2030	0.4696
	1.78, 0.50	61, 20	0.3197	0.3529	0.0640	0.4576
Commercial	1.55	61	0.4452	0.4790	0.2996	0.5848
	1.52, 0.54	62, 25	0.4076	0.4431	0.0969	0.5581
Residential	1.60	61	0.4219	0.4558	0.2815	0.5647
	1.58, 0.49	61, 23	0.3675	0.4070	0.0999	0.5247
Industrial	1.63	61	0.3879	0.4232	0.2685	0.5376
	1.66, 0.45	61, 22	0.3362	0.3775	0.0924	0.4993

Among all four types practical loads, DG of maximum size is required for constant load model, for every objective optimization. Therefore, the reduction in respective objective is also maximum for constant load model. Similar results are obtained for all practical loads during Type-III DG placement but only the results for constant load model are presented in Table 4.5.

The placement of Type-III DG follows the pattern of Type-I DG placement, *i.e.*, the size of DG is maximum when VDI is objective. The optimal location is governed by objectives as it is bus 58 corresponding to VDI and 61 for PLI, QLI, and OEI for single DG placement. It is also concluded that similar to Type-I DG, placement of multiple Type-III DG is more effective as the values of PLI, QLI, VDI and OEI through single objective optimization are higher for single DG placement then the respective values obtained with the placement of two DGs. This suggests

Table 4.5: Optimal Size and Site of Type-III DG and Indices Values for Single Objective Optimization

Objective	DG Size (MVA @ pf)	DG Site	*PLI*	*QLI*	*VDI*	*OEI*
PLI	2.23 @ 0.83	61	0.1029	0.1410	0.1207	0.2816
	2.10 @ 0.83, 0.48 @ 0.83	61, 26	0.0453	0.0911	0.0134	0.2368
QLI	2.31 @ 0.83	61	0.1034	0.1400	0.1135	0.2833
	2.27 @ 0.83, 0.48 @ 0.83	61, 26	0.0466	0.0904	0.0089	0.2381
VDI	2.87 @ 0.83	58	0.2556	0.2649	0.0859	0.4062
	2.14 @ 0.83, 0.62 @ 0.83	61, 26	0.0492	0.0913	0.0060	0.2402
OEI	2.24 @ 0.83	61	0.1029	0.1407	0.1197	0.2825
	2.10 @ 0.83, 0.48 @ 0.83	61, 26	0.0453	0.0911	0.0134	0.2368

that the placement of two DGs is yielding better optimization. Another conclusion derived from Table 4.5 is that there is a reduction in all indices after placement of DG irrespective of the considered objective. Moreover, it is also observed that Type-III DG placement is more useful for the single as well as multiple DG placement as compared to Type-I DG placement. The effect of load models on Type-I and Type-III DG for multi-objective placement is discussed in detail in the following section.

4.7.2 DG Placement for Multi-objective Optimization

The placement of DG is carried out by obtaining MOF from the objective indices for two cases. In the first case PLI and VDI are considered simultaneously, and in the second case, all the four objectives (PLI, QLI, VDI, and OEI) are considered simultaneously. The effect of load models is also considered during the placement of Type-I as well as Type-III DG for such non Pareto based multi-objective optimization.

4.7.2.1 Case I: Optimizing PLI and VDI using Non-Pareto based Approach

The placement of single as well as multiple DGs has been investigated by considering PLI and VDI simultaneously by assigning fuzzy membership function to each performance index. For

all types of voltage-dependent loads optimal size, site and the corresponding value of each index after placement of Type-I and Type-III DGs are summarized in Table 4.6 and 4.7 respectively.

Table 4.6: Optimal Size and Site of Type-I DG for Placement of Single DG and Multiple DG and Indices Values for PLI and VDI Optimization

Load Model	DG Size (MW)	DG Site	*PLI*	*QLI*	*VDI*	*OEI*
Constant	2.09	61	0.3766	0.3997	0.1666	0.5029
	1.91, 0.48	61, 26	0.3312	0.3609	0.0477	0.4669
Commercial	1.94	61	0.4603	0.4862	0.2159	0.5979
	1.93, 0.48	63, 26	0.4016	0.4366	0.0436	0.5737
Residential	1.87	61	0.4309	0.4597	0.2356	0.4597
	1.79, 0.55	61, 26	0.3943	0.4259	0.0543	0.5460
Industrial	2.14	61	0.4427	0.4647	0.1787	0.5805
	1.95, 0.44	61, 26	0.3757	0.4093	0.0528	0.5300

Table 4.7: Optimal Size and Site of Type-III DG for Placement of Single DG and Multiple DG and Indices Values for for PLI and VDI Optimization

Load Model	DG Size (MVA @ pf)	DG Site	*PLI*	*QLI*	*VDI*	*OEI*
Constant	2.41 @ 0.82	61	0.1067	0.1412	0.1084	0.2859
	2.31@ 0.82, 0.64 @ 0.82	61, 26	0.0544	0.0943	0.0069	0.2446
Commercial	2.26 @ 0.84	61	0.1318	0.1791	0.1418	0.3521
	1.89 @ 0.84, 0.66 @ 0.84	61, 26	0.0796	0.1331	0.0173	0.3135
Residential	2.15 @ 0.85	61	0.1308	0.1788	0.1478	0.3458
	1.85 @ 0.85, 0.70 @ 0.85	61, 26	0.0858	0.1358	0.0200	0.3726
Industrial	2.18 @ 0.87	61	0.1342	0.1801	0.1401	0.3453
	1.87 @ 0.87, 0.66 @ 0.87	61, 26	0.0793	0.1311	0.0170	0.3042

These results are compared to the single objective optimization results presented in Tables 4.1 and 4.3, which summarize the results corresponding to the minimization of PLI and minimization of VDI respectively for Type-I DG placement. From Tables 4.1 and 4.3, it is clear that the value of PLI is minimum, while VDI is maximum when only PLI is the objective, whereas VDI is minimum and PLI is maximum when only VDI is the objective for all types of loads. When compared to multi-objective placement the value of PLI and VDI is compromised in comparison to the single objective case as evident from Tables 4.1, 4.3 and 4.6. Similar observations are made for the placement of Type-III DG also.

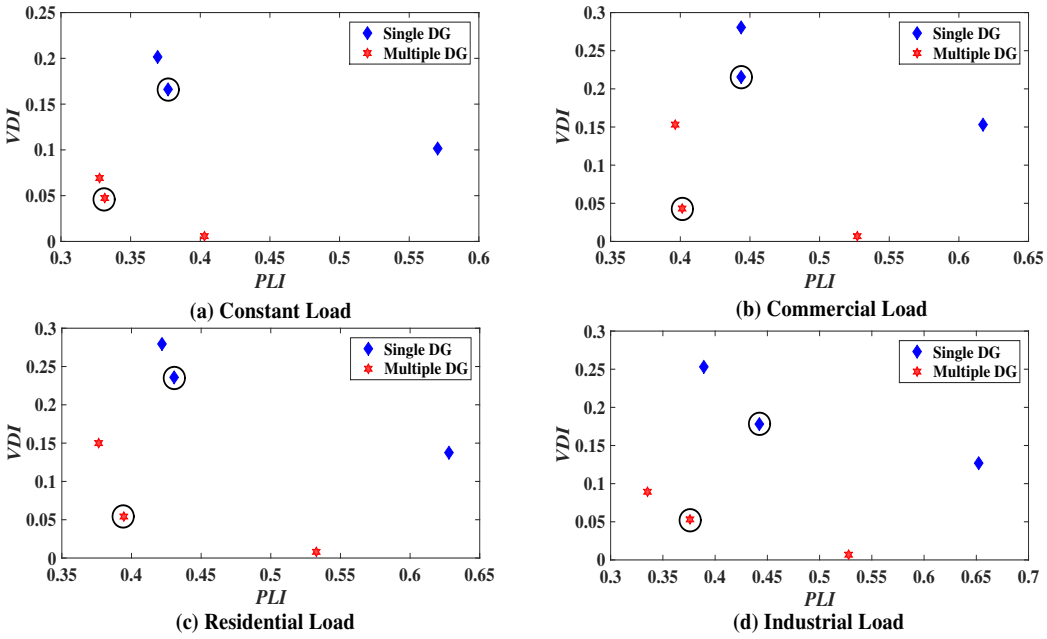

Fig. 4.4: Variation of PLI versus VDI for Voltage-dependent Loads

The results of multi-objective optimization, while compared with single objective optimization, PLI and VDI form the non-dominated set of solutions. The variation of PLI with variation in VDI for placement of single as well as multiple Type-I DGs is shown in Figure 4.4 (a-d) for different load models. The encircled solutions corresponds to multi-objective optimization while; the extreme solutions corresponds to individual objectives. As the optimal solution corresponding to the multiple DG placement is more dominant, *i.e.*, near to the origin as compared to single DG placement, thus the placement of multiple DGs is more beneficial.

4.7.2.2 Case-II Optimizing All Indices Simultaneously using Non-Pareto based Approach

In the second case of multi-objective optimization based placement of DG, all four indices PLI, QLI, VDI, and OEI are combined by assigning fuzzy membership to each index. The optimal size and site of Type-I and Type-III DG and all indices are tabulated in Table 4.8 and Table 4.9, respectively. It is observed from results that type of load is affecting DG size.

The placement of multiple DGs is more advantageous as compared to single DG placement and it results in reduced values of indices. The reduced values of PLI and QLI show the

Table 4.8: Optimal Size and Site of Type-I DG for Single and Multiple DG Placement and Indices Values for Multi-objective Optimization of All Indices

Load Model	DG Size (MW)	DG Site	*PLI*	*QLI*	*VDI*	*OEI*
Constant	1.97	61	0.3712	0.3964	0.1838	0.4984
	1.85, 0.48	61, 27	0.3308	0.3608	0.0546	0.4665
Commercial	1.92	61	0.4580	0.4845	0.2197	0.5961
	1.80, 0.44	61, 20	0.3963	0.4335	0.0771	0.5505
Residential	1.91	61	0.4355	0.4631	0.2166	0.5761
	1.85, 0.49	61, 19	0.3802	0.4168	0.0600	0.5354
Industrial	1.86	61	0.4000	0.4306	0.2216	0.5473
	1.85, 0.41	61, 22	0.3521	0.3906	0.0741	0.5117

Table 4.9: Optimal Size and Site of Type-III DG for Single and Multiple DG Placement and Indices Values for Multi-objective Optimization of All Indices

Objective	DG Size (MVA @ pf)	DG Site	*PLI*	*QLI*	*VDI*	*OEI*
Constant	2.31 @ 0.82	61	0.1036	0.1400	0.1135	0.2833
	2.08 @ 0.82, 0.65 @ 0.82	61, 23	0.0518	0.0935	0.0075	0.2422
Commercial	2.11 @ 0.84	61	0.1332	0.1832	0.1555	0.3523
	1.78 @ 0.84, 0.48 @ 0.84	61, 26	0.0817	0.1418	0.0401	0.3136
Residential	2.12 @ 0.85	61	0.1313	0.1797	0.1501	0.3460
	1.78 @ 0.85, 0.45 @ 0.85	61, 26	0.0813	0.1403	0.0429	0.3082
Industrial	2.12 @ 0.87	61	0.1344	.01815	0.1413	0.3454
	1.80 @ 0.87, 0.47 @ 0.87	61, 26	0.0792	0.1364	0.0354	0.3036

reduction in active and reactive power losses respectively and reduced values of VDI show improvement in voltage profile of all buses. The reduction in OEI means that integration of DG in DN is economical, as it reduces the losses and cost of DG is being overcome by the reduction in losses. Also Type-III DG is more advantageous for multi-objective DG placement.

The multi-objective optimization, as summarized in Tables 4.6, 4.7, 4.8 and 4.9, yields the lower values of indices with two DG placement in comparison to single DG placement. With multiple DGs of optimum size, the compensation is affected at multiple locations, and thereby the load burden is not reflected on the substation. Such multiple DG placement thereby results in reduced losses and improved bus voltage profile.

4.7.2.3 True Pareto Based Optimization of PLI and VDI

The true multi-objective optimization of PLI and VDI is giving the Pareto optimal fronts which are shown in Figure 4.5 (a) and (b) corresponding to the optimal placement of single and multiple Type-I DGs. Whereas the Pareto optimal front for placement of single and multiple Type-III DGs is shown in Figure 4.6 (a) and (b), respectively. Correspondingly the best compromised solution are summarized in Table 4.10.

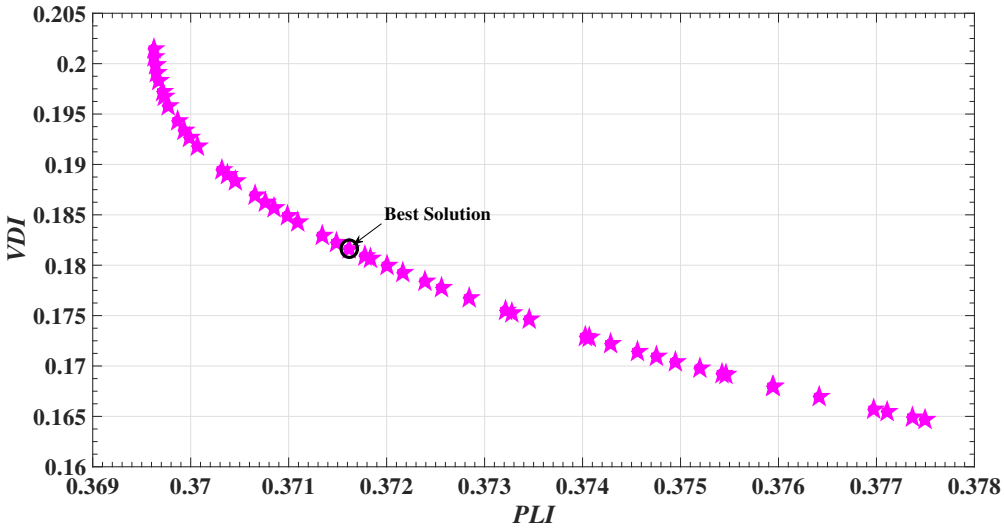

(a) Single DG

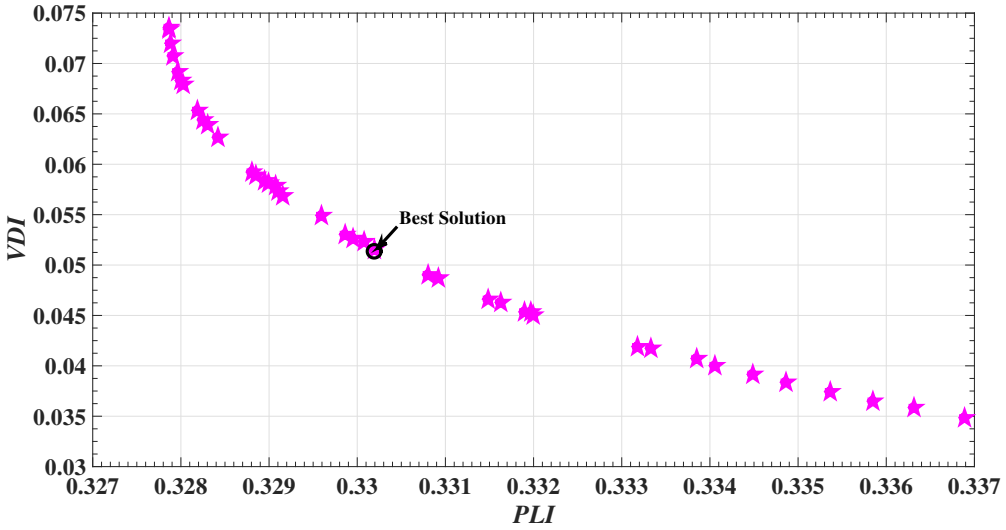

(b) Multiple DG

Fig. 4.5: Pareto Front for Placement of Type-I DG

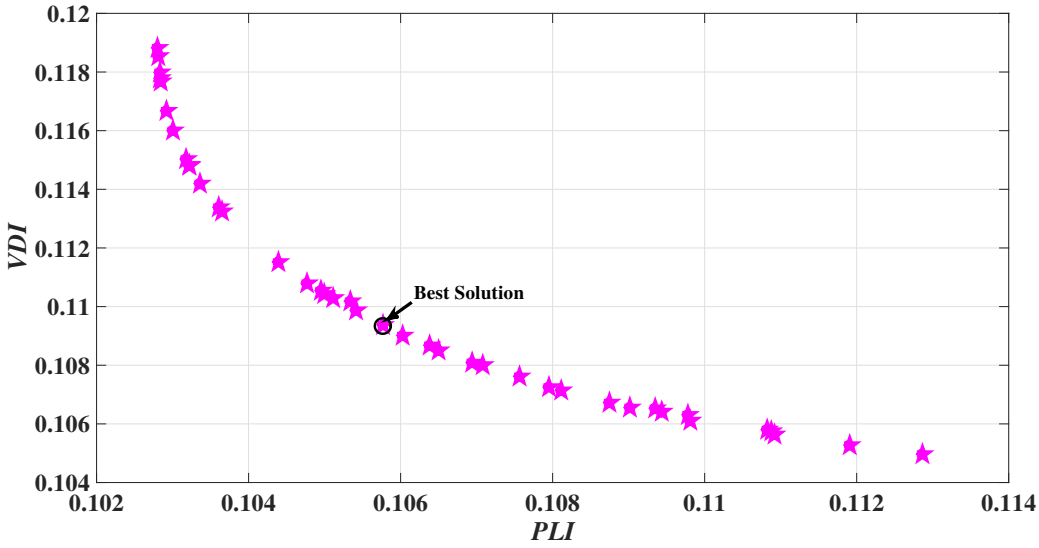

(a) Single DG

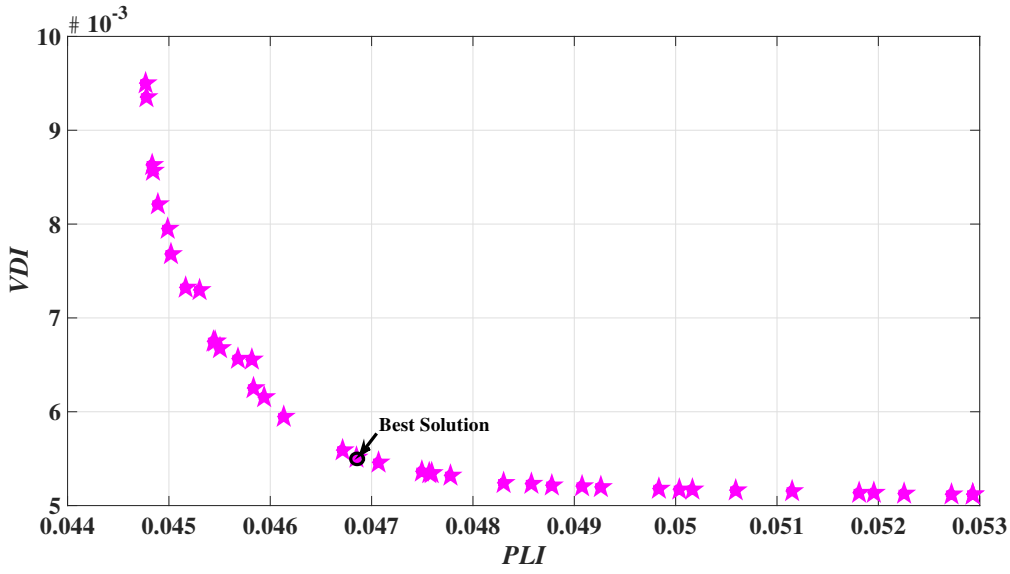

(b) Multiple DG

Fig. 4.6: Pareto Front for Placement of Type-III DG

The Pareto fronts are well diversified. As expected, the placement of multiple DGs is yielding better optimization of both PLI and VDI. The compromised solution corresponding to placement of Type-III multiple DGs is near to origin. It is also observed from Table 4.10 that similar to MOF based optimization, the placement of Type-III DG is more beneficial in comparison to Type-I DG.

Table 4.10: Optimal Allocation of Single and Multiple Type-I and Type-III DG for True Pareto Based Multi-objective Optimization

DG Type	DG Size	DG Site	*PLI*	*VDI*
Type-I	2.03 MW	61	0.3716	0.1816
	1.89 MW, 0.47 MW	61, 26	0.3302	0.0515
Type-III	2.39 MVA @ 0.82 pf	61	0.1058	0.1094
	2.21 MVA @ 0.82 pf, 0.56 MVA @ 0.82 pf	61, 26	0.0469	0.0055

4.7.3 Bus Voltage after DG Placement

The placement of DGs of optimal size at the optimal site improves the voltage of all buses of the RDN. The variation of the voltage of each bus before and after placement of optimal sized Type-I and Type-III DG at respective optimal sites for multi-objective optimization after considering all indices is shown in Figures 4.7 - 4.10 for four different types of loads. The plot of voltage indicates that the improvement in bus voltage is better with the placement of multiple DGs as compared to single DG for almost all buses. For a few buses, the increase in voltage is more corresponding to single DG. This is due to the location and size of DG, as the size of a single DG is large in comparison to the size of multiple DG for the same location. The larger size of DG results in more enhancement of bus voltage for Type-I and Type-III DG. For example, considering constant load model, the size of Type-I for single DG placement is 1.97 MW for bus 61, while for multiple DG placement, it is 1.85 MW for bus 61.

It is also observed from Figures 4.7 - 4.10, that the enhancement in voltage is more with the integration of Type-III DG at single and multiple optimal locations as compared to Type-I DG (both single and multiple) in the first cluster of buses. For the second cluster of buses the improvement in voltage is maximum with multiple Type-III DG integration followed by multiple Type-I DG, and it is minimum with the integration of single Type-I DG. Similar trends are observed for commercial, residential and industrial load model. Also, the voltage of all buses is within the limits of voltage constraints for all types of load after placement of single as well as multiple DG. The minimum bus voltage is found at bus 65 for all load models. The effect of DG allocation on minimum bus voltage is summarized in Tables 4.11, 4.12, 4.13 and 4.14 for constant, commercial, residential and industrial load models, respectively.

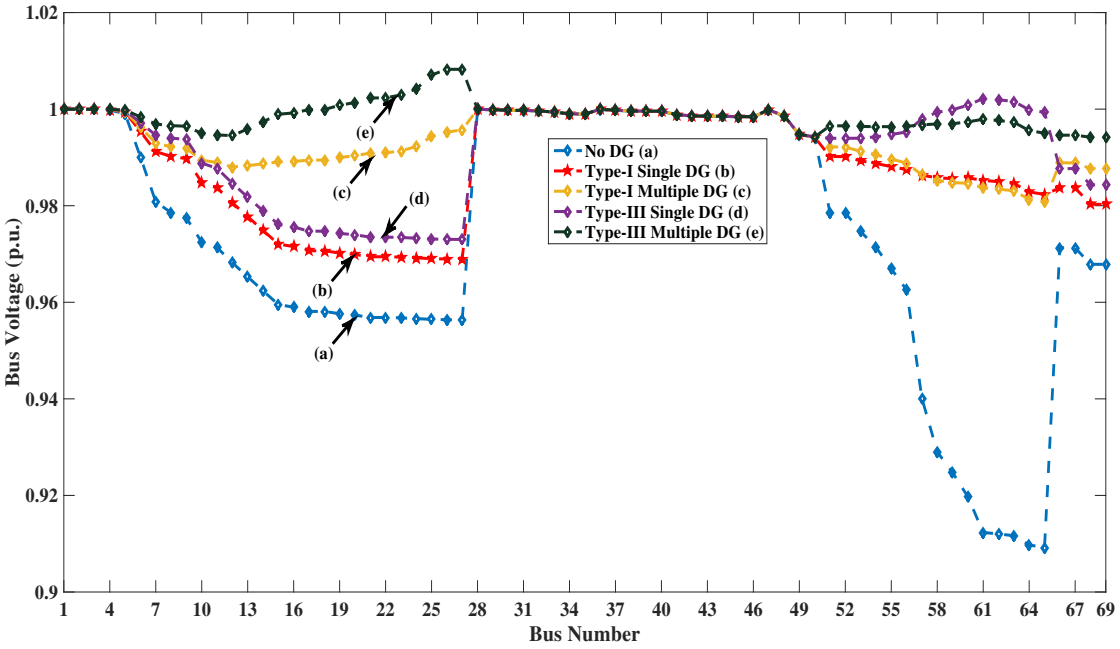

Fig. 4.7: Variation of Bus Voltage Before and After Placement of Type-I and Type-III DG for Constant Load

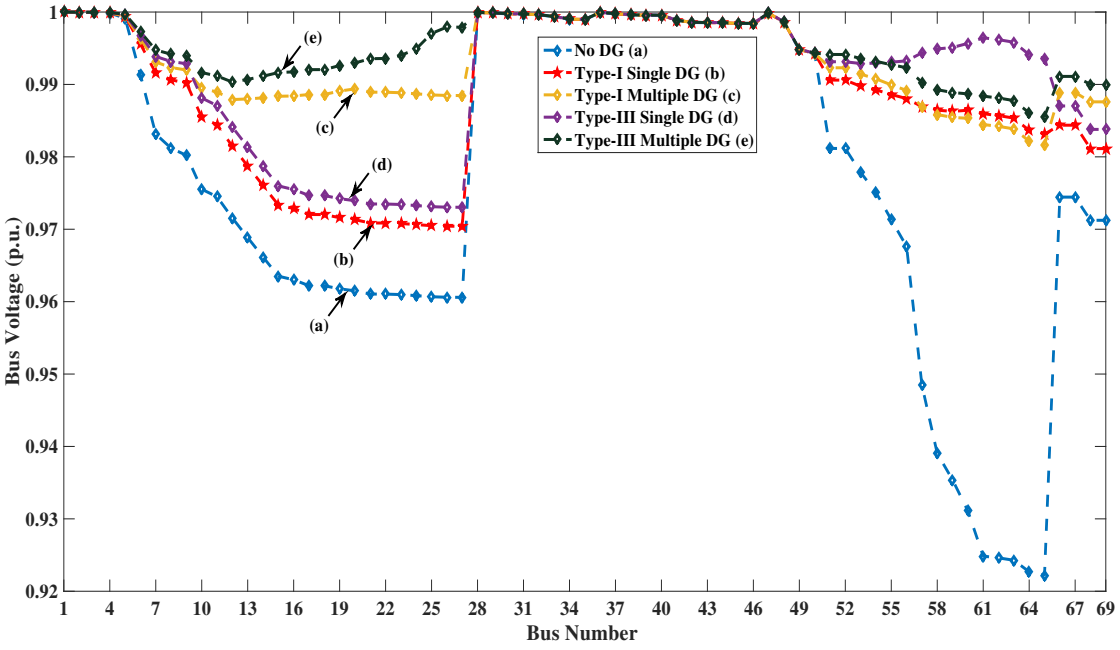

Fig. 4.8: Variation of Bus Voltage Before and After Placement of Type-I and Type-III DG for Commercial Load

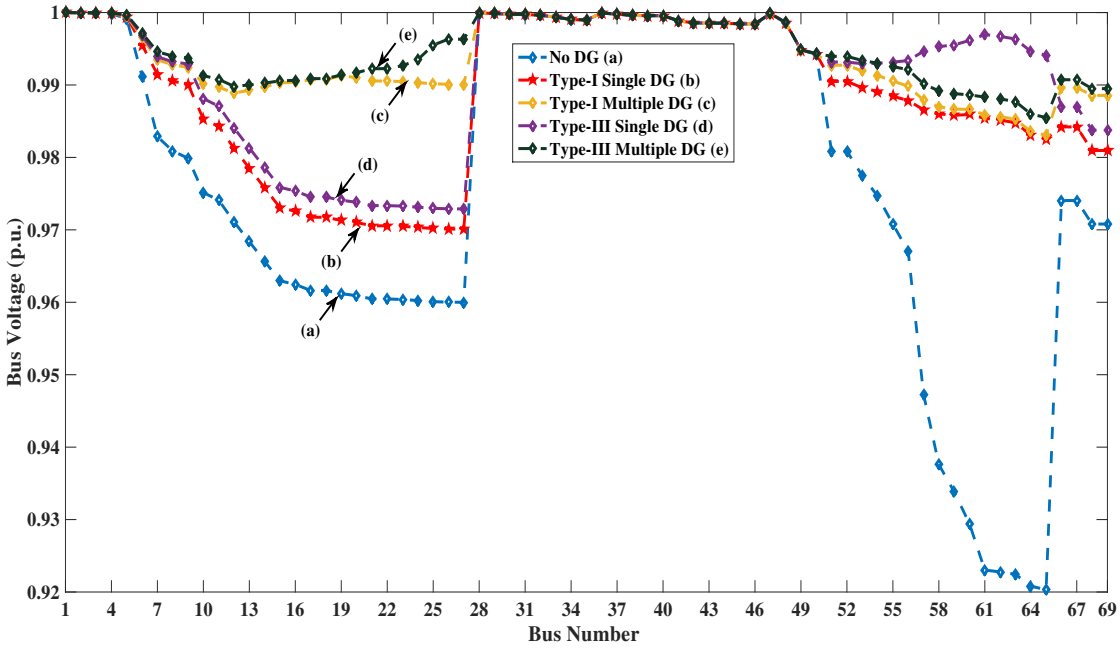

Fig. 4.9: Variation of Bus Voltage Before and After Placement of Type-I and Type-III DG for Residential Load

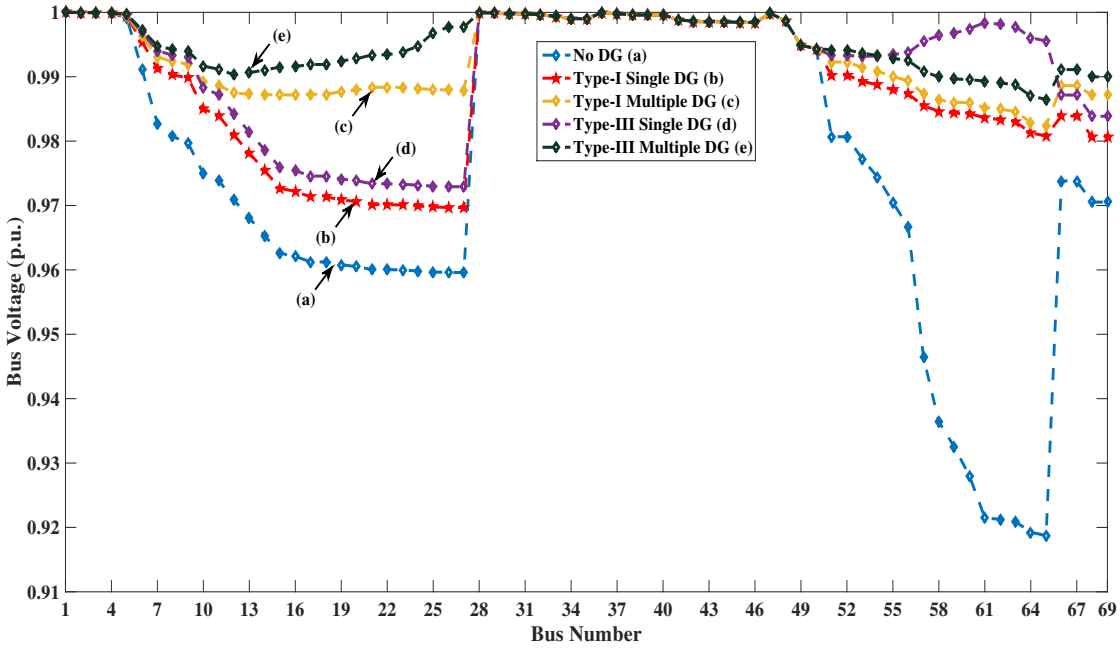

Fig. 4.10: Variation of Bus Voltage Before and After Placement of Type-I and Type-III DG for Industrial Load

Table 4.11: Minimum Bus Voltage Before and After DG Integration for Constant Load

DG Type	Minimum Bus Voltage @ Bus
No DG	0.9092 @ 65
Type-I DG (Single)	0.9689 @ 27
Type-I DG (Multiple)	0.9808 @ 65
Type-III DG (Single)	0.9730 @ 27
Type-III DG (Multiple)	0. 9942 @ 69

Table 4.12: Minimum Bus Voltage Before and After DG Integration for Commercial Load

DG Type	Minimum Bus Voltage @ Bus
No DG	0.9222 @ 65
Type-I DG (Single)	0.9704 @ 27
Type-I DG (Multiple)	0.9817 @ 65
Type-III DG (Single)	0.9730 @ 27
Type-III DG (Multiple)	0. 9856 @ 65

Table 4.13: Minimum Bus Voltage Before and After DG Integration for Residential Load

DG Type	Minimum Bus Voltage @ Bus
No DG	0.9203 @ 65
Type-I DG (Single)	0.9701 @ 27
Type-I DG (Multiple)	0.9831 @ 65
Type-III DG (Single)	0.9729 @ 27
Type-III DG (Multiple)	0. 9855 @ 65

The minimum bus voltage is improved significantly by the integration of single as well as multiple DGs. As the location of single DG is in the first cluster of buses for all loads, so the bus with minimum bus voltage after optimal allocation of Type-I and Type-III shifts to the second cluster, *i.e.*, bus 27. The integration of multiple DG further improves the voltage of all buses with more impact on the second cluster as second DG is installed on bus selected from the second

cluster. This results in shifting of the bus with minimum bus voltage, to the first cluster as given in Tables 4.11, 4.12, 4.13, and 4.14.

Table 4.14: Minimum Bus Voltage Before and After DG Integration for Industrial Load

DG Type	Minimum Bus Voltage @ Bus
No DG	0.9187 @ 65
Type-I DG (Single)	0.9697 @ 27
Type-I DG (Multiple)	0.9824 @ 65
Type-III DG (Single)	0.9729 @ 27
Type-III DG (Multiple)	0. 9869 @ 65

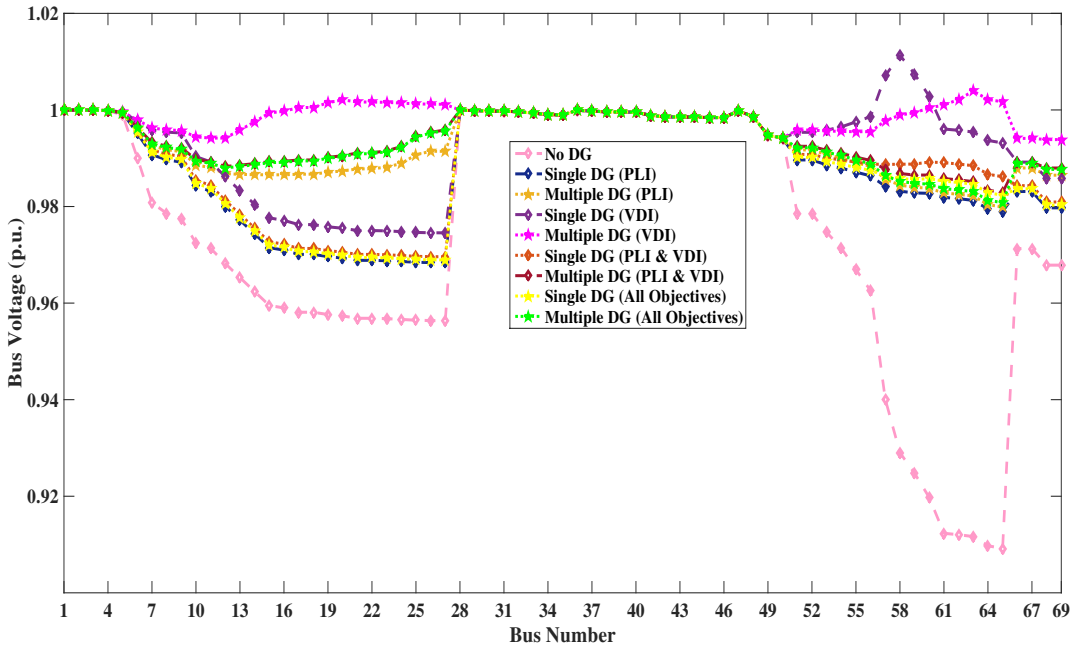

Fig. 4.11: Bus Voltage for Constant Load for Optimal Size of Type-I DG Corresponding to Different Objectives

The effect of objective selection on voltage profile of all buses is shown in Figure 4.11 considering Type-I DG for constant load model. Significant improvement in voltage of all buses is achieved after optimal integration of DG corresponding to all individual objectives and two cases of multi-objective optimization, but it is maximum for placement of multiple DGs corresponding to objective VDI except at few buses of the first cluster. This is due to the large size and location of single DG corresponding to objective VDI. Although there is an enhancement in voltage with the placement of optimal DG obtained corresponding to each objective, but the DG corresponding to PLI is resulting in minimum enhancement of bus voltages. Table 4.15 summarizes the effect of objective selection on the minimum bus voltage for constant load model.

Table 4.15: Effect of Objective on Minimum Bus Voltage After Integration of Type-I DG

Objective	Number of DGs	Minimum Bus Voltage @ Bus
——	No DG	0.9092 @ 65
PLI	Single	0.9684 @ 27
	Multiple	0.9799 @ 65
VDI	Single	0.9745 @ 27
	Multiple	0. 9939 @ 69
PLI & VDI	Single	0.9696 @ 27
	Multiple	0.9829 @ 65
All Objectives	Single	0.9689 @ 27
	Multiple	0. 9808 @ 65

4.8 CONCLUDING REMARKS

In this chapter, the multi-objective optimization based formulations are presented to decide the optimal placement of single and multiple DGs. The multi-objective optimization is solved by both non Pareto and Pareto front based formulations. For non Pareto approach, a MOF is derived by combining objectives through fuzzy decision. The optimization problems are solved by PSO. The modified PSO is used to suit Pareto based multi-objective optimization using concept of non-domination. The search space for the selection of optimal sites for DG placement is reduced by forming the cluster of buses. The proposed approach is implemented on 69-bus RDN for different voltage sensitive loads, such as residential, commercial and industrial. The optimal size and site of Type-I and Type-III DG are obtained by the presented approach. It is observed that the load types significantly affects the sites and sizes of DGs. It is also found that the integration of Type-III DG is more useful as it is yielding more reduction in all performances indices. The significant improvement in the voltage profile is observed at all buses after optimal sized DG integration at the optimal site. Moreover, the placement of multiple DGs is found to be more effective in improving the system performance as compared to placement of single DG. Two DGs are sufficient to improve the overall performance, for both single and multi-objective optimization for different loads. The true Pareto based optimization is yielding well diverse Pareto optimal front. The compromised optimal solution yielded from Pareto front and MOF formulation are different .

In this Chapter, the placement of single and multiple DGs have been investigated for multi-objective optimization. The placement of capacitors can significantly improve the DN

performance as far as losses and voltage profiles are concerned. Therefore, the concurrent allocation of DG and capacitor in RDN is the main focus to be investigated on the basis of single as well as multi-objective optimization for practical voltage-dependent loads in next Chapter 5.

Chapter–5

Optimal DG and Capacitor Placement

5.1 OVERVIEW

The capacitors have been prominently used to improve voltage profile, reduce reactive burden and diminution of losses. The allocation of DGs has gained interest as it benefits the system by diminishing losses as well as enhancing voltage of all buses, and by supplying increased load demand. The benefits of both DG and capacitor placement can be attained by the concurrent allocation of both in DNs. The simultaneous allocation of DG and capacitor is beneficial from economical view also, as the cost of DG is much higher. It is essential to find the optimal location and size of DG and capacitor to achieve the benefits of diminution in losses and enhancement in voltage profile. In this Chapter, separate and concurrent allocation of DG and capacitor is determined using both single and multi-objective optimization. The PLI and VDI are considered as objectives for the optimization. PSO is employed for single objective optimization and the multi-objective problem. The multi-objective optimization is investigated through a non Pareto based and true Pareto based formulation. A MOF is formulated by assigning fuzzy membership to each objective for non Pareto based formulation while the PLI and VDI are considered simultaneously for optimization using true Pareto based formulation.

5.2 OBJECTIVES FOR DG AND CAPACITOR PLACEMENT

The optimal allocation of DG and capacitor is attempted for the optimization of two objectives namely the active power loss index (PLI) and voltage deviation index (VDI). These objectives are given as:

Active Power Loss Index (PLI)

The power losses alter after assimilation of DG as well as capacitors in RDNs. The effectiveness of DG and capacitor assimilation on active power loss is deliberated by this index. Before the placement of DG and/or capacitor the value of PLI is 1, and it is desirable to diminish PLI. It is expressed as:

$$PLI = \frac{P_{loss}^{DG/Cap}}{P_{loss}} \tag{5.1}$$

where P_{loss} and $P_{loss}^{DG/Cap}$ are loss before and after placement of DG and/or capacitor respectively.

Voltage Deviation Index (VDI)

The optimal allocation of DG and/or capacitor has another benefit, *i.e.*, enhancement in voltage profile of all buses. This improvement is indicated by the diminished value of VDI, which indicates the deviation of bus voltages from reference bus. The VDI is 1 before placement of DG and/or capacitor, and it is desired to reduce its value to the minimum. It is expressed as:

$$VDI = \frac{VD^{DG/Cap}}{VD} \tag{5.2}$$

where VD and $VD^{DG/Cap}$ are measure of deviation in the bus voltage with respect to reference voltage before and after integration of DG and/or capacitor respectively. The VD is given by equation (4.9) and $V^{DG/Cap}$ is defined as:

$$VD^{DG/Cap} = \sum_{i=2}^{n} \left(\frac{V_{nom} - V_i^{DG/Cap}}{V_{nom}} \right)^2 \tag{5.3}$$

where $V_i^{DG/Cap}$ is voltage of i^{th} bus placement of DG and/or capacitor and V_{nom} is the nominal voltage taken as 1 p.u.

5.2.1 Multi-objective Problem Formulation

For DG and capacitor placement, PLI and VDI are considered as objectives. These objectives are conflicting as the decrease in PLI results in an increase in VDI and vice-versa.

These objectives are optimized by the true Pareto front based optimization. Correspondingly, the objective function is expressed as:

$$min(F) = min(PLI, VDI) \tag{5.4}$$

A set of Pareto optimal solutions is obtained through modified PSO. A compromised solution is selected by fuzzy cardinal ranking, which satisfies both objectives.

Also, these objectives are combined to formulate the MOF, which is optimized by PSO. The MOF framed by coalescing two objectives is expressed as:

$$minMOF = min[\mu_{PLI} \times PLI + \mu_{VDI} \times VDI] \tag{5.5}$$

The fuzzy membership value (μ) is computed for both PLI and VDI using equation (4.14).

The inequality constraints of bus voltage bounds and MVA capability of lines given by equations (4.16) and (4.17) respectively are imposed on objective functions represented by equation (5.4) and (5.5).

5.3 OPTIMAL ALLOCATION OF DG AND CAPACITOR USING PSO

5.3.1 Algorithm for MOF Based Optimization

Step 1 Read the DN line and bus data and the type of load.

Step 2 Carry-out the base case load flow using $BIBC$ and $BCBV$ matrices (Teng, 2008).

Step 3 Calculate the indices *i.e.*, PLI and VDI before placement of DG and/or capacitor.

Step 4 Initialize the particles positions that are random DGs and capacitors at random buses in the search space and set the iteration counter $k = 0$.

Step 5 For these positions, calculate load flow and check for constraints satisfaction. Compute the performance indices and corresponding membership functions using equation (4.14).

Step 6 Obtain the objective function from equation (5.5).

Step 7 For the positions, assign them as individual best positions (*pbest*). Also, identify the best of the *pbest* as global best (*gbest*).

Step 8 Update the particles positions by accounting their adaptive weight and current positions, *pbest* and *gbest* and increase iterations as $k = k + 1$.

Step 9 Go to Step 5 until the convergence is achieved.

5.3.2 Algorithm for Pareto Based Optimization

Step 1 Read the DN line data, bus data and the type of load.

Step 2 Carry-out the base case load flow using $BIBC$ and $BCBV$ matrices.

Step 3 Calculate the indices, namely PLI and VDI before placement of DG.

Step 4 Identify the cluster of buses for obtaining optimal site of DG and capacitor.

Step 5 Initialize the particles positions that are random DGs at random buses in the search space and set the iteration counter $k = 0$.

Step 6 For these positions, calculate load flow and check for constraints satisfaction. Compute the PLI and VDI.

Step 7 Assign these positions as individual best x_i^{pbest}.

Step 8 Apply non-dominated sorting to $\mathbf{X}^{pbest}$ to obtain a solution vector non-dominated solutions $\mathbf{X}^{gbest}$.

Step 9 Obtain the particle positions by using current position x_i, its best x_i^{pbest} and a randomly picked solution from non-dominated set $\mathbf{X}^{gbest}$.

Step 10 Obtain x_i^{pbest} as the non-dominated value between x_i^{pbest} and x_i.

Step 11 Set iteration $k = k + 1$.

Step 12 Go to Step 6 until the convergence is achieved.

Step 13 Compute the normalized membership β for each Pareto-optimal solution. Select the solution with maximum β as best compromised solution.

5.4 RESULTS AND DISCUSSIONS

For the location and sizing of DG and capacitors, two cases of optimization are considered, *i.e.* (i) single objective optimization where objectives are considered individually and (ii) multi-objective optimization. The multiple objectives are optimized through MOF based approach and true Pareto based approach. The approaches implemented for optimal allocation of DG and capacitor in this work are tested on 33-bus RDN and 69-bus RDN. The total load on 33-bus RDN is $3.720+j2.300$ MVA, while 69-bus RDN has a total load of $3.803 + j2.694$ MVA.

Table 5.1: Base Case Results for 33-bus RDN and 69-bus RDN

Load Model	Effective Load (MVA)	Active Power Loss (kW)	Voltage Deviation	*PLI*	*VDI*
33-Bus RDN					
Constant	3.720+j2.300	210.987	0.1338	1	1
Commercial	3.466+j1.940	159.501	0.0993	1	1
Residential	3.559+j1.875	164.541	0.1024	1	1
Industrial	3.773+j2.099	167.792	0.1034	1	1
69-Bus RDN					
Constant	3.803+j2.694	225.005	0.0993	1	1
Commercial	3.568+j2.340	165.050	0.0756	1	1
Residential	3.654+j2.274	170.834	0.0788	1	1
Industrial	3.773+j2.099	175.104	0.0813	1	1

As the practical loads are dependent on bus voltage magnitude, the effective load for different voltage-dependent load models reduces as tabulated in Table 5.1. The base case analysis for 33-bus RDN and 69-bus RDN is summarized through active power loss, voltage deviation, PLI, and VDI for various practical load models in Table 5.1. The algorithm is implemented under MATLAB, R2014b in MAC operating system. The PSO swarm size is taken as 50 and the algorithm has been implemented for 100 iterations for single as well as multi-objective optimization. The best results are presented after 10 runs of PSO.

5.4.1 Single Objective DG and Capacitor Placement

The DG and capacitor are placed individually as well as simultaneously considering PLI and VDI as separate objectives. The effectiveness of integrating DG and capacitor individually

and concurrently is investigated for 33-bus and 69-bus RDNs considering constant load model. Tables 5.2 and 5.3 present the optimal allocation of DG and capacitor individually as well as simultaneously for 33-bus RDN and 69-bus RDN, respectively. From Table 5.2 and 5.3 following observations are made:

Table 5.2: Optimal Size and Location of DG and Capacitor, PLI and VDI for 33-Bus RDN

Objective	**DG Size (MW) @ Location**	**Capacitor Size (MVAr) @ Location**	***PLI***	***VDI***
PLI	2.5839 @ 6	———	0.5262	0.2830
	———	1.2563 @ 30	0.7174	0.6268
	2.5501 @ 6	1.7379 @ 6	0.3216	0.1242
VDI	3.7362 @ 6	———	0.5716	0.1673
	———	2.2066 @ 30	0.8617	0.4424
	3.2843 @ 6	3.4211 @ 6	0.5207	0.0300

Table 5.3: Optimal Size and Location of DG and Capacitor, PLI and VDI for 69-Bus RDN

Objective	**DG Size (MW) @ Location**	**Capacitor Size (MVAr) @ Location**	***PLI***	***VDI***
PLI	1.8729 @ 61	———	0.3696	0.2015
	———	1.3310 @ 61	0.6758	0.6445
	1.8507 @ 61	1.2919 @ 61	0.1029	0.1172
VDI	2.9815 @ 58	———	0.5706	0.1016
	———	2.6752 @ 58	0.9395	0.4605
	2.2506 @ 61	2.4841 @ 61	0.3797	0.0779

- The optimal size and site of DG and capacitor is determined by the selection of objective.
- The integration of DG and capacitor results in the reduction of losses and voltage deviation.
- The size of DG and capacitor is large when VDI is selected as objective in comparison to the size of DG and capacitor obtained corresponding to objective PLI.
- The integration of DG and capacitor simultaneously is more effective in comparison to individual placement of DG and capacitor.
- The concurrent allocation of DG and capacitor yields a reduced size of DG as compared to individual DG allocation.

It is observed from Tables 5.2 and 5.3 that, the size and location of both DG and capacitor are governed by the objective. The optimal location of capacitor and DG is the same for 69-bus RDN; while it is different for 33-bus RDN when DG and capacitor are placed individually. It is also observed that integration of capacitor along with DG reduces the size of DG as compared to its size when only DG is placed which leads additional benefit regarding cost, as the cost of DG is much higher in comparison to the cost of a capacitor. The enhancement in voltage profile of all buses is indicated by index VDI as it is reducing after integration of DG and capacitor. Also, the diminution in value of PLI from its initial value indicates diminution in active power losses after placement of DG and capacitor either individually or simultaneously. Although the placement of both DG and capacitor is beneficial, but DG is more efficient in comparison to capacitor when placed individually, while when DG and capacitor are placed simultaneously, the diminution in PLI and VDI is even more.

As shown in Table 5.2, with the integration of individual DG, individual capacitor and simultaneous DG and capacitor of optimum size at respective optimum locations for optimizing PLI in 33-bus RDN; PLI reduces to 0.5262, 0.7174 and 0.3216, respectively and VDI reduces to 0.2830, 0.6268 and 0.1242, respectively. The improvement in PLI or VDI is minimum with individual capacitor placement. With the optimal integration of DG and capacitor separately and concurrently corresponding to VDI optimization, PLI reduces to 0.5716, 0.8617 and 0.5207; VDI reduces to 0.1673, 0.4424 and 0.0300 respectively for 33-bus RDN. The results of Tables 5.2 and 5.3 also reflect that both PLI and VDI reduce after separate and simulataneous integration of DG and capacitor regardless of considered objective, although the diminution in master objective is more. Similar observations are made for 69-bus RDN. As the simultaneous placement of DG and capacitor is found more effective, so it is considered for single and multi-objective optimization for voltage-dependent practical loads.

The optimal placement of DG and capacitor for various voltage-dependent practical loads is presented in Table 5.4 and Table 5.5 for PLI and VDI optimization, respectively. It is observed from these tables that, for both 33-bus and 69-bus RDNs the optimal size of DG and capacitor is affected by load model while the optimal location is independent of the load model. Also, there is a significant reduction in PLI and VDI after placement of DG and capacitor for all load models. It is also observed from Tables 5.4 and 5.5 that the capacity of DG and capacitor is largest for the constant load.

Table 5.4: Effect of Load Model on DG and Capacitor Placement for Objective PLI

Load Model	DG Size (MW) @ Location	Capacitor Size (MVAr) @ Location	PLI	VDI
33-Bus RDN				
Constant	2.5501 @ 6	1.7379 @ 6	0.3216	0.1242
Commercial	2.5008 @ 6	1.3715 @ 6	0.3863	0.1626
Residential	2.1326 @ 6	1.2349 @ 6	0.3856	0.2257
Industrial	2.3939 @ 6	1.4007 @ 6	0.3675	0.1711
69-Bus RDN				
Constant	1.8507 @ 61	1.2919 @ 61	0.1029	0.1177
Commercial	1.8501 @ 61	1.1715 @ 61	0.1331	0.1472
Residential	1.8472 @ 61	1.1850 @ 61	0.1288	0.1432
Industrial	1.8065 @ 61	1.2961 @ 61	0.1237	0.1387

Table 5.5: Effect of Load Model on DG and Capacitor Placement for Objective VDI

Load Model	DG Size (MW) @ Location	Capacitor Size (MVAr) @ Location	PLI	VDI
33-Bus RDN				
Constant	3.2843 @ 6	3.4211 @ 6	0.5207	0.0300
Commercial	3.0288 @ 6	3.2579 @ 6	0.6167	0.0415
Residential	3.2813 @ 6	2.7889 @ 6	0.5289	0.0441
Industrial	2.8387 @ 6	3.3969 @ 6	0.6168	0.0424
69-Bus RDN				
Constant	2.1020 @ 58	2.8663 @ 58	0.4861	0.0414
Commercial	2.0535 @ 58	2.4745 @ 58	0.4991	0.0985
Residential	2.0843 @ 58	2.4702 @ 58	0.4820	0.0951
Industrial	2.0285 @ 58	2.6705 @ 58	0.5392	0.0917

5.4.2 MOF Optimization for DG and Capacitor Placement

The placement of DG and capacitor separately and concurrently for optimization of PLI and VDI is achieved through formulation of MOF using non Pareto based approach.

The optimal allocation of DG and capacitor individually and simultaneously, for the constant load attained by non Pareto based optimization though PSO is summarized in Table5.6 for both 33-bus and 69-bus RDNs. Similar to single objective optimization, concurrent placement of DG and capacitor is best suited to optimize PLI and VDI.

Table 5.6: Non Pareto Based Multi-Objective Optimal Placement of DG and Capacitor

Test System	**DG Size (MW) @ Location**	**Capacitor Size (MVAr) @ Location**	***PLI***	***VDI***
33-Bus RDN	3.0357 @ 6	———	0.5390	0.2092
	———	1.6888 @ 30	0.7479	0.5340
	2.7572 @ 6	1.9894 @ 6	0.3273	0.0889
69-Bus RDN	2.0812 @ 61	———	0.3763	0.1673
	———	1.7568 @ 61	0.7073	0.5598
	1.9942 @ 61	1.3810 @ 61	0.1078	0.1074

It is also observed from Tables 5.2, 5.3 and 5.6 that, the size of DG and capacitor obtained corresponding to the multi-objective problem is large, as compared to their size obtained corresponding to objective PLI; while it is small as compared to their size obtained corresponding to objective VDI. For 33-bus RDN considering constant load model, the size of DG corresponding to objectives PLI, VDI, and both PLI and VDI is 2.5501 MW, 3.2843 MW and 2.7572 MW respectively; while the size of the capacitor is 1.7379 MVAr, 3.4211 MVAr and 1.9894 MVAr respectively. The similar trend is followed in 69-bus RDN.

It is also concluded from Tables 5.2, 5.3 and 5.6 that, DG and capacitor size is a compromised solution for the multi-objective problem in comparison to the single-objective problem. For example, the reduction in PLI is 0.3216, 0.5207 and 0.3273 after concurrent integration of DG and capacitor for 33-bus RDN obtained corresponding to objectives PLI, VDI and both PLI and VDI, respectively. The VDI reduces to 0.1242, 0.0300 and 0.0889 after simultaneous integration of DG and capacitor of optimal size obtained corresponding to objectives PLI, VDI and both PLI and VDI, respectively. The diminution in PLI is maximum when the objective is PLI and minimum when the objective is VDI, while diminution in VDI is maximum, when VDI is objective and minimum when PLI is objective, and the compromised values of PLI and VDI are attained when both objectives are considered simultaneously. In case of multi-objective optimization, individual objectives are inferior as compared to corresponding single objective optimization. Similar observations are made for 69-bus RDN also.

Table 5.7: Optimal Size and Site of DG and Capacitor Considering PLI and VDI as Objectives

Load Model	DG Size (MW) @ Location	Capacitor Size (MVAr) @ Location	*PLI*	*VDI*
33-Bus RDN				
Constant	2.7572 @ 6	1.9894 @ 6	0.3273	0.0889
Commercial	2.7621 @ 6	1.5140 @ 6	0.3947	0.1226
Residential	2.9565 @ 6	1.5388 @ 6	0.3982	0.1018
Industrial	2.8743 @ 6	1.4993 @ 6	0.3818	0.1104
69-Bus RDN				
Constant	1.9942 @ 61	1.3810 @ 61	0.1078	0.1074
Commercial	1.9424 @ 61	1.1950 @ 61	0.1354	0.1395
Residential	1.9492 @ 61	1.1896 @ 61	0.1323	0.1356
Industrial	1.9889 @ 61	1.3949 @ 61	0.1298	0.1250

As it has been identified for multi-objective problem also, the concurrent allocation of DG and capacitor is beneficial in comparison to their individual placement, so the effect of load models is considered only on concurrent allocation. The similar trend is followed in the placement of DG and capacitor for practical voltage-dependent load models *i.e.* commercial, residential and industrial as in case of constant load model. Table 5.7 summarizes the optimal size and site of DG and capacitor as well as PLI and VDI for 33-bus RDN and 69-bus RDN for multi-objective optimization. It is accomplished that the optimum size of DG and capacitor is contingent on load model while optimal location remains same for all loads for both 33-bus RDN and 69-bus RDN.

5.4.3 Pareto Based Optimization for DG and Capacitor Placement

The PLI and VDI are optimized through true Pareto based approach by simultaneous allocation of DG and capacitor. The Pareto fronts indicating set of non-dominating solutions, obtained for simultaneous allocation of DG and capacitor are shown in Figure 5.1 and Figure 5.2 for 33-bus and 69-bus RDNs, respectively. The compromised solution optimizes both PLI and VDI upto some extent. The individual and simultaneous DG and capacitor optimal allocation yielded through true Pareto based optimization is summarized in Table 5.8 for constant load model.

Similar to non Pareto based approach, simultaneous placement of DG and capacitor is more beneficial as compared to their individual placement. As shown in Figure 5.1 and Figure 5.2 the Pareto fronts are well diverse for both 33-bus and 69-bus RDNs. While, comparing the best compromised solution summarized in Table 5.8 with optimal solution yielded by MOF formulation summarized in Table 5.6, it is observed that different solutions are yielded. The difference is mainly due to different formulation.

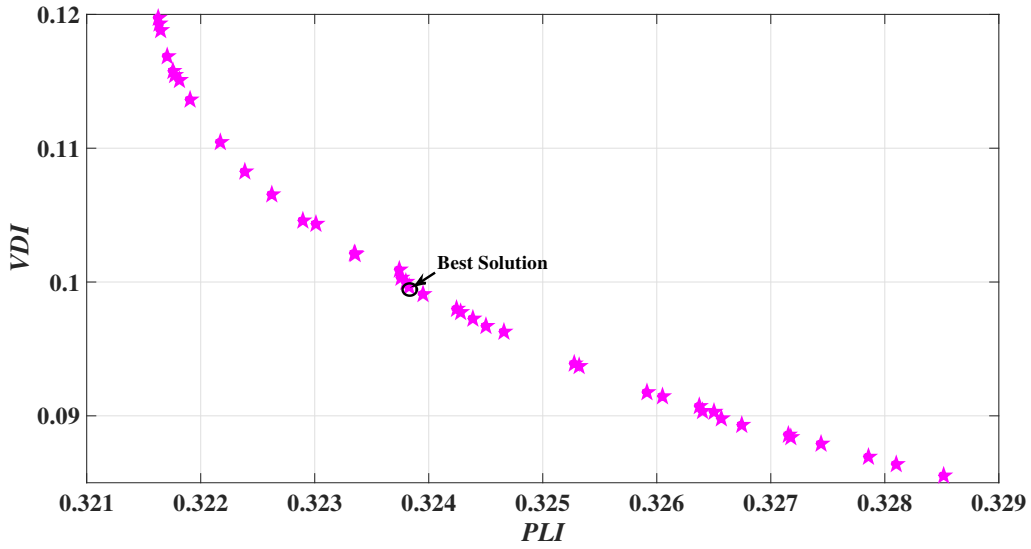

Fig. 5.1: Pareto Front for Concurrent DG and Capacitor Placement for 33-Bus RDN

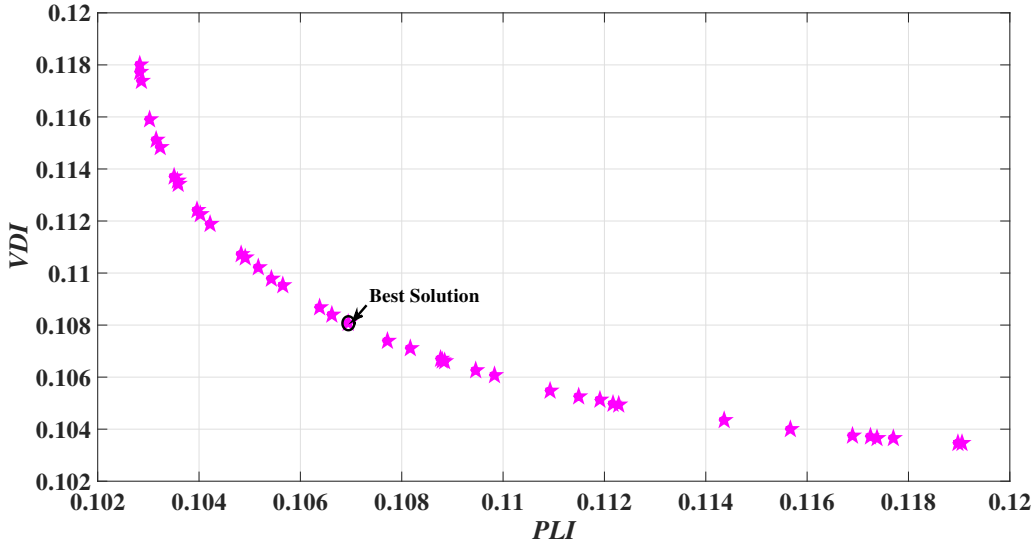

Fig. 5.2: Pareto Front for Concurrent DG and Capacitor Placement for 69-Bus RDN

Table 5.8: Pareto Based Multi-Objective Optimal Placement of DG and Capacitor

Test System	DG Size (MW) @ Location	Capacitor Size (MVAr) @ Location	*PLI*	*VDI*
33-Bus RDN	2.8883 @ 6	———	0.5320	0.2318
	———	1.6880 @ 30	0.7450	0.5381
	2.7143 @ 6	1.8663 @ 6	0.3238	0.0996
69-Bus RDN	1.9864 @ 61	———	0.3716	0.1817
	———	1.5928 @ 61	0.6878	0.5910
	1.9774 @ 61	1.3787 @ 61	0.1069	0.1081

5.4.4 Bus Voltage after DG and Capacitor Placement

As the integration of DG and capacitor in DN enhances the voltage profile, thus the effect of individual and concurrent integration of DG and capacitor is investigated. The enhancement in the voltage level of 33-bus RDN and 69-bus RDN is shown correspondingly in Figures 5.3 and 5.4 following the allocation of optimal sized only DG, only capacitor and both DG and capacitor at the corresponding optimum site for constant load model achieved by PSO. Although both DG and capacitor are effectual for enhancement of voltage individually, but the simultaneous placement of DG and capacitor is most effective, and individual capacitor placement is least effective.

The minimum bus voltage before DG and capacitor placement is found to be 0.9038 at bus 18 and 0.9092 at bus 65 for 33-bus RDN and 69-bus RDN, respectively. The enhancement in voltage of bus 18 in 33-bus RDN and bus 65 in 69-bus RDN after allocation of optimum sized DG and capacitor at optimum location obtained from multi-objective optimization for constant load model is tabulated in Table 5.9.

Table 5.9: Enhancement in Voltage of Bus with Lowest Voltage

Test System	33-Bus RDN	69-Bus RDN
Before DG and Capacitor Placement	0.9038	0.9092
With Only Capacitor Placement	0.9204	0.9369
With Only DG Placement	0.9487	0.9860
Both DG and Capacitor Placement	0.9634	1.0035

As optimal size and site of DG and capacitor are influenced by considered objective, the effect of objective selection is also investigated on the voltage enhancement. Figures 5.5 and 5.6

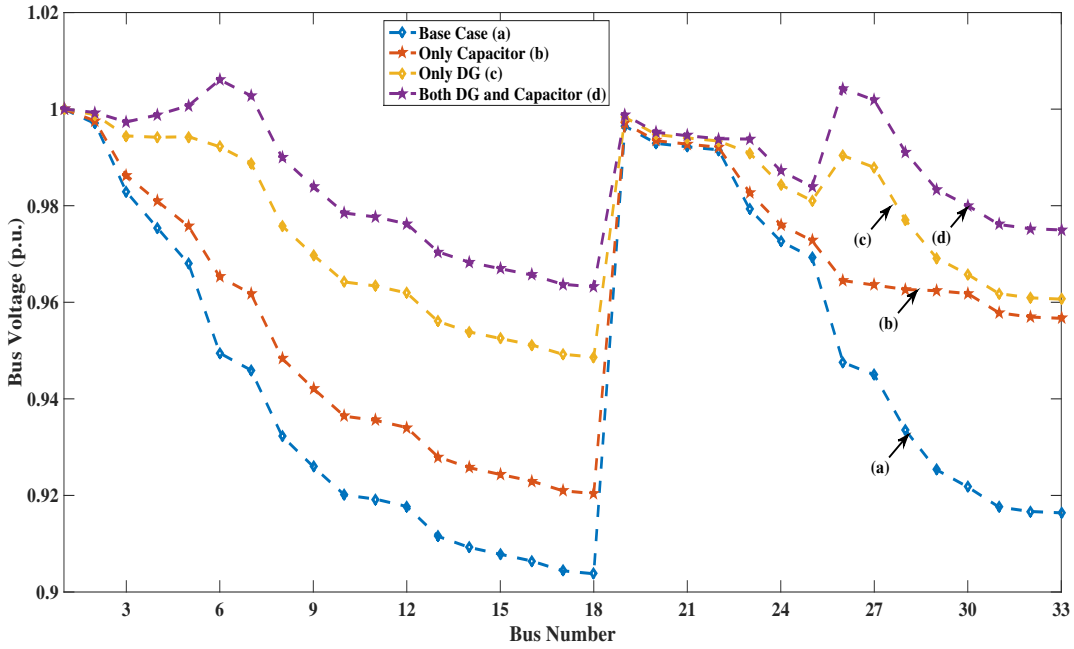

Fig. 5.3: Voltage Variation for Constant Load Model 33-bus RDS for Multi-Objective Optimization

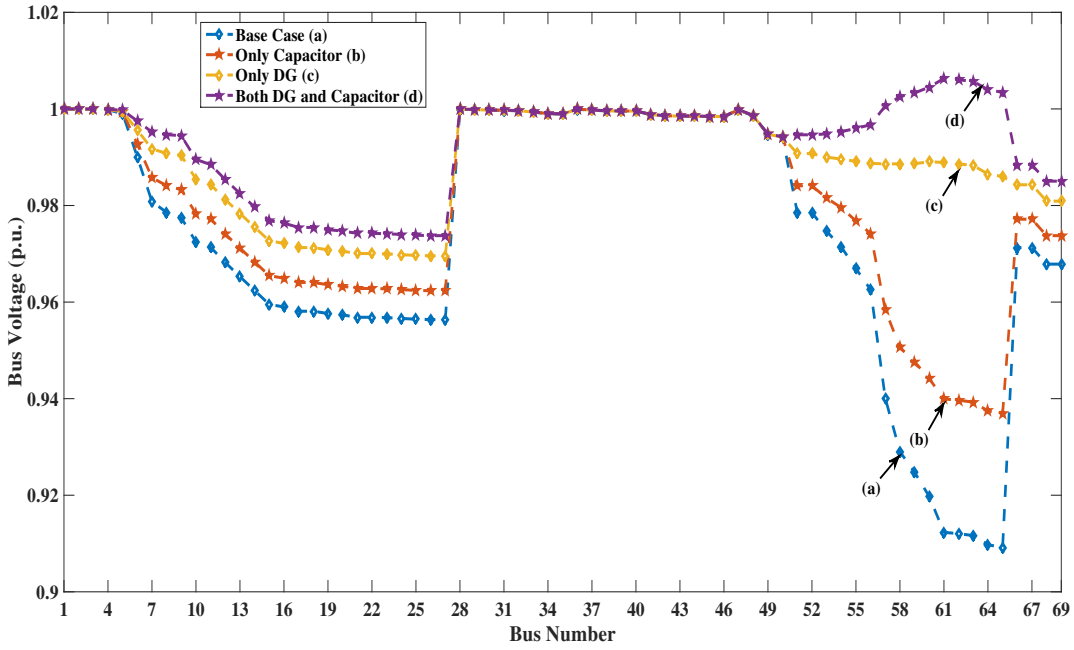

Fig. 5.4: Voltage Variation for Constant Load Model 69-bus RDS for Multi-Objective Optimization

illustrate the influence of objective selection on the voltage level of all buses for 33-bus RDN and 69-bus RDN, respectively after optimal allocation of DG and capacitor corresponding to three cases of objectives.

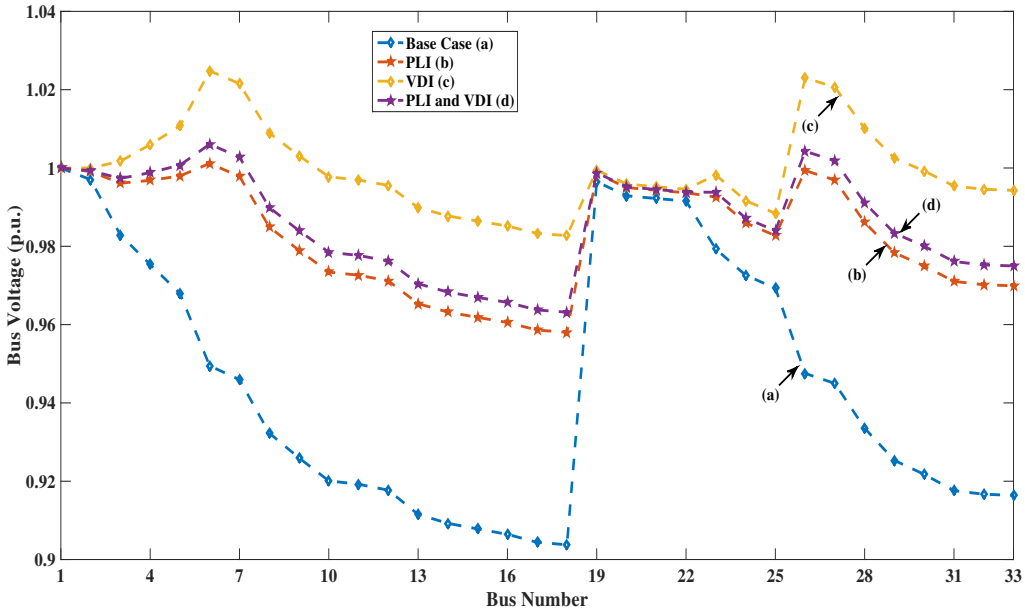

Fig. 5.5: Effect of Objective on Voltage of 33-Bus RDN for Integration of DG and Capacitor

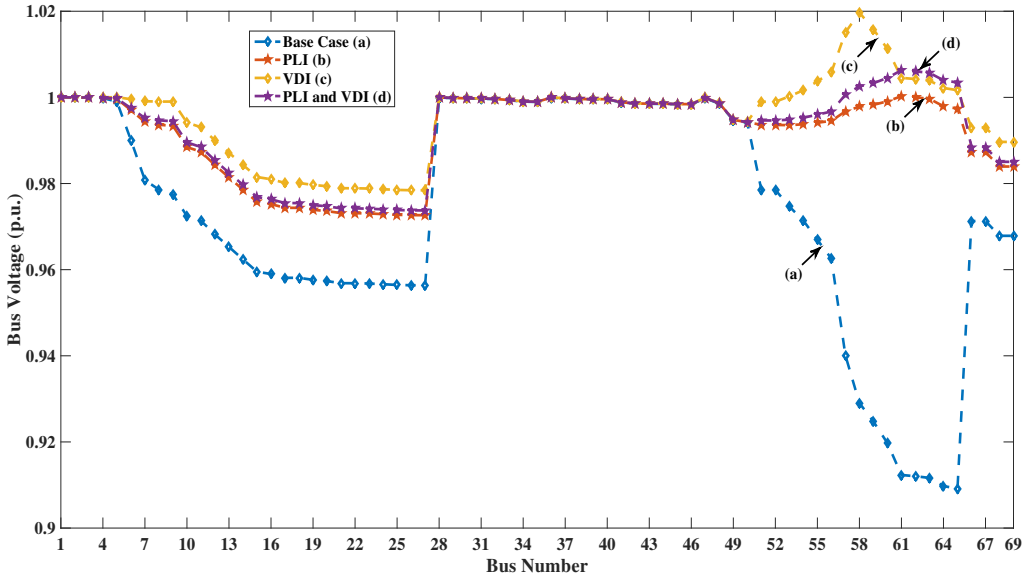

Fig. 5.6: Effect of Objective on Voltage of 69-Bus RDN for Integration of DG and Capacitor

Although there is a substantial enhancement in voltage profile in each case in comparison to the base case, but maximum improvement is obtained corresponding to objective VDI, minimum

corresponding to PLI and intermediary for the multi-objective case. Also, the voltage of all buses is within limits imposed by bus voltage constraint. A summary of the effect of objective selection on the minimum bus voltage for constant load model is presented in Table 5.10. Similar effect of objective on bus voltage is observed for the voltage-dependent load models.

Table 5.10: Minimum Bus Voltage After Integrating Both DG and Capacitor

Objective	**33-Bus RDN**	**69-Bus RDN**
	Minimum Bus Voltage @ Bus	
Base Case	0.9038 @ 18	0.9092 @ 65
PLI	0.9580 @ 18	0.9726 @ 27
VDI	0.9827 @ 18	0.9784 @ 27
PLI & VDI	0.9632 @ 18	0.9738 @ 27

5.4.5 Comparative Results

The proposed approaches are verified on 33-bus RDN as well as on 69-bus RDN for distinct load models. The results obtained by proposed approach are justified by comparing them with already published results in literature for constant load model. Table 5.11, using the results from Table 5.2 and Table 5.3, summarizes the comparison of size, location and diminution in active and reactive power after placement of both DG and capacitor simultaneously corresponding to objective PLI. It is found that the optimal capacity and location of DG and capacitor obtained using the proposed PSO are more effective in reducing both active and reactive power losses in comparison to PSO (Kansal *et al.*, 2015) because of identification of potential buses and better search.

Table 5.11: Comparative Results for Optimization of PLI for Constant Load Model

Approach	**PSO (Kansal *et al.*, 2015)**	**Proposed PSO**	**PSO (Kansal *et al.*, 2015)**	**Proposed PSO**
Test System	**33-bus RDN**		**69-bus RDN**	
DG Size (MW) @ Location	1.5000 @ 30	2.5501 @ 6	1.5000 @ 61	1.8507 @ 61
Capacitor Size (MVAr) @ Location	0.9000 @ 30	1.7379 @ 6	1.2000 @ 61	1.2919 @ 61
Active Power loss (kW)	75.650	67.864	27.200	23.150
Reactive Power loss (kVAr)	56.130	54.824	17.400	14.344

The comparison of results pertaining to multi-objective optimization through Pareto and non-pareto based approaches, utilizing the results from Table 5.6 and Table 5.8, are summarized in Table 5.12. It is observed that the reduced size of both DG and capacitor is achieved through Pareto based approach for both 33-bus and 69-bus RDNs. Corresponding to these values of DG and capacitor, both active and reactive power losses are reduced. As the optimization was carried out with the consideration of PLI and VDI, the results from non-pareto and Pareto based formulations are found to be non-dominating (improvement in PLI, deteriorate VDI) for both the DNs.

Table 5.12: Comparative Results for Multi-objective Optimization for Constant Power Load

Approach	**Non Pareto based**	**Pareto based**	**Non Pareto based**	**Pareto based**
Test System	**33-bus RDN**		**69-bus RDN**	
DG Size (MW) @ Location	2.7573 @ 6	2.7143 @ 6	1.9942 @ 61	1.9774 @ 61
Capacitor Size (MVAr) @ Location	1.9894 @ 6	1.8663 @ 6	1.3810 @ 61	1.3787 @ 61
Active Power loss (kW)	69.067	68.323	24.247	24.062
Reactive Power loss (kVAr)	55.959	55.369	14.496	14.446
PLI	0.3273	0.3238	0.1078	0.1069
VDI	0.0889	0.0996	0.1074	0.1081

5.5 CONCLUDING REMARKS

In this Chapter, the concurrent optimal allocation of DG and capacitor is achieved for single as well as multi-objective optimization. In addition to concurrent placement of DG and capacitor, both are optimally placed individually also. For multi-objective optimization, two formulations are employed. A single solution is yielded through optimization of MOF formulated by assigning fuzzy membership to objectives while a set of non dominated solutions is yielded by true Pareto based approach. The optimal solutions are obtained through PSO for all formulations.

The suggested methodologies are realized on 33-bus RDN and 69-bus RDN for various voltage-dependent loads. It is accomplished that, the location and size of DG and capacitor are significantly affected by the type of load and objective. It is also perceived that the voltage level of all buses is enhanced significantly after assimilation of DG and capacitor of optimum size at the optimum location. Moreover, the simultaneous allocation of DG and capacitor is more

effective in comparison to the individual allocation of DG and capacitor due to higher reduction in the both indices. Also with the simultaneous allocation of DG and capacitor, the size of DG significantly reduces which, improves the economy of overall RDN, as the cost of DG is high. Diverse Pareto fronts are obtained for Pareto based formulation. The optimal solutions from MOF and best compromised solutions from Pareto based optimization are different.

The analysis on optimal allocation of DGs so far is carried out for voltage-dependent practical loads. The practical aspect has been extended to find the allocation of DG and capacitor by including the uncertainty in load in the next Chapter 6.

Chapter–6

Probabilistic Allocation of DG and Capacitor for Uncertain Load

6.1 OVERVIEW

The optimal placement of DGs has been done in last decades extensively, but it is mostly done with deterministic approach. The loads in practical DNs are not constant, but possess some amount of randomness / uncertainty due to the presence of number of consumers utilizing different loads. The uncertainty in load patterns calls for the need of probabilistic approach in modeling and analysis. As the optimal size of DG and capacitor are governed by the load of DN, the uncertainty in load has impact on DG and capacitor size. The optimal allocation of DG and capacitor in presence of these uncertainties is termed as probabilistic allocation.

The random variations in load of practical DN are considered in this Chapter for determination of optimal size of DG and capacitor. These variations are specified by probabilistic measures of mean and standard deviation to base load. The load has been sampled by two different techniques namely Monte Carlo Simulation (MCS) and Latin Hypercube Sampling (LHS). The MCS randomly generates samples of data whereas LHS generates normally distributed load samples. The MCS although requires large number of samples and higher simulation time, it is the benchmark method used in probabilistic analysis to validate other sampling methods. The LHS can be regarded as a constrained version of MCS sampling without getting struck to samples getting clustered around an interval.

The probabilistic allocation defines the probability and probable size of DG and capacitor for uncertain randomly varying loads. The probabilistic allocation of individual DG, and DG and capacitor concurrently is investigated for single and multi-objective optimization.

6.2 MONTE CARLO SIMULATION

The MCS is a sampling technique in which, random values are chosen for variables *i.e.* active and reactive power loads. The random value is decided on the basis of mean and standard deviation describing density function. For optimal placement of DG and capacitor, the optimization is solved using these random values of variables. The optimization outcome is recorded, and the procedure is repeated for next set of random values of the variables. A typical MCS repeats the procedure for M samples using randomly selected values each time.

The random sample, x can be formulated mathematically as:

$$x = randn \times \sigma(x) \times \mu(x) + \mu(x) \tag{6.1}$$

where $randn$ is normally distributed random number; $\mu(x)$ is mean of variable x; $\sigma(x)$ is standard deviation of variable x.

The MCS is employed to generate samples of load data for determination of optimal size of DG and capacitor. The major steps required in MCS are:

1. Sample the input variables *i.e.* active and reactive power loads on each bus, from the given probability distributions.
2. Obtain the output vector of variables of interest *i.e.* power loss, voltage deviation, bus voltages, DG and capacitor size, corresponding to each input vector by deterministic allocation of individual DG or DG and capacitor concurrently.
3. The steps 1 and 2 are repeated for sufficiently large number of samples.
4. From the output vector, compute the frequency and probability distribution of output variables of interest.

6.3 LATIN HYPERCUBE SAMPLING

It is an efficient sampling technique that covers the random distribution of a variable entirely. In LHS, the sampling of variable is not repeated. In this technique, the sample size is predefined and

the probability distribution function (PDF) is divided into M samples. One sample is selected from each interval randomly. The sampling of variable is done over the entire spectrum of PDF including the tail-end values.

The LHS technique has two phases *i.e.* sampling and permutation. The sampling leads to normally distributed representative samples of the uncertain variable. The permutation is performed to reduce the correlations between different variables.

By using LHS, a random sample x can be formulated mathematically as:

$$x = \mu(x) + ltqnorm(P) \times \sigma(x) \tag{6.2}$$

where $\mu(x)$ is mean of variable x; $\sigma(x)$ is standard deviation of variable x; $ltqnorm(P)$ returns the lower tail quantile for the standard normal distribution function and P is given as:

$$P = \frac{randperm(M) - randn(M)}{M} \tag{6.3}$$

where M is sample size; $randperm$ is random permutation; $randn$ is normally distributed random number.

The procedure for generating samples of load data employing LHS can be presented as follows:

1. Specify sample size.
2. Construct the distribution function of active and reactive power load.
3. Divide the load distribution functions into M subintervals with equal probability.
4. Randomly sample the load without repetition from each subinterval
5. Perform the random permutation to generate load samples.

6.4 OBJECTIVES FOR PROBABILISTIC ALLOCATION OF DG AND CAPACITOR

The probabilistic allocation of DG separately, DG and capacitor simultaneously, performed for uncertain randomly varying active and reactive power loads. The active power loss index (PLI)

and voltage deviation index (VDI) are contemplated as objectives for probabilistic allocation. The formulation of PLI and VDI is presented by equation (5.1) and equation (5.2) respectively, and reproduced here as equation (6.4) and equation (6.5) for ready reference.

$$PLI = \frac{P_{loss}^{DG/Cap}}{P_{loss}} \tag{6.4}$$

$$VDI = \frac{VD^{DG/Cap}}{VD} \tag{6.5}$$

These are considered separately and simultaneously formulating single objective and multi-objective problem respectively. The MOF formulated by equation (5.5) for multi-objective optimization is reproduced here as equation (6.6).

$$minMOF = min[\mu_{PLI} \times PLI + \mu_{VDI} \times VDI] \tag{6.6}$$

The value of PLI and VDI is 1 before the placement of DG and capacitor and it is desirable to diminish these indices by optimal integration of DG separately, and DG and capacitor simultaneously. The PLI is measure of active power loss reduction while VDI is measure of diminution in voltage deviation of all buses of DN.

6.5 ALGORITHM FOR PROBABILISTIC ALLOCATION OF DG AND CAPACITOR

The load data obtained from two different methods of sampling is utilized for the probabilistic allocation of DG; and DG and capacitor concurrently. The procedure of sampling is although distinct for MCS and LHS, the computational procedure for probabilistic allocation is same. The probabilistic allocation is carried out for single objective optimization of different indices and MOF optimization for multi-objective. The MOF is resulting in single membership to be optimized. Therefore, optimization algorithm steps are similar. The procedure for the probabilistic allocation of DG and capacitor concurrently, employing MCS or LHS can be attained through the following steps:

Step 1 Read the DN line and bus data, the sample size (M) and probabilistic distributions (*i.e.* mean and standard deviation) of uncertain active and reactive power load on each bus.

Step 2 Count the number of input variables as K, which depends on buses.

Step 3 For MCS employ sampling procedure described in section 6.2 while for LHS employ the sampling and permutation procedures described in section 6.3 to yield the sampling matrix with dimension $K \times M$.

Step 4 Set the sample count $m = 1$.

Step 5 Perform deterministic allocation of individual DG or DG and capacitor concurrently using PSO, with the m^{th} column of the sampling matrix to obtain the values of PLI (power loss), VDI (voltage deviation), bus voltages, DG and capacitor size.

Step 6 Set $m = m + 1$; go to Step 5 if $m \leq M$ for deterministic allocation of individual DG or DG and capacitor concurrently, using the next column of the sampling matrix.

Step 7 Compute the statistical information (*i.e* mean and standard deviation) of output variables such as power loss, voltage deviation, bus voltages, DG and capacitor size.

6.6 RESULTS AND DISCUSSIONS

The probabilistic allocation of only DG, and DG and capacitor simultaneously is attained for uncertainty in active and reactive power load. This uncertainty is accommodated by sampling of load data by MCS and LHS described in sections 6.2 and 6.3, respectively. The sampled load data is utilized for single as well multi-objective placement of individual DG, and DG and capacitor concurrently through the PSO algorithm described in section 6.5. The allocation is carried out at bus 6 for 33-bus RDN because it resulted as optimal location for DG and capacitor placement in Chapter 5.

The algorithms for sampling and optimization using PSO are implemented in MATLAB, R2014b in MAC operating system. The swarm size is considered as 50 and algorithm is evaluated for 100 iterations. The sample size is taken as 1000 and 100 for MCS and LHS, respectively. The probability distributions for active and reactive load are formulated by considering base load as mean with 10% variation. After random sampling, the mean and standard deviation are calculated again, which differ slightly and are given in Appendix C, as Table C.1.

The probable optimal size of DG and capacitor are achieved for all load samples. Correspondingly, the frequency distribution is presented by histograms. The PDFs for DG and capacitor size are also obtained and a comparison is made between the results obtained through two sampling techniques. The reduction in active power loss and voltage deviation is also analyzed by PDFs. The analysis of voltage variation is done for bus 6 and bus 18. It is worth mentioning that bus 6 has been selected for location for DG and capacitor integration, whereas bus 18, is the bus with lowest voltage for base case load as obtained in Chapter 5. The allocation of DG individually and concurrently with capacitor is achieved for separate and simultaneous optimization of PLI and VDI forming single and multi-objective problems, which are discussed in following sections.

6.6.1 Single Objective Allocation of DG

The probabilistic allocation of DG for single objective optimization is investigated for minimization of PLI and minimization of VDI.

With the sampling, different DG sizes are expected corresponding to each load sample, however some sizes are repetitive. The frequency of DG size repetition achieved through MCS and LHS is shown in Figures 6.1 (a) and (c), respectively. It is observed from Figures 6.1 (a) and (c) that the variation in DG size is more for MCS as compared to LHS. The PDF of DG size occurrence is computed and presented in Figures 6.1 (b) and (d) for MCS and LHS, respectively. These PDFs follow the normal distribution, which is on the expected lines because the load variation is considered with normal distribution.

The mean DG size and deviation in DG size obtained from two different techniques, are summarized in Table 6.1. Both sampling methods are yielding the DG size approximately as 2.59 MW for the load variation of 10% for integration at bus 6 in 33-bus RDN. This DG size is regarded as probable DG size because it has maximum probability for occurrence for randomly varying load.

The probable optimal size of DG is also attained for optimization of VDI. The histograms indicating the frequency of DG size repetition are presented in Figures 6.2 (a) and (c)

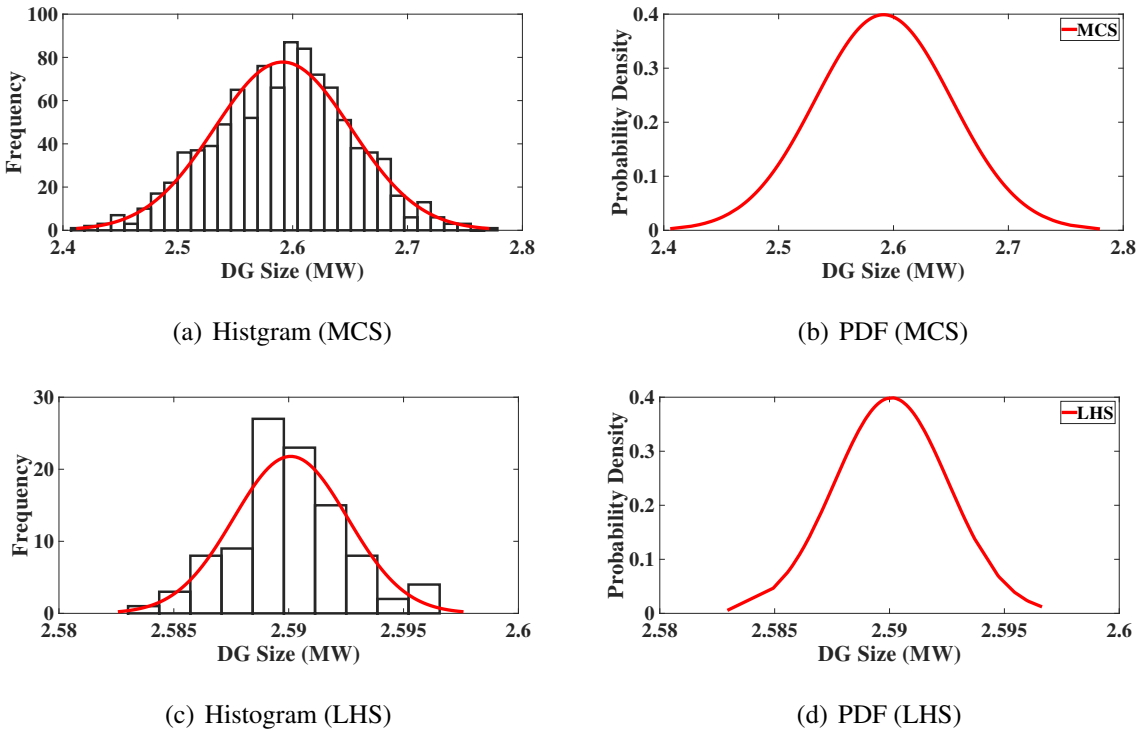

(a) Histgram (MCS)

(b) PDF (MCS)

(c) Histogram (LHS)

(d) PDF (LHS)

Fig. 6.1: Histogram and PDF of DG Size for PLI Optimization

Table 6.1: DG Size Statistics for Optimization of PLI

MCS		**LHS**	
μ	σ	μ	σ
2.5914 MW	0.0594 MW	2.5901 MW	0.0025 MW

corresponding to load samples generated through MCS and LHS. Correspondingly, the PDFs of DG size are shown in Figures 6.2 (b) and (d) for MCS and LHS, respectively. The probable DG sizes yielded for minimizing VDI through MCS and LHS are presented in Table 6.2. Similar to DG size acquired in PLI optimization, it is observed from Figures 6.2 (a-d) that the variation in DG size is less for LHS in comparison to MCS.

It is evident from Tables 6.1 and 6.2 that the probable DG size for VDI optimization is large as compared to PLI optimization.

Table 6.2: DG Size Statistics for Optimization of VDI

MCS		**LHS**	
μ	σ	μ	σ
3.7382 MW	0.0849 MW	3.7362 MW	7.6799 $\times 10^{-4}$ MW

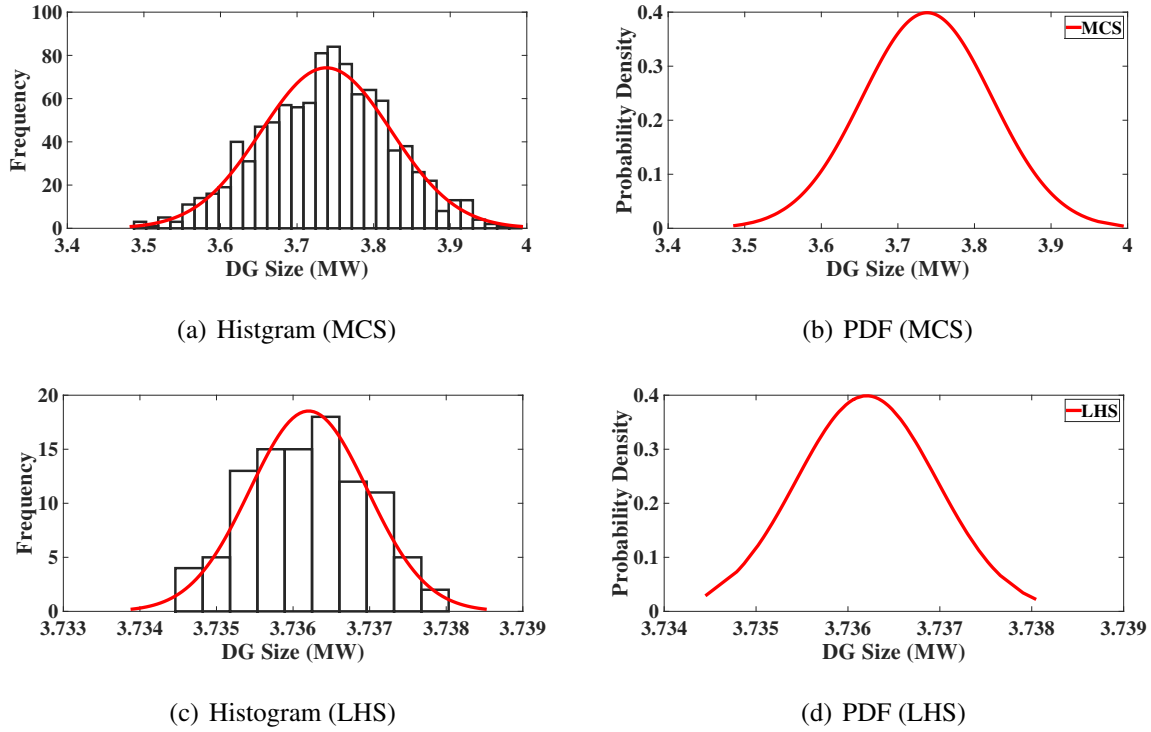

(a) Histgram (MCS)

(b) PDF (MCS)

(c) Histogram (LHS)

(d) PDF (LHS)

Fig. 6.2: Histogram and PDF of DG Size for VDI Optimization

6.6.2 Multi-Objective Allocation of DG

The probabilistic allocation of DG for multi-objective optimization is investigated for minimization of both PLI and VDI simultaneously. The MOF formulated by equation (6.6) is optimized through PSO. The histograms and PDFs resulted from MCS and LHS are presented in Figures 6.3 (a-d).

The probable mean DG size for MCS and LHS are comparable. The deviation in DG size from mean is more for MCS, as evident from Table 6.3. It is inferred from Figures 6.3 (b) and (d), that DG size follows the normal distribution, as it is governed by load variation.

Table 6.3: DG Size Statistics for Multi-objective Optimization

MCS		**LHS**	
μ	σ	μ	σ
3.0374 MW	0.0649 MW	3.0372 MW	0.0024 MW

The probable DG size attained through LHS is 2.5901 MW, 3.7362MW and 3.0372 MW corresponding to minimizing PLI, VDI separately and PLI and VDI simultaneously. A similar

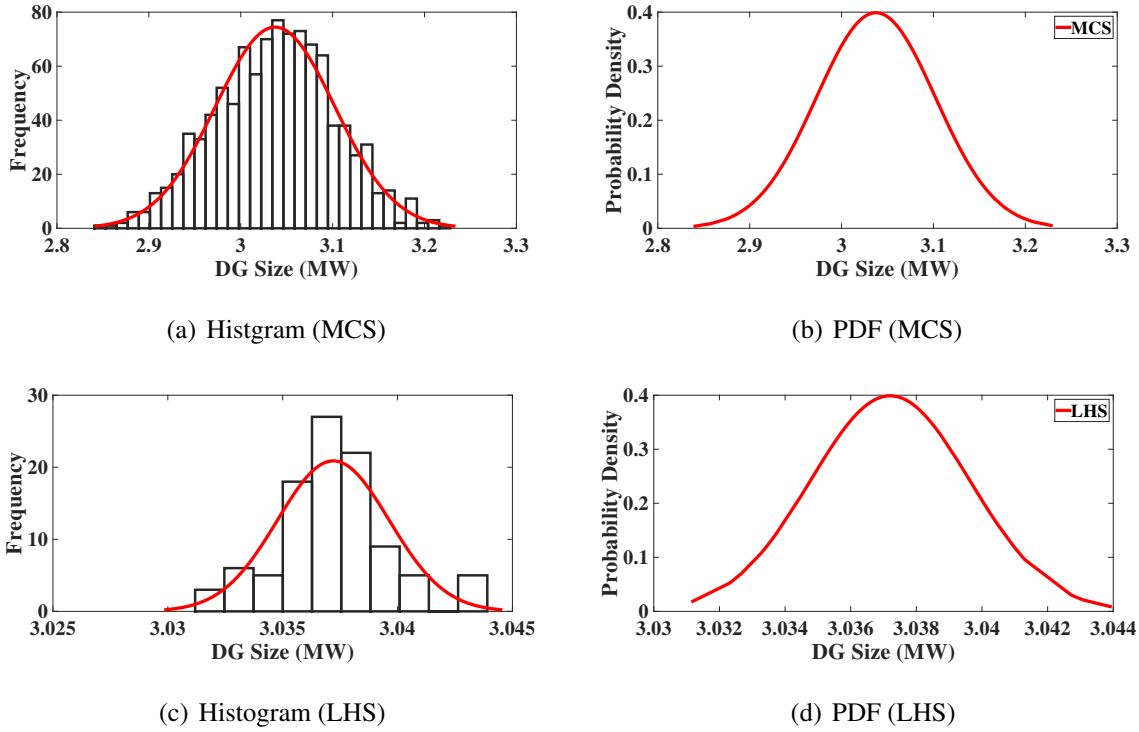

(a) Histgram (MCS)

(b) PDF (MCS)

(c) Histogram (LHS)

(d) PDF (LHS)

Fig. 6.3: Histogram and PDF of DG Size for Multi-objective Optimization

observation is made for MCS from Tables 6.1, 6.2 and 6.3. Although, both PLI and VDI are reduced by integration of DGs, but the large sized DGs result in more reduction in VDI and less reduction in PLI and vice versa. Thus, it is concluded that the probable DG size obtained corresponding to multi-objective optimization is a compromised solution.

The probable DG size attained through probabilistic allocation is compared with its size attained in Chapter 5 through deterministic approach for individual and concurrent optimization of PLI and VDI. The comparison is summarized in Table 6.4 and it is inferred that the DG sizes are comparable for deterministic and probabilistic approach for predefined optimal location.

Table 6.4: Comparison of DG Size for Deterministic and Probabilistic Allocation

Objective	**Deterministic**	**Probabilistic (MCS)**	**Probabilistic (LHS)**
PLI	2.5839 MW	2.5914 MW	2.5901 MW
VDI	3.7362 MW	3.7382 MW	3.7362 MW
PLI* and *VDI	3.0357 MW	3.0374 MW	3.0372 MW

6.6.3 Single Objective Allocation of DG and Capacitor

The size of both DG and capacitor are evaluated for each load sample generated by MCS and LHS sampling. With the consideration of samples, 1000 different DG and capacitor sizes are yielded through MCS and 100 from LHS. The histograms of DG and capacitor size repetition are shown in Figures 6.4 (a), (c), (e) and (g) for MCS and LHS, where the corresponding PDFs are shown in Figures 6.4 (b), (d), (f) and (h). It is observed that the variation in DG and capacitor size is large for MCS as compared to LHS. It is also observed that the DG as well as capacitor size follows the normal distribution.

Table 6.5: DG and Capacitor Size Statistics for Optimization of PLI

MCS		**LHS**	
μ	σ	μ	σ
DG Size (MW)			
2.5673	0.0752	2.5671	0.0522
Capacitor Size (MVAr)			
1.7670	0.0816	1.7647	0.0418

The mean and standard deviation of DG and capacitor size are summarized in Table 6.5. It is observed that the probable DG and capacitor size obtained by MCS and LHS are comparable while the deviation in DG as well as capacitor sizes is less for LHS. The DG of 2.5671 MW and capacitor of 1.7647 MVAr achieved through LHS are best suited for concurrent allocation in 33-bus RDN at bus 6, when variation in randomly varying practical load is 10%.

The histograms and PDFs of yielded DG and capacitor size for VDI minimization are demonstrated in Figure 6.5. The size of DG as well as capacitor, for VDI optimization is higher as compared to their size obtained corresponding to PLI optimization.

The mean and standard deviation of DG and capacitor size for VDI optimization are summarized in Table 6.6. The variation in DG as well as capacitor size is again less for LHS as compared to MCS. The DG of 3.0802 MW and capacitor of 3.7362 MVAr, as resulted from LHS sampling, are best for integration at bus 6 for varying load.

Comparing Tables 6.2 and 6.6, it is observed that the DG size reduces significantly when DG and capacitor are allocated concurrently. The DG size are 3.7362 MW and 3.0802 MW for

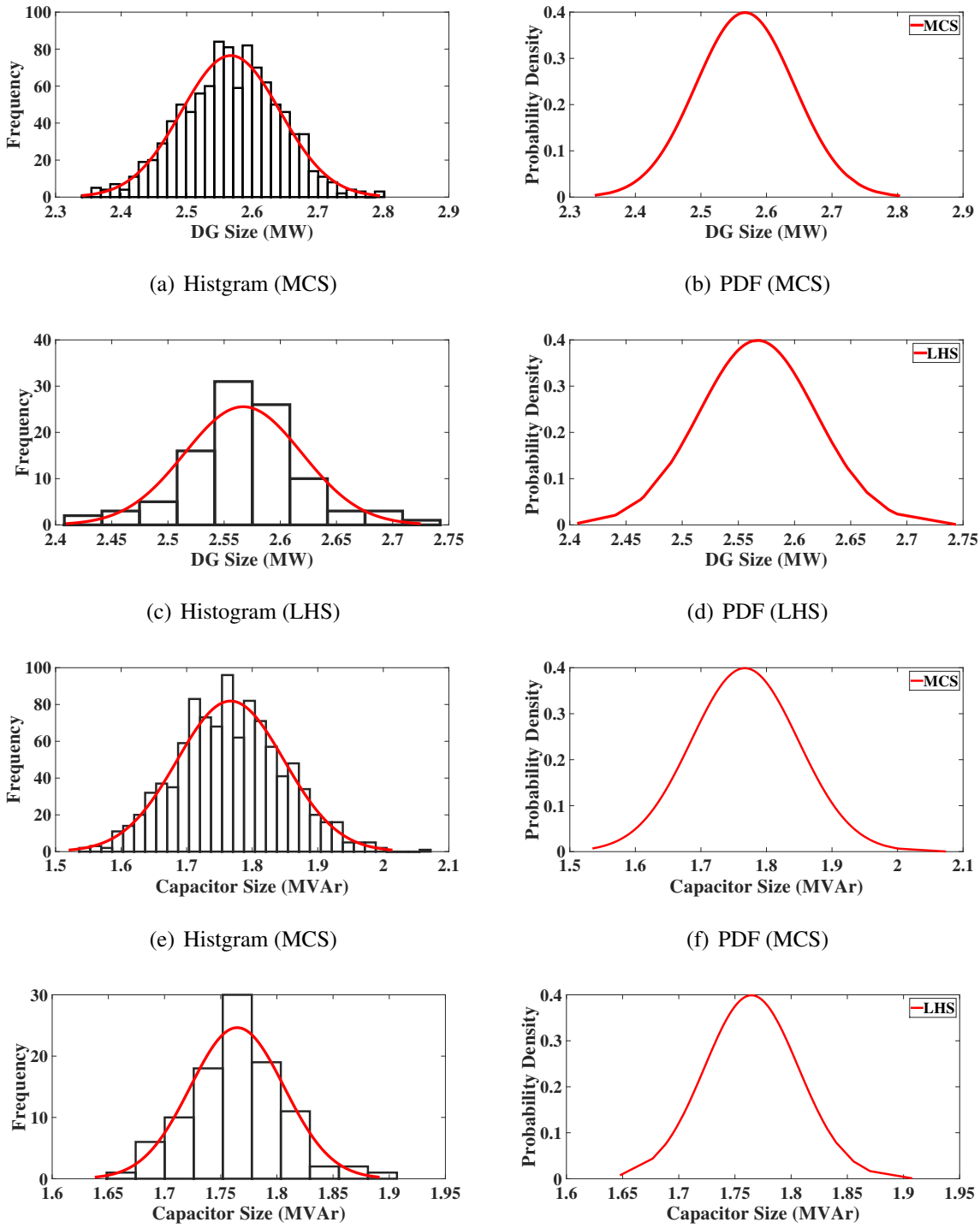

(a) Histgram (MCS) (b) PDF (MCS)

(c) Histogram (LHS) (d) PDF (LHS)

(e) Histgram (MCS) (f) PDF (MCS)

(g) Histogram (LHS) (h) PDF (LHS)

Fig. 6.4: Histogram and PDF of DG and Capacitor Size for PLI Optimization

only DG allocation and for allocating both DG and capacitor, respectively. The reduced DG size is due to capacitor, which is helping in increased voltage profile.

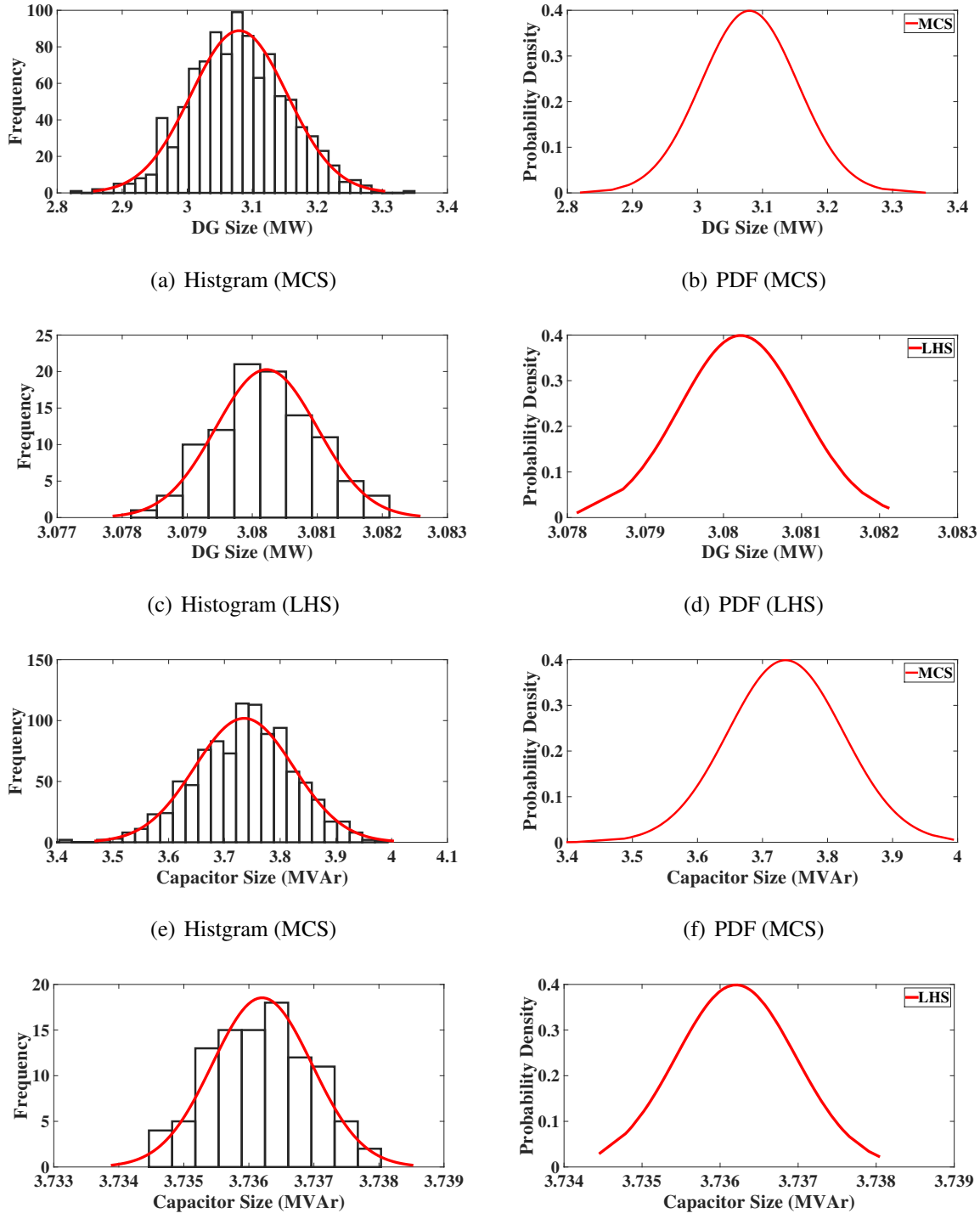

(a) Histgram (MCS) (b) PDF (MCS)

(c) Histogram (LHS) (d) PDF (LHS)

(e) Histgram (MCS) (f) PDF (MCS)

(g) Histogram (LHS) (h) PDF (LHS)

Fig. 6.5: Histogram and PDF of DG and Capacitor Size for VDI Optimization

Table 6.6: DG and Capacitor Size Statistics for Optimization of VDI

MCS		**LHS**	
μ	σ	μ	σ
DG Size (MW)			
3.0798	0.0742	3.0802	7.8201×10^{-4}
Capacitor Size (MVAr)			
3.7355	0.0887	3.7362	7.6799×10^{-4}

6.6.4 Multi-Objective Allocation of DG and Capacitor

The probabilistic allocation of DG and capacitor is simultaneously carried out by optimization of PLI and VDI. The histogram of DG and capacitor size resulted from MCS and LHS are presented in Figures 6.6 (a), (c), (e) and (g). These histograms indicate the frequency of DG and capacitor size repetition. It is evident from Figures 6.6 (a) and (e), that DG size corresponding to maximum frequency of occurrence is different from MCS and LHS sampling. Correspondingly, the PDFs are demonstrated in Figures 6.6 (b), (d), (f) and (h).

Table 6.7: DG and Capacitor Size Statistics for Multi-objective Optimization

MCS		**LHS**	
μ	σ	μ	σ
DG Size (MW)			
2.7676	0.0709	2.7690	0.0570
Capacitor Size (MVAr)			
1.8942	0.0818	1.9116	0.0562

The comparative mean and standard deviation of DG and capacitor size obtained by MCS and LHS is summarized in Table 6.7. The DG of 2.7690 MW and capacitor of 1.9116 MVAr at bus 6 are suitable for integration in 33-bus RDN for 10% variation in load. It is also observed from Tables 6.5, 6.6 and 6.7, that the probable DG size for optimization of PLI, VDI and multi-objective optimization is 2.5673 MW, 3.0798 MW and 2.7676 MW, respectively for MCS. A similar observation is made for DG size attained by LHS for three different cases of optimization. Thus, it is inferred that the DG size obtained corresponding to multi-objective optimization is a compromised solution between the DG size for VDI or PLI optimization. The capacitor size is also a compromised solution for multi-objective optimization. Moreover, it is

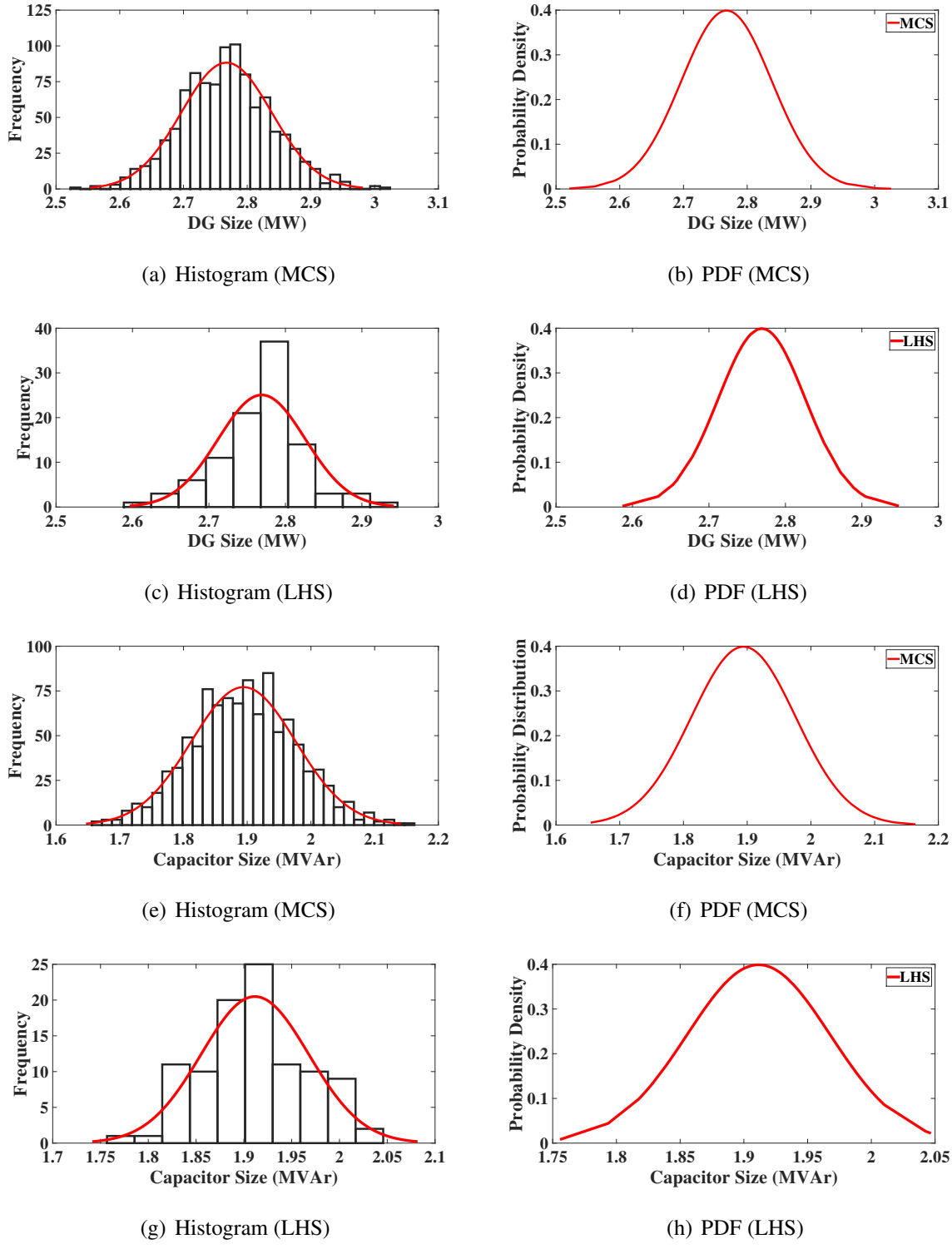

(a) Histogram (MCS) (b) PDF (MCS)

(c) Histogram (LHS) (d) PDF (LHS)

(e) Histogram (MCS) (f) PDF (MCS)

(g) Histogram (LHS) (h) PDF (LHS)

Fig. 6.6: Histogram and PDF of DG and Capacitor Size for Multi-Objective Optimization

also observed that probable DG size is reduced with allocation of capacitor as compared to its size when allocated separately for multi-objective optimization.

The optimal size of DG as well as capacitor achieved through probabilistic and deterministic approach are compared and summarized in Table 6.8. The deterministic approach results are taken from Tables 5.2 and 5.6 and the probabilistic approach results from Tables 6.5, 6.6 and 6.7. From Table 6.8 it is observed that, the probable sizes of DG and capacitor for uncertain load are comparable with deterministic size for single as well as multi-objective optimization. It is inferred from probabilistic allocation that the time expended for LHS is less and results are even better or comparable to results from MCS.

Table 6.8: Comparison of DG and Capacitor Size for Deterministic and Probabilistic Allocation

Objective	**Parameter**	**Deterministic**	**Probabilistic (MCS)**	**Probabilistic (LHS)**
PLI	**DG Size (MW)**	2.5501	2.5673	2.5671
	Capacitor Size (MVAr)	1.7379	1.7670	1.7647
VDI	**DG Size (MW)**	3.2843	3.0798	3.0802
	Capacitor Size (MVAr)	3.4211	3.7355	3.7362
PLI* and *VDI	**DG Size (MW)**	2.7572	2.7676	2.7690
	Capacitor Size (MVAr)	1.9894	1.8942	1.9116

6.6.5 Effect of DG and Capacitor Allocation on Power Loss and Voltage

The analysis of probable optimal size attained through LHS for multi-objective problem is done by integrating DG separately, and DG and capacitor concurrently. The probable optimal placement is done at optimum location *i.e.* bus 6 and the effect of their integration on active power loss and voltage deviation is evaluated. The reduction in active power loss and voltage deviation is reflecting upon the reduction in PLI and VDI, respectively.

The PDFs of active power loss corresponding to base case and with the integration of individual DG, DG and capacitor simultaneously are demonstrated in Figures 6.7 (a), (b) and (c). The PDFs of active power loss follow the normal distribution for base case and with integration of DG and capacitor. The summary of mean and standard deviation of active power losses is presented in Table 6.9. The mean percentage reduction in losses by placement of DG separately,

and DG and capacitor concurrently is 46.090% and 61.277% respectively, as evident from Table 6.9.

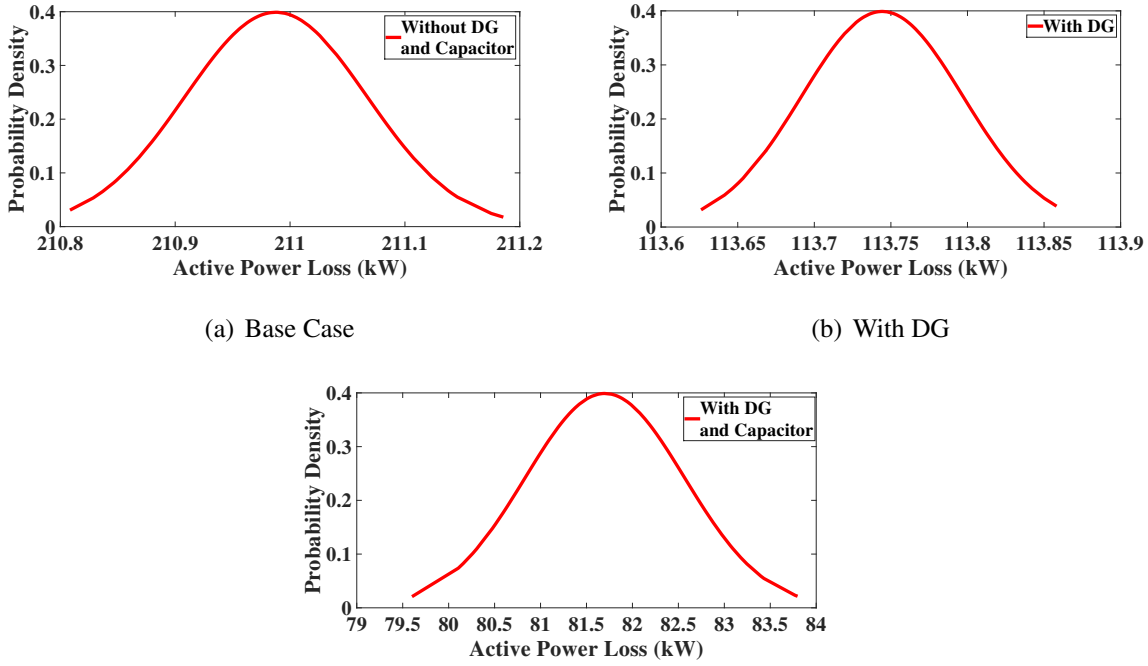

(a) Base Case

(b) With DG

(c) With DG and Capacitor

Fig. 6.7: Power Loss PDF Before and After Integration of DG and Capacitor

Table 6.9: Active Power Loss Statistics for Multi-objective Optimization

Base Case		With DG		With DG and Capacitor	
μ	σ	μ	σ	μ	σ
210.9878 kW	0.0793 kW	113.7444 kW	0.0527 kW	81.7001 kW	0.8681 kW

In addition to power loss reduction, there is improvement in voltage of all buses and thus the reduction in voltage deviation with DG placement. The PDF for voltage deviation before DG and capacitor integration is shown in Figure 6.8 (a) while Figures 6.8 (b) and (c) are demonstrating the PDFs of voltage deviation corresponding to integration of DG separately, and DG and capacitor simultaneously.

The mean voltage deviation corresponding to base case and with integration of DG and capacitor and the corresponding standard deviation are tabulated in Table 6.10. It is evident from Table 6.10 that, the voltage deviation is reduced effectively by integration of DG and capacitor. In addition to voltage deviation, the voltage of bus 6 and bus 18 is also analyzed. The DG and capacitor size evaluated through LHS are considered for the analysis of bus voltages.

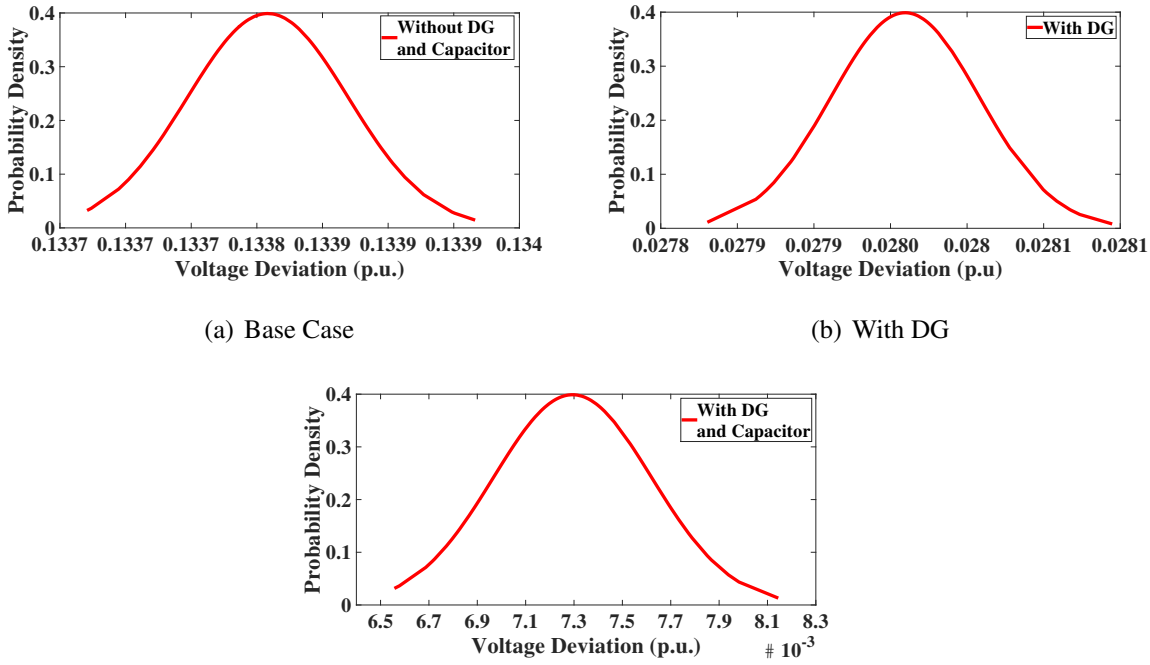

(a) Base Case

(b) With DG

(c) With DG and Capacitor

Fig. 6.8: Voltage Deviation PDF Before and After Integration of DG and Capacitor

Table 6.10: Voltage Deviation Statistics for Multi-objective Optimization

Base Case		**With DG**		**With DG and Capacitor**	
μ	σ	μ	σ	μ	σ
0.1338	6.1476×10^{-4}	0.0280	4.8659×10^{-5}	0.0073	3.2702×10^{-4}

The PDFs of bus 6 voltage, obtained after individual integration of DG and concurrent integration of DG and capacitor are shown in Figures 6.9 (a) and (b), respectively. The statistics of voltage at bus 6 are summarized in Table 6.11. The mean voltage of bus 6 is 0.9495 p.u. before DG and capacitor placement and it is enhanced to 0.9922 p.u. and 1.0127 p.u with integration of individual DG, and DG and capacitor simultaneously, respectively.

Table 6.11: Bus 6 Voltage Statistics for Multi-objective Optimization

With DG		**With DG and Capacitor**	
μ	σ	μ	σ
0.9922 p.u.	3.1586×10^{-5} p.u.	1.0127 p.u.	5.9650×10^{-4} p.u.

The mean voltage of bus 18 is 0.9038 p.u. before the integration of DG and capacitor as determined from base case load flow. The improvement in voltage of bus 18 is indicated by increase of voltage to a mean of 0.9487 p.u. by DG integration and 0.9701 p.u. by concurrent

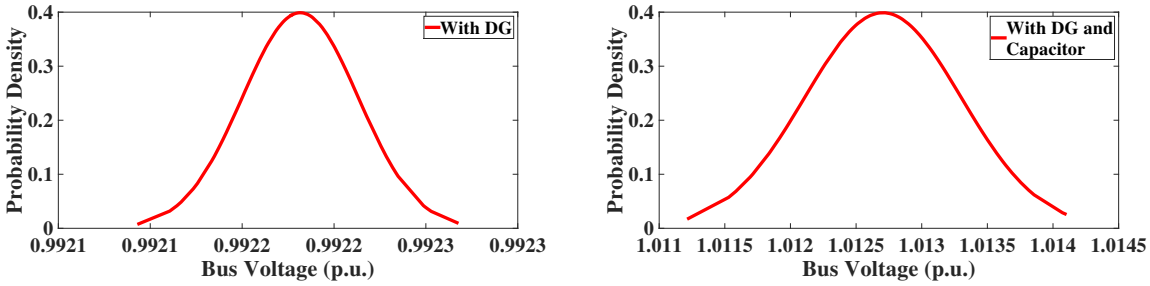

(a) With DG (b) With DG and Capacitor

Fig. 6.9: Voltage of Bus 6 after DG and Capacitor Integration

integration of DG and capacitor, as evident from Table 6.12. The PDFs for bus 18 voltage corresponding to individual DG, and simultaneous DG and capacitor allocation are presented in Figures 6.10 (a) and (b). Similar to bus 6 voltage PDFs, the PDFs of bus 18 voltage are also following normal distribution.

Table 6.12: Bus 18 Voltage Statistics for Multi-objective Optimization

With DG		**With DG and Capacitor**	
μ	σ	μ	σ
0.9487 p.u.	3.7519×10^{-5} p.u.	0.9701 p.u.	6.2715×10^{-4} p.u.

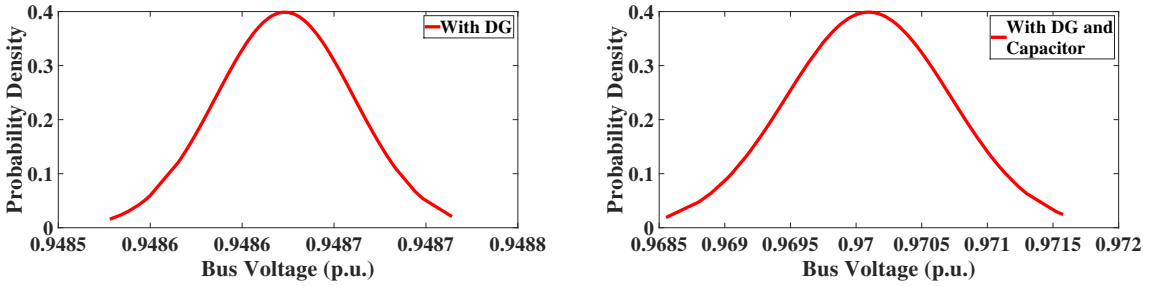

(a) With DG (b) With DG and Capacitor

Fig. 6.10: Voltage of Bus 18 after DG and Capacitor Integration

6.7 CONCLUDING REMARKS

In this Chapter, the optimal allocation of separate DG, and concurrent DG and capacitor are obtained in presence of uncertain random variations in the load of practical DNs. The uncertain randomly varying load is obtained by sampling of load data through MCS and LHS for 10%

variation in both active and reactive power load connected to each bus of 33-bus RDN. The probable size of separate DG and concurrent DG and capacitor is evaluated corresponding to each load sample for a predefined optimal location *i.e.* bus 6. The DG and capacitor size are attained to optimize PLI and VDI separately as well as concurrently by individual DG integration, and simultaneous integration of DG and capacitor. It is concluded that the DG and capacitor size attained corresponding to load samples generated by MCS and LHS follow the normal distribution. It is also concluded that the probable optimal size of DG and capacitor are similar for samples using MCS and LHS but the deviation in DG, as well as capacitor size, is more for MCS. Moreover, it is also found that the less computation time is required for LHS without loss of accuracy because of small sample size. Also, it is found that the DG and capacitor size yielded for multi-objective optimization are compromised solutions in comparison to their size corresponding to single-objective optimization of PLI and VDI. The probable DG size reduces considerably when a capacitor is integrated along with DG.

The important findings of the research work and the scope for future work are summarized in next Chapter 7.

Chapter–7

Conclusions and Scope for Future Work

The usage of DGs is economical and environment-friendly option to supply load demand. These DGs are integrated in the low voltage DNs and thereby not much expansion of existing transmission network is needed. The optimal sized DG(s) must be integrated at optimal location(s) for optimum performance measured through loss reduction, improvement in voltage profile *etc*. The investigations have been carried out while assuming that the locations are available for placement of limited number of moderate size DGs. The algorithms are developed to find the optimal allocation of DGs for RDNs for single as well as multi-objective formulation for the practical network having voltage-dependent and probabilistic loads. The algorithms have been developed using analytical expressions and particle swarm optimization (PSO). The main findings of the research work carried out in this Thesis are summarized in the following section.

7.1 SUMMARY OF IMPORTANT FINDINGS

In Chapter-3, the optimal size and site of different types of DG are attained to diminish the active power losses. The optimization is realized through an analytical expression based approach and through PSO for all four Types of DGs. The allocation is investigated for DNs with the consideration of voltage-dependent practical loads. The main conclusions of this Chapter are summarized as:

- The analytical approach computes the optimal size of DG to be placed at each bus. The allocation of DG at a bus leading to minimum loss is selected as optimal site whereas, the PSO provides global optimal site and size.

- For all types of DG, the optimal size yielded by PSO is more effective for loss minimization as compared to DG size obtained by analytical expressions.

- Among all types of DGs, Type-III DG operating at lagging power factor is best for improvement of DN performance followed by Type-I operating at unity power factor.

- The effect of practical voltage-dependent loads on the optimal allocation of Type-I and Type-III DGs is also considered. The size of both Type-I and Type-III DG is affected by the consideration of practical-voltage dependent loads. The size is minimum for commercial loads.

- The results obtained by PSO are also compared with results obtained by other methods such as GA and ABC. The PSO formulation provides better results.

The Chapter-4 is directed on optimal allocation of DGs using multi-objective optimization formulation through PSO. The optimal allocation of Type-I and Type-III DGs is carried out for four performance parameters namely PLI, QLI, VDI and OEI that are optimized individually as well as simultaneously. The multi-objective optimization is carried out by combining objectives through fuzzy-decision making and on the basis of true Pareto based approach for voltage-dependent practical loads. The major contributions are:

- The placement of Type-I and Type-III DGs is considered for single and multiple locations. The allocation of multiple DGs is more effective for single as well as multi-objective optimization.

- The integration of Type-III DG is resulting in better performance for both formulations.

- The size, as well as the location of single and multiple DGs, is governed by the objective considered and nature of practical load.

- Modified PSO is able to handle true Pareto based multi-objective formulation.

- The well diverse optimal Pareto front comprising of number of solutions, is obtained for optimizing PLI and VDI simultaneously. The MOF formulation is yielding single optimal solution.

- The best compromised result from Pareto based, and solution from MOF based multi-objective optimization are different.

In Chapter-5, the optimal allocation of Type-I DG, capacitor, and DG and capacitor concurrently are investigated for individual and simultaneous optimization of PLI and VDI for practical loads. The multi-objective allocation is investigated through Pareto-based and non Pareto MOF based optimization using PSO. The main findings of this Chapter are:

- The VDI minimization is yielding higher value of DG and/or capacitor size in comparison to size attained for PLI minimization.
- The optimal integration of DG and capacitor simultaneously is most effective for both single and multi-objective optimization.
- The size of optimal DG reduces with the use of capacitor for all voltage-dependent practical loads.
- Well diverse Pareto fronts are resulted from true Pareto based optimization while a single optimal solution is obtained through MOF optimization.
- The results attained for multi-objective optimization through Pareto and non Pareto based formulations are different.

The uncertainty in practical network is realized though random load variation. Correspondingly, the optimal allocation DG separately and DG and capacitor simultaneously is investigated in Chapter 6 for individual and simultaneous optimization of PLI and VDI. The MCS and LHS methods are used while considering 10% variation in active and reactive power load demand. The following conclusions are derived from this study:

- Probable DG and capacitor size attained corresponding to load samples generated by MCS and LHS follow the normal distribution.
- The probable optimal size of DG and capacitor are similar for samples using MCS and LHS but the deviation in DG, as well as capacitor size, is more for MCS.

- The less computation time is required for LHS without loss of accuracy because of small sample size.
- Probable DG and capacitor size yielded for multi-objective optimization are compromised solutions in comparison to their size corresponding to single-objective optimization of PLI and VDI.
- The probable DG size reduces considerably when a capacitor is integrated along with DG.

7.2 SCOPE FOR FURTHER WORK

The research work is a continuous process. An end of a research project is the beginning to a lot other avenues for further work. As a consequence of the investigations carried out in this Thesis on *Optimal Placement of Dispersed Generators for Practical Distribution Networks*, the basic objectives have been brought to a successful conclusions and the following aspects are identified for further research.

- Although the practical loads are modelled through voltage-dependent residential, industrial loads. The excessive use of power electronic based appliances may increase the harmonics significantly. The performance of different types of DGs under the influence of harmonics and correspondingly the optimal allocation shall be analyzed.
- The DGs have been allocated mainly on the basis of real and reactive power injection. The renewable resources such as wind and solar are inherently of intermittent nature. Their realistic modeling can be considered in DG allocation.
- The integration of DG may give rise to reverse power flows. This shall be accounted for both deterministic and probabilistic modeling of DG allocation.
- The optimal allocation of DGs although depends on objective and type of DGs. The performance improves significantly if more number of DGs are placed, but involves cost and operational difficulty. Therefore, the investigations shall be carried out on identifying an ideal number of DGs and capacitors for integration in DN.

List of Publications

SCI/SCIE

1. Navdeep Kaur, Sanjay K. Jain. "Analytical approach for optimal allocation of distributed generators to minimize losses". **Journal of Electrical Engineering and Technology** (2016), (Impact factor: **0.597**). **[Chapter 3]**

   doi : 10.5370/JEET.2016.11.6.1582

2. Navdeep Kaur, Sanjay K. Jain. "Multi-objective optimization approach for placement of multiple DGs for voltage sensitive loads". **Energies** (2017), (Impact factor: **2.676**). **[Chapter 4]**

   doi : 10.3390/en10111733

Scopus Indexed Book Chapters / Conferences

1. Navdeep Kaur, Sanjay K. Jain. "A Review on techniques for placement of distributed generators". ***7th IEEE India International Conference on Power Electronics (IICPE)*** (2016). **[Chapter 2]**

   doi : 10.1109/IICPE.2016.8079474

2. Navdeep Kaur, Sanjay K. Jain. "Placement of distributed generators for loss minimization and voltage improvement using particle swarm optimization". ***7th IEEE India International Conference on Power Electronics (IICPE)*** (2016). **[Chapter 3]**

   doi : 10.1109/IICPE.2016.8079426

3. Navdeep Kaur, Sanjay K. Jain. "Hybrid methodology for optimal allocation of synchronous generator-based DG". ***Ambient Communications and Computer Systems*** (2017) (**Scopous Indexed book chapter**). **[Chapter 3]**

   doi : 10.1007/978-981-10-7386-1_8

4. Navdeep Kaur, Sanjay K. Jain. “Optimal allocation of dispersed generators for voltage dependent practical loads”. presented in ***PSC2018 IEEE Conference held on 4-7 September, 2018 at Charleston, SC, USA*** . **[Chapter 4]**

Papers Under Review

1. “Multi-objective Probabilistic Allocation of DG and Capacitor for Practical Uncertain Load” is under review with IET Generation, Transmission and Distribution. **[Chapter 6]**

References

Abd-El-Motaleb, A. M. and Bekdach, S. K. (2016), 'Optimal sizing of distributed generation considering uncertainties in a hybrid power system', *International Journal of Electrical Power and Energy Systems*, **82**, 179–188.

Abdelaziz, A. Y., Hegazy, Y. G., El-Khattam, W. and Othman, M. M. (2015), 'Optimal planning of distributed generators in distribution networks using modified firefly method', *Electric Power Components and Systems*, **43**(3), 320–333.

Abou El-Ela, A. A., Allam, S. M. and Shatla, M. M. (2010), 'Maximal optimal benefits of distributed generation using genetic algorithms', *Electric Power Systems Research*, **80**(7), 869–877.

Abri, R. S. A., El-saadany, E. F. and Atwa, Y. M. (2013), 'Optimal placement and sizing method to improve the voltage stability margin in a distribution system using distributed generation', *IEEE Transactions on Power Systems*, **28**(1), 326–334.

Abu-Mouti, F. S. and El-Hawary, M. E. (2011), 'Optimal distributed generation allocation and sizing in distribution systems via artificial bee colony algorithm', *IEEE Transactions on Power Delivery*, **26**(4), 2090–2101.

Acharya, N., Mahat, P. and Mithulananthan, N. (2006), 'An analytical approach for DG allocation in primary distribution network', *International Journal of Electrical Power and Energy Systems*, **28**(10), 669–678.

Ackermann, T., Andersson, G. and Soder, L. (2001), 'Distributed generation: a definition', *Electric Power Sysytems Research*, **57**, 195–204.

Akorede, M., Hizam, H., Aris, I. and Ab Kadir, M. (2011), 'Effective method for optimal allocation of distributed generation units in meshed electric power systems', *IET Generation, Transmission & Distribution*, **5**(2), 276–287.

Ali, E. S., Abd Elazim, S. M. and Abdelaziz, A. Y. (2017), 'Ant lion optimization algorithm for optimal location and sizing of renewable distributed generations', *Renewable Energy*, **101**, 1311–1324.

Aman, M. M., Jasmon, G. B., Bakar, A. H. and Mokhlis, H. (2013), 'A new approach for optimum DG placement and sizing based on voltage stability maximization and minimization of power losses', *Energy Conversion and Management*, **70**, 202–210.

Aman, M. M., Jasmon, G. B., Mokhlis, H. and Bakar, A. H. A. (2012), 'Optimal placement and sizing of a DG based on a new power stability index and line losses', *International Journal of Electrical Power and Energy Systems*, **43**(1), 1296–1304.

Arabali, A., Ghofrani, M., Etezadi-Amoli, M. and Fadali, M. S. (2014), 'Stochastic performance assessment and sizing for a hybrid power system of solar/wind/energy storage', *IEEE Transactions on Sustainable Energy*, **5**(2), 363–371.

Atwa, Y. and El-Saadany, E. (2011), 'Probabilistic approach for optimal allocation of wind-based distributed generation in distribution systems', *IET Renewable Power Generation*, **5**(1), 79–88.

Atwa, Y. M., El-Saadany, E. F., Salama, M. M. A. and Seethapathy, R. (2010), 'Optimal renewable resources mix for distribution system energy loss minimization', *IEEE Transactions on Power Systems*, **25**(1), 360–370.

Bahrami, S. and Imari, A. (2014), 'Optimal placement of distributed generation units for constructing virtual power plant using binary particle swarm optimization algorithm', *Journal of Electrical & Electronic Systems*, **3**(127), 796–2332.

Banerjee, R. (2006), 'Comparison of options for distributed generation in india', *Energy Policy*, **34**(1), 101 – 111.

Baran, M. E. and Wu, F. F. (1989*a*), 'Optimal capacitor placement on radial distribution systems', *IEEE Transactions on Power Delivery*, **4**(1), 725–734.

Baran, M. and Wu, F. F. (1989*b*), 'Optimal sizing of capacitors placed on a radial distribution system', *IEEE Transactions on Power Delivery*, **4**(1), 735–743.

Biswas, S., Goswami, S. K. and Chatterjee, A. (2012), 'Optimum distributed generation placement with voltage sag effect minimization', *Energy Conversion and Management*, **53**(1), 163–174.

Bohre, A. K., Agnihotri, G. and Dubey, M. (2016), 'Optimal sizing and sitting of DG with load models using soft computing techniques in practical distribution system', *IET Generation, Transmission & Distribution*, **10**(11), 2606–2621.

Borges, C. L. T. and Falcão, D. M. (2006), 'Optimal distributed generation allocation for reliability, losses, and voltage improvement', *International Journal of Electrical Power and Energy Systems*, **28**(6), 413–420.

Carpinelli, G., Celli, G., Mocci, S., Pilo, F. and Russo, A. (2005), 'Optimisation of embedded generation sizing and siting by using a double trade-off method', *IEE Proceedings-Generation, Transmission and Distribution*, **152**(4), 503–513.

Carpinelli, G., Celli, G., Pilo, F. and Russo, A. (2003), 'Embedded generation planning under uncertainty including power quality issues', *European Transactions on Electrical Power*, **13**(6), 381–389.

Carvalho, P. M. S., Correia, P. F. and Ferreira, L. A. F. M. (2008), 'Distributed reactive power generation control for voltage rise mitigation in distribution networks', *IEEE Transactions on Power Systems*, **23**(2), 766–772.

Celli, G., Ghiani, E., Mocci, S. and Pilo, F. (2005), 'A multiobjective evolutionary algorithm for the sizing and siting of distributed generation', *IEEE Transactions on Power Systems*, **20**(2), 750–757.

Chandrashekhar Reddy, S., Prasad, P. V. N. and Jaya Laxmi, A. (2013), 'Placement of distributed generator, capacitor and DG and capacitor in distribution system for loss reduction and reliability improvement', *Journal of Electrical Engineering*, **13**(4), 329–337.

Cheng, C. S. and Shirmohammadi, D. (1995), 'A three-phase power flow method for real-time distribution system analysis', *IEEE Transactions on Power Systems*, **10**(2), 671–679.

Darfoun, M. A. and El-Hawary, M. E. (2015), 'Multi-objective optimization approach for optimal distributed generation sizing and placement', *Electric Power Components and Systems*, **43**(7), 828–836.

Dehghanian, P., Hosseini, S. H., Moeini-Aghtaie, M. and Arabali, A. (2013), 'Optimal siting of DG units in power systems from a probabilistic multi-objective optimization perspective', *International Journal of Electrical Power and Energy Systems*, **51**, 14–26.

Devi, S. and Geethanjali, M. (2014), 'Application of modified bacterial foraging optimization algorithm for optimal placement and sizing of distributed generation', *Expert Systems with Applications*, **41**(6), 2772–2781.

Dinakara Prasasd Reddy, P., Veera Reddy, V. and Gowri Manohar, T. (2017), 'Ant lion optimization algorithm for optimal sizing of renewable energy resources for loss reduction in distribution systems', *Journal of Electrical Systems and Information Technology*, pp. 1–18.

Divya, K. and Rao, P. N. (2006), 'Models for wind turbine generating systems and their application in load flow studies', *Electric Power Systems Research*, **76**(9), 844 – 856.

Dixit, M., Kundu, P. and Jariwala, H. R. (2017), 'Incorporation of distributed generation and shunt capacitor in radial distribution system for techno-economic benefits', *Engineering Science and Technology, an International Journal*, **20**(2), 482–493.

Doagou-Mojarrad, H., Gharehpetian, G. B., Rastegar, H. and Olamaei, J. (2013), 'Optimal placement and sizing of DG (distributed generation) units in distribution networks by novel hybrid evolutionary algorithm', *Energy*, **54**, 129–138.

Driesen, J. and Belmans, R. (2006), Distributed generation: challenges and possible solutions, *in* 'IEEE Power Engineering Society General Meeting, 18-22 June 2006, Montreal, Que., Canada', pp. 1–8.

El-Fergany, A. (2015), 'Optimal allocation of multi-type distributed generators using backtracking search optimization algorithm', *International Journal of Electrical Power and Energy Systems*, **64**, 1197–1205.

El-Khattam, W., Hegazy, Y. G. and Salama, M. M. A. (2005), 'An integrated distributed generation optimization model for distribution system planning', *IEEE Transactions on Power Systems*, **20**(2), 1158–1165.

El-Saadany, E. F. and Abdelsalam, A. A. (2013), 'Probabilistic approach for optimal planning of distributed generators with controlling harmonic distortions', *IET Generation, Transmission & Distribution*, **7**(10), 1105–1115.

El-Zonkoly, A. M. (2011), 'Optimal placement of multi-distributed generation units including different load models using particle swarm optimization', *IET Generation, Transmission & Distribution*, **5**(7), 760–771.

Elsaiah, S., Benidris, M. and Mitra, J. (2014), 'Analytical approach for placement and sizing of distributed generation on distribution systems', *IET Generation, Transmission & Distribution*, **8**(6), 1039–1049.

Esmaeilian, H. R., Darijany, O. and Mohammadian, M. (2012), 'Optimal placement and sizing of DG units and capacitors simultaneously in radial distribution networks based on voltage stability security margin', *Turkish Journal of Electrical Engineering & Computer Sciences*, pp. 1–14.

Esmaili, M., Firozjaee, E. C. and Shayanfar, H. A. (2014), 'Optimal placement of distributed generations considering voltage stability and power losses with observing voltage-related constraints', *Applied Energy*, **113**, 1252–1260.

Evangelopoulos, V. A. and Georgilakis, P. S. (2014), 'Optimal distributed generation placement under uncertainties based on point estimate method embedded genetic algorithm', *IET Generation, Transmission & Distribution*, **8**(3), 389–400.

Farhat, I. A. (2013), 'Ant colony optimization for optimal distributed generation in distribution systems', *International Journal of Computer, Information, Systems and Control Engineering*, **7**, 1094–1098.

Fathy, A. (2015), 'An efficient and reliable method for optimal allocating of the distributed generation based on optimal teaching learning algorithm', *WSEAS Transcations on Power Systems*, **10**, 188–197.

Feijoo, A. E. and Cidras, J. (2000), 'Modeling of wind farms in the load flow analysis', *IEEE Transactions on Power Systems*, **15**(1), 110–115.

Gampa, S. R. and Das, D. (2015), 'Optimum placement and sizing of DGs considering average hourly variations of load', *International Journal of Electrical Power and Energy Systems*, **66**, 25–40.

Garcia, P. A. N., Pereira, J. L. R., Carneiro, S., Costa, V. M. D. and Martins, N. (2000), 'Three-phase power flow calculations using the current injection method', *IEEE Transactions on Power Systems*, **15**(2), 508–514.

Gautam, D. and Mithulananthan, N. (2007), 'Optimal DG placement in deregulated electricity market', *Electric Power Systems Research*, **77**, 1627–1636.

Ghaffarzadeh, N. and Sadeghi, H. (2016), 'A new efficient BBO based method for simultaneous placement of inverter-based DG units and capacitors considering harmonic limits', *International Journal of Electrical Power and Energy Systems*, **80**, 37–45.

Ghosh, S. and Das, D. (1999), 'Method for load-flow solution of radial distribution networks', *IEE Proceedings - Generation, Transmission and Distribution*, **146**(6), 641–648.

Ghosh, S., Ghoshal, S. and Ghosh, S. (2010), 'Optimal sizing and placement of distributed generation in a network system', *International Journal of Electrical Power & Energy Systems*, **32**(8), 849–856.

Gomez-Gonzalez, M., Lopez, A. and Jurado, F. (2012), 'Optimization of distributed generation systems using a new discrete PSO and OPF', *Electric Power Systems Research*, **84**(1), 174–180.

Gopiya Naik, S., Khatod, D. K. and Sharma, M. P. (2013), 'Optimal allocation of combined DG and capacitor for real power loss minimization in distribution networks', *International Journal of Electrical Power and Energy Systems*, **53**, 967–973.

Gözel, T. and Hocaoglu, M. H. (2009), 'An analytical method for the sizing and siting of distributed generators in radial systems', *Electric Power Systems Research*, **79**(6), 912–918.

Haghifam, M., Falaghi, H. and Malik, O. P. (2008), 'Risk-based distributed generation placement', *IET Generation, Transmission & Distribution*, **2**(2), 252–260.

Haque, M. (2000), 'A general load flow method for distribution systems', *Electric Power Systems Research*, **54**(1), 47 – 54.

Harrison, G. P. and Wallace, A. R. (2005), 'Optimal power flow evaluation of distribution network capacity for the connection of distributed generation', *IEE Proceedings-Generation, Transmission and Distribution*, **152**(1), 115–122.

Hedayati, H., Nabaviniaki, S. A. and Akbarimajd, A. (2008), 'A new method for placement of DG units in distribution networks', *IEEE Transactions on Power Delivery*, **23**(3), 1904–1909.

Hemdan, N. G. A. and Kurrat, M. (2011), 'Efficient integration of distributed generation for meeting the increased load demand', *International Journal of Electrical Power and Energy Systems*, **33**(9), 1572–1583.

Hosseini, S. A., Karimi Madahi, S. S., Razavi, F., Karami, M. and Ghadimi, A. A. (2013), 'Optimal sizing and siting distributed generation resources using a multiobjective algorithm', *Turkish Journal of Electrical Engineering and Computer Sciences*, **21**(3), 825–850.

Hung, D. Q. and Mithulananthan, N. (2013), 'Multiple distributed generator placement in primary distribution networks for loss reduction', *IEEE Transactions on Industrial Electronics*, **60**(4), 1700–1708.

Hung, D. Q. and Mithulananthan, N. (2014), 'Loss reduction and loadability enhancement with DG: A dual-index analytical approach', *Applied Energy*, **115**, 233–241.

Hung, D. Q., Mithulananthan, N. and Bansal, R. C. (2010), 'Analytical expressions for DG allocation in primary distribution networks', *IEEE Transactions on Energy Conversion*, **25**(3), 814–820.

Hung, D. Q., Mithulananthan, N. and Bansal, R. C. (2013), 'Analytical strategies for renewable distributed generation integration considering energy loss minimization', *Applied Energy*, **105**, 75–85.

Hung, D. Q., Mithulananthan, N. and Bansal, R. C. (2014), 'An optimal investment planning framework for multiple distributed generation units in industrial distribution systems', *Applied Energy*, **124**, 62–72.

Injeti, S. K. and Kumar, N. P. (2013), 'A novel approach to identify optimal access point and capacity of multiple DGs in a small, medium and large scale radial distribution systems', *International Journal of Electrical Power and Energy Systems*, **45**(1), 142–151.

Ishak, R., Mohamed, A., Abdalla, A. N. and Wanik, M. Z. C. (2014), 'Optimal placement and sizing of distributed generators based on a novel MPSI index', *International Journal of Electrical Power and Energy Systems*, **60**, 389–398.

Jabr, R. A. and Pal, B. C. (2009), 'Ordinal optimisation approach for locating and sizing of distributed generation', *IET Generation, Transmission & Distribution*, **3**(8), 713–723.

Jamian, J. J., Mustafa, M. W. and Mokhlis, H. (2015), 'Optimal multiple distributed generation output through rank evolutionary particle swarm optimization', *Neurocomputing*, **152**, 190–198.

Kansal, S., Kumar, V. and Tyagi, B. (2013), 'Optimal placement of different type of DG sources in distribution networks', *International Journal of Electrical Power and Energy Systems*, **53**(1), 752–760.

Kansal, S., Kumar, V. and Tyagi, B. (2015), 'Integration of DG and capacitor in power distribution systems', *International Journal of Distributed Energy Resources and Smart Grids*, **11**(2), 109–127.

Kansal, S., Kumar, V. and Tyagi, B. (2016), 'Hybrid approach for optimal placement of multiple DGs of multiple types in distribution networks', *International Journal of Electrical Power and Energy Systems*, **75**, 226–235.

Kanwar, N., Gupta, N., Niazi, K. R. and Swarnkar, A. (2015*a*), 'Improved meta-heuristic techniques for simultaneous capacitor and DG allocation in radial distribution networks', *International Journal of Electrical Power and Energy Systems*, **73**, 653–664.

Kanwar, N., Gupta, N., Niazi, K. R. and Swarnkar, A. (2015*b*), 'Optimal distributed generation allocation in radial distribution systems considering customer-wise dedicated feeders and load patterns', *Journal of Modern Power Systems and Clean Energy*, **3**(4), 475–484.

Karimyan, P., Gharehpetian, G. B., Abedi, M. and Gavili, A. (2014), 'Long term scheduling for optimal allocation and sizing of DG unit considering load variations and DG type', *International Journal of Electrical Power and Energy Systems*, **54**, 277–287.

Kashem, M. A., Ganapathy, V., Jasmon, G. B. and Buhari, M. I. (2000), A novel method for loss minimization in distribution networks, *in* 'International Conference on Electric Utility Deregulation and Restructuring and Power Technologies. Proceedings', pp. 251–256.

Kaur, S., Kumbhar, G. and Sharma, J. (2014), 'A MINLP technique for optimal placement of multiple DG units in distribution systems', *International Journal of Electrical Power and Energy Systems*, **63**, 609–617.

Kayal, P. and Chanda, C. (2013), 'Placement of wind and solar based DGs in distribution system for power loss minimization and voltage stability improvement', *International Journal of Electrical Power and Energy Systems*, **53**, 795–809.

Keane, A. and O'Malley, M. (2005), 'Optimal allocation of embedded generation on distribution networks', *IEEE Transactions on Power Systems*, **20**(3), 1640–1646.

Kefayat, M., Lashkar Ara, A. and Nabavi Niaki, S. A. (2015), 'A hybrid of ant colony optimization and artificial bee colony algorithm for probabilistic optimal placement and sizing of distributed energy resources', *Energy Conversion and Management*, **92**, 149–161.

Kennedy, J. and Eberhart, R. (1995), Particle swarm optimization, *in* 'IEEE International Conference on Neural Networks, 1995, 27 Nov-1 Dec 1995, Perth, WA, Australia', Vol. 4, pp. 1942–1948.

Kersting, W. H. (2002), *Distribution system modelling and analysis*, CRC Press.

Khalesi, N., Rezaei, N. and Haghifam, M. R. (2011), 'DG allocation with application of dynamic programming for loss reduction and reliability improvement', *International Journal of Electrical Power and Energy Systems*, **33**(2), 288–295.

Khan, N. A., Ghoshal, S. P. and Ghosh, S. (2015), 'Optimal allocation of distributed generation and shunt capacitors for the reduction of total voltage deviation and total line loss in radial distribution systems using binary collective animal behavior optimization algorithm', *Electric Power Components and Systems*, **43**(2), 119–133.

Khodabakhshian, A. and Andishgar, M. H. (2016), 'Simultaneous placement and sizing of DGs and shunt capacitors in distribution systems by using IMDE algorithm', *International Journal of Electrical Power and Energy Systems*, **82**, 599–607.

Khushalani, S., Solanki, J. M. and Schulz, N. N. (2007), 'Development of three-phase unbalanced power flow using PV and PQ models for distributed generation and study of the impact of DG models', *IEEE Transactions on Power Systems*, **22**(3), 1019–1025.

Kim, K.-h., Song, K.-b., Joo, S.-k., Lee, Y.-j. and Kim, J.-o. (2008), 'Multiobjective distributed generation placement using fuzzy goal programming with genetic algorithm', *European Transactions on Electrical Power*, **18**(3), 217–230.

Kumar, A. and Gao, W. (2010), 'Optimal distributed generation location using mixed integer non-linear programming in hybrid electricity markets', *IET Generation, Transmission & Distribution*, **4**(2), 281–298.

Kumawat, M., Gupta, N., Jain, N. and Bansal, R. C. (2017), 'Swarm-intelligence-based optimal planning of distributed generators in distribution network for minimizing energy loss', *Electric Power Components and Systems*, **45**(6), 589–600.

Lakervi, E. and Holmes, E. (2003), *Electrical distribution network design*, IET.

Lee, S. H. and Park, J. W. (2009), 'Selection of optimal location and size of multiple distributed generations by using kalman filter algorithm', *IEEE Transactions on Power Systems*, **24**(3), 1393–1400.

Li, M., Yang, S. and Liu, X. (2016), 'Pareto or non-pareto: Bi-criterion evolution in multiobjective optimization', *IEEE Transactions on Evolutionary Computation*, **20**(5), 645–665.

Lin, W.-M. and Teng, J.-H. (2000), 'Three-phase distribution network fast-decoupled power flow solutions', *International Journal of Electrical Power and Energy Systems*, **22**, 375 – 380.

Liu, K. Y., Sheng, W., Liu, Y., Meng, X. and Liu, Y. (2015), 'Optimal sitting and sizing of DGs in distribution system considering time sequence characteristics of loads and DGs', *International Journal of Electrical Power and Energy Systems*, **69**, 430–440.

Liu, Z., Wen, F. and Ledwich, G. (2011), 'Optimal siting and sizing of distributed generators in distribution systems considering uncertainties', *IEEE Transactions on Power Delivery*, **26**(4), 2541–2551.

Lopez, P. R., Jurado, F., Reyes, N. R., Galan, S. G. and Gomez, M. (2008), 'Particle swarm optimization for biomass-fuelled systems with technical constraints', *Engineering Applications of Artificial Intelligence*, **21**(8), 1389–1396.

Losi, A. and Russo, M. (2005), 'Dispersed generation modeling for object-oriented distribution load flow', *IEEE Transactions on Power Delivery*, **20**(2), 1532–1540.

Luo, G. X. and Semlyen, A. (1990), 'Efficient load flow for large weakly meshed networks', *IEEE Transactions on Power Systems*, **5**(4), 1309–1316.

Mahesh, K., Nallagownden, P. and Elamvazuthi, I. (2016), 'Advanced pareto front non-dominated sorting multi-objective particle swarm optimization for optimal placement and sizing of distributed generation', *Energies*, **9**(12), 982.

Martín García, J. A. and Gil Mena, A. J. (2013), 'Optimal distributed generation location and size using a modified teaching-learning based optimization algorithm', *International Journal of Electrical Power and Energy Systems*, **50**, 65–75.

Mistry, K. D. and Roy, R. (2014), 'Enhancement of loading capacity of distribution system through distributed generator placement considering techno-economic benefits with load growth', *International Journal of Electrical Power and Energy Systems*, **54**, 505–515.

Mithulananthan, N. (2017), 'Optimal allocation of distributed generation using hybrid grey wolf optimizer', *IEEE Access*, pp. 14807–14818.

Moghaddas-Tafreshi, S. and Mashhour, E. (2009), 'Distributed generation modeling for power flow studies and a three-phase unbalanced power flow solution for radial distribution systems considering distributed generation', *Electric Power Systems Research*, **79**(4), 680 – 686.

Mohamed, I. A. and Kowsalya, M. (2014), 'Optimal size and siting of multiple distributed generators in distribution system using bacterial foraging optimization', *Swarm and Evolutionary Computation*, **15**, 58–65.

Mohandas, N., Balamurugan, R. and Lakshminarasimman, L. (2015), 'Optimal location and sizing of real power DG units to improve the voltage stability in the distribution system using ABC algorithm united with chaos', *International Journal of Electrical Power and Energy Systems*, **66**, 41–52.

Mohanty, B. and Tripathy, S. (2016), 'A teaching learning based optimization technique for optimal location and size of DG in distribution network', *Journal of Electrical Systems and Information Technology*, **3**(1), 33–44.

Moradi, M. H. and Abedini, M. (2012), 'A combination of genetic algorithm and particle swarm optimization for optimal DG location and sizing in distribution systems', *International Journal of Electrical Power and Energy Systems*, **34**(1), 66–74.

Moradi, M. H., Zeinalzadeh, A., Mohammadi, Y. and Abedini, M. (2014), 'An efficient hybrid method for solving the optimal sitting and sizing problem of DG and shunt capacitor banks simultaneously based on imperialist competitive algorithm and genetic algorithm', *International Journal of Electrical Power and Energy Systems*, **54**, 101–111.

Moravej, Z. and Akhlaghi, A. (2013), 'A novel approach based on cuckoo search for DG allocation in distribution network', *International Journal of Electrical Power and Energy Systems*, **44**(1), 672–679.

Mukhopadhyay, S. and Singh, B. (2009), Distributed generation - basic policy, perspective planning, and achievement so far in india, *in* 'IEEE Power Energy Society General Meeting, 26-30 July 2009, Calgary, AB, Canada', pp. 1–7.

Musa, H. and Adamu, S. S. (2013), Enhanced PSO based multi-objective distributed generation placement and sizing for power loss reduction and voltage stability index improvement, *in* 'IEEE Energytech, 21-23 May 2013, Cleveland, OH, USA', pp. 1–6.

Muthukumar, K. and Jayalalitha, S. (2016), 'Optimal placement and sizing of distributed generators and shunt capacitors for power loss minimization in radial distribution networks using hybrid heuristic search optimization technique', *International Journal of Electrical Power and Energy Systems*, **78**, 299–319.

Naik, S. N. G., Khatod, D. K. and Sharma, M. P. (2015), 'Analytical approach for optimal siting and sizing of distributed generation in radial distribution networks', *IET Generation, Transmission & Distribution*, **9**(3), 209–220.

Nayanatara, C., Baskaran, J. and Kothari, D. P. (2016), 'Hybrid optimization implemented for distributed generation parameters in a power system network', *International Journal of Electrical Power and Energy Systems*, **78**, 690–699.

Nekooei, K., Farsangi, M. M., Nezamabadi-Pour, H. and Lee, K. Y. (2013), 'An improved multi-objective harmony search for optimal placement of DGs in distribution systems', *IEEE Transactions on Smart Grid*, **4**(1), 557–567.

Nguyen, T. T., Truong, A. V. and Phung, T. A. (2016), 'A novel method based on adaptive cuckoo search for optimal network reconfiguration and distributed generation allocation in distribution network', *International Journal of Electrical Power and Energy Systems*, **78**, 801–815.

Ochoa, L. F. and Harrison, G. P. (2011), 'Minimizing energy losses: optimal accommodation and smart operation of renewable distributed generation', *IEEE Transactions on Power Systems*, **26**(1), 198–205.

Pepermans, G., Driesen, J., Haeseldonckx, D., Belmans, R. and D'haeseleer, W. (2005), 'Distributed generation: definition, benefits and issues', *Energy Policy*, **33**(6), 787 – 798.

Poornazaryan, B., Karimyan, P., Gharehpetian, G. B. and Abedi, M. (2016), 'Optimal allocation and sizing of DG units considering voltage stability, losses and load variations', *International Journal of Electrical Power and Energy Systems*, **79**, 42–52.

Pradhan, S., Singh, B. and Panigrahi, B. K. (2018), 'A digital disturbance estimator (DDE) for multiobjective grid connected solar PV based distributed generating system', *IEEE Transactions on Industry Applications*, **54**(5), 5318–5330.

Prenc, R., Škrlec, D. and Komen, V. (2013), 'Distributed generation allocation based on average daily load and power production curves', *International Journal of Electrical Power and Energy Systems*, **53**(1), 612–622.

Rahmani-Andebili, M. (2016), 'Simultaneous placement of DG and capacitor in distribution network', *Electric Power Systems Research*, **131**, 1–10.

Rajendran, A. and Narayanan, K. (2017), 'Optimal installation of different DG types in radial distribution system considering load growth', *Electric Power Components and Systems*, **45**(7), 739–751.

Rama Prabha, D. and Jayabarathi, T. (2016), 'Optimal placement and sizing of multiple distributed generating units in distribution networks by invasive weed optimization algorithm', *Ain Shams Engineering Journal*, **7**(2), 683–694.

Rama Prabha, D., Jayabarathi, T., Umamageswari, R. and Saranya, S. (2015), 'Optimal location and sizing of distributed generation unit using intelligent water drop algorithm', *Sustainable Energy Technologies and Assessments*, **11**, 106–113.

Ranjan, R. and Das, D. (2003), 'Simple and efficient computer algorithm to solve radial distribution networks', *Electric Power Components and Systems*, **31**(1), 95–107.

Ranjan, R., Venkatesh, B., Chaturvedi, A. and Das, D. (2004), 'Power flow solution of three-phase unbalanced radial distribution network', *Electric Power Components and Systems*, **32**(4), 421–433.

Rao, B. N. and Abhyankar, A. R. (2014), Optimal placement of distributed generator using monte carlo simulation, *in* 'Eighteenth Power Systems Conference (NPSC), National, 18-20 Dec. 2014, Guwahati, India', pp. 1 – 6.

Rao, R. S., Ravindra, K., Satish, K. and Narasimham, S. V. L. (2013), 'Power loss minimization in distribution system using network reconfiguration in the presence of distributed generation', *IEEE Transactions on Power Systems*, **28**(1), 317–325.

Rashtchi, V. and Darabian, M. (2012), 'A new BFA-based approach for optimal siting and sizing of distributed generation in distribution system', *International Journal of Automation and Control*, **1**(1), 9–18.

Ravikumar Pandi, V., Zeineldin, H. H. and Xiao, W. (2013), 'Determining optimal location and size of distributed generation resources considering harmonic and protection coordination limits', *IEEE Transactions on Power Systems*, **28**(2), 1245–1254.

Reddy, G. H., Chakrapani, P., Goswami, A. K. and Choudhury, N. B. (2017), 'Optimal distributed generation placement in distribution system to improve reliability and critical loads pick up after natural disasters', *Engineering Science and Technology, an International Journal*, **20**(3), 825–832.

Rotaru, F., Chicco, G., Grigoras, G. and Cartina, G. (2012), 'Two-stage distributed generation optimal sizing with clustering-based node selection', *International Journal of Electrical Power and Energy Systems*, **40**(1), 120–129.

Saha, S. and Mukherjee, V. (2016), 'Optimal placement and sizing of DGs in RDS using chaos embedded SOS algorithm', *IET Generation, Transmission & Distribution*, **10**(14), 3671–3680.

Sajjadi, S. M., Haghifam, M. R. and Salehi, J. (2013), 'Simultaneous placement of distributed generation and capacitors in distribution networks considering voltage stability index', *International Journal of Electrical Power and Energy Systems*, **46**(1), 366–375.

Sharma, S., Bhattacharjee, S. and Bhattacharya, A. (2016), 'Quasi-oppositional swine influenza model based optimization with quarantine for optimal allocation of DG in radial distribution network', *International Journal of Electrical Power and Energy Systems*, **74**, 348–373.

Sheng, W., Liu, K. Y., Liu, Y., Meng, X. and Li, Y. (2015), 'Optimal placement and sizing of distributed generation via an improved nondominated sorting genetic algorithm II', *IEEE Transactions on Power Delivery*, **30**(2), 569–578.

Shirmohammadi, D., Hong, H. W., Semlyen, A. and Luo, G. X. (1988), 'A compensation-based power flow method for weakly meshed distribution and transmission networks', *IEEE Transactions on Power Systems*, **3**(2), 753–762.

Shukla, T. N., Singh, S. P., Srinivasarao, V. and Naik, K. B. (2010), 'Optimal sizing of distributed generation placed on radial distribution systems', *Electric Power Components and Systems*, **38**, 260–274.

Singh, D. and Misra, R. K. (2007), 'Effect of load models in distributed generation planning', *IEEE Transactions on Power Systems*, **22**(4), 2204–2212.

Singh, D., Singh, D. and Verma, K. S. (2009*a*), 'Distributed generation planning strategy with load models in radial distribution system', *International Journal of Computer and Electrical Engineering*, (3), 362–365.

Singh, D., Singh, D. and Verma, K. S. (2009*b*), 'Multiobjective optimization for DG planning with load models', *IEEE Transactions on Power Systems*, **24**(1), 427–436.

Singh, R. K. and Goswami, S. K. (2009), 'Optimum siting and sizing of distributed generations in radial and networked systems', *Electric Power Components and Systems*, **37**(2), 127–145.

Singh, R. K. and Goswami, S. K. (2010), 'Optimum allocation of distributed generations based on nodal pricing for profit, loss reduction, and voltage improvement including voltage rise issue', *International Journal of Electrical Power and Energy Systems*, **32**(6), 637–644.

Singh, R. K. and Goswami, S. K. (2011), 'Multi-objective optimization of distributed generation planning using impact indices and trade-off technique', *Electric Power Components and Systems*, **39**, 1175–1190.

Teng, J. H. (2003), 'A direct approach for distribution system load flow solutions', *IEEE Transactions on Power Delivery*, **18**(3), 882–887.

Teng, J. H. (2008), 'Modelling distributed generations in three-phase distribution load flow', *IET Generation, Transmission & Distribution*, **2**(3), 330–340.

Thukaram, D., Banda, H. W. and Jerome, J. (1999), 'A robust three phase power flow algorithm for radial distribution systems', *Electric Power Systems Research*, **50**(3), 227 – 236.

Tolba, M. A., Rezk, H., Tulsky, V., Zaki Diab, A. A., Abdelaziz, A. Y. and Vanin, A. (2018), 'Impact of optimum allocation of renewable distributed generations on distribution networks based on different optimization algorithms', *Energies*, **11**, 245.

Ugranli, F. and Karatepe, E. (2013), 'Multiple-distributed generation planning under load uncertainty and different penetration levels', *International Journal of Electrical Power and Energy Systems*, **46**(1), 132–144.

Vieira, J. C. M., Freitas, W. and Morelato, A. (2004), 'Phase-decoupled method for three-phase power-flow analysis of unbalanced distribution systems', *IEE Proceedings - Generation, Transmission and Distribution*, **151**(5), 568–574.

Vinothkumar, K. and Selvan, M. P. (2011), 'Fuzzy embedded genetic algorithm method for distributed generation planning', *Electric Power Components and Systems*, **39**, 346–366.

Vinothkumar, K. and Selvan, M. P. (2012), 'Distributed generation planning: A new approach based on goal programming', *Electric Power Components and Systems*, **40**, 497–512.

Viral, R. and Khatod, D. (2012), 'Optimal planning of distributed generation systems in distribution system: A review', *Renewable and Sustainable Energy Reviews*, **16**(7), 5146 – 5165.

Viral, R. and Khatod, D. K. (2015), 'An analytical approach for sizing and siting of DGs in balanced radial distribution networks for loss minimization', *International Journal of Electrical Power and Energy Systems*, **67**, 191–201.

Vita, V. (2017), 'Development of a decision-making algorithm for the optimum size and placement of distributed generation units in distribution networks', *Energies*, **10**, 1433.

Wang, C. and Nehrir, M. H. (2004), 'Analytical approaches for optimal placement of distributed generation sources in power systems', *IEEE Transactions on Power Systems*, **19**(4), 2068–2076.

Wang, L. W. L. and Singh, C. (2008), 'Reliability-constrained optimum placement of reclosers and distributed generators in distribution networks using an ant colony system algorithm', *IEEE Transactions on Systems, Man, and Cybernetics, Part C (Applications and Reviews)*, **38**(6), 757–764.

Yammani, C., Maheswarapu, S. and Kumari, M. S. (2014), 'Optimal placement and sizing of DER's with load variations using bat algorithm', *Arabian Journal for Science and Engineering*, **39**(6), 4891–4899.

Yammani, C., Maheswarapu, S. and Matam, S. K. (2016), 'A multi-objective shuffled bat algorithm for optimal placement and sizing of multi distributed generations with different load models', *International Journal of Electrical Power and Energy Systems*, **79**, 120–131.

Zeinalzadeh, A., Mohammadi, Y. and Moradi, M. H. (2015), 'Optimal multi objective placement and sizing of multiple DGs and shunt capacitor banks simultaneously considering load uncertainty via MOPSO approach', *International Journal of Electrical Power and Energy Systems*, **67**, 336–349.

Zhan, H., Wang, C., Wang, Y., Yang, X., Zhang, X., Wu, C. and Chen, Y. (2016), 'Relay protection coordination integrated optimal placement and sizing of distributed generation sources in distribution networks', *IEEE Transactions on Smart Grid*, **7**(1), 55–65.

Zhang, L., Tang, W., Liu, Y. and Lv, T. (2015), 'Multiobjective optimization and decision-making for DG planning considering benefits between distribution company and DGs owner', *International Journal of Electrical Power and Energy Systems*, **73**, 465–474.

Zhang, X., Karady, G. G. and Ariaratnam, S. T. (2014), 'Optimal allocation of CHP-based distributed generation on urban energy distribution networks', *IEEE Transactions on Sustainable Energy*, **5**(1), 246–253.

Zheng, Y., Dong, Z. Y., Meng, K., Yang, H., Lai, M. and Wong, K. P. (2017), 'Multi-objective distributed wind generation planning in an unbalanced distribution system', *CSEE Journal of Power and Energy Systems*, **3**(2), 186–195.

Zhu, Y. and Tomsovic, K. (2002), 'Adaptive power flow method for distribution systems with dispersed generation', *IEEE Transactions on Power Delivery*, **17**(3), 822–827.

Zimmerman, R. D. and Chiang, H.-D. (1995), 'Fast decoupled power flow for unbalanced radial distribution systems', *IEEE Transactions on Power Systems*, **10**(4), 2045–2052.

Zongo, O. A. and Oonsivilai, A. (2017), 'Optimal placement of distributed generator for power loss minimization and voltage stability improvement', *Energy Procedia*, **138**, 134–139.

Zou, K., Agalgaonkar, A. P., Muttaqi, K. M. and Perera, S. (2012), 'Distribution system planning with incorporating DG reactive capability and system uncertainties', *IEEE Transactions on Sustainable Energy*, **3**(1), 112–123.

Appendices

Appendix–A

Load Flow using BIBC and BCBV

The load flow of RDN is obtained by utilizing topological $BIBC$ and ($BCBV$) matrices (Teng, 2003). The $BIBC$ relates branch currents to nus injections while the ($BCBV$) bus voltages to branch currents.

The relation between branch currents $[B]$ and bus injection currents $[I]$ using $BIBC$ matrix is expressed as:

$$[B] = [BIBC][I] \tag{A.1}$$

The elements of $BIBC$ are either 0 or +1 only. For a RDN with m branches and n buses, the dimension of $BIBC$ matrix are $m \times (n-1)$. The substation bus is assigned number 1.

The $BCBV$ matrix, relates branch current $[B]$ to change in bus voltage $[\Delta V]$. This relationship can be expressed as:

$$[\Delta V] = [BCBV][B] \tag{A.2}$$

For a RDN with m branches and n buses, the dimension of $BCBV$ matrix is $(n-1) \times m$.

The equations (A.1) and (A.2) are combined to obtain the relationship between bus current injection and bus voltages as:

$$[\Delta V] = [BCBV][BIBC][I]$$

$$[\Delta V] = [DLF][I] \tag{A.3}$$

The algorithm starts with flat voltage profile at all buses. Corresponding to load $S_i = P_i + jQ_i$, the equivalent current injection I_i^k at the k^{th} iteration is computed as:

$$I_i^k = \left(\frac{P_i + jQ_i}{V_i^k}\right)^* \tag{A.4}$$

$[\Delta V]$ and $[V]$ are updated in every iteration as:

$$\begin{aligned}[\Delta V^k] &= [DLF][I^k] \\ [V^{k+1}] &= [V^0] + [\Delta V^{k+1}]\end{aligned} \tag{A.5}$$

The convergence is decided when $\left|V^{k+1} - V^k\right| \leq \epsilon$ is achieved at all buses.

Appendix–B

Test Data

B.1 33-BUS RDN

The single line diagram of 12.66 kV, 33-bus RDN, which is used as test system in this thesis is illustrated in Figure B.1. The relevant bus and branch data for this test system given in Table B.1 (Kashem *et al.*, 2000).

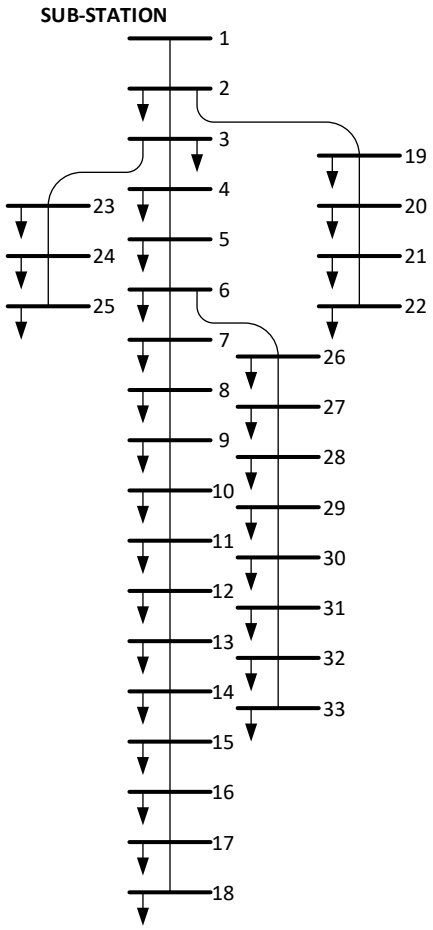

Fig. B.1: Single Line Diagram of 33-Bus RDN

Table B.1: Branch and Bus Data for 33-bus RDN

Branch Number	Bus Number		Branch Parameters		Load at Receiving End Bus	
	Sending End	Receiving End	Resistance (Ω)	Reactance (Ω)	Active power (kW)	Reactive power (kVAr)
1	1	2	0.0922	0.0470	100	60
2	2	3	0.4930	0.2511	90	40
3	3	4	0.3660	0.1864	120	80
4	4	5	0.3811	0.1941	60	30
5	5	6	0.8190	0.7070	60	20
6	6	7	0.1872	0.6188	200	100
7	7	8	1.7114	1.2351	200	100
8	8	9	1.0300	0.7400	60	20
9	9	10	1.0440	0.7400	60	20
10	10	11	0.1966	0.0650	45	30
11	11	12	0.3744	0.1238	60	35
12	12	13	1.4680	1.1550	60	35
13	13	14	0.5416	0.7129	120	80
14	14	15	0.5910	0.5260	60	10
15	15	16	0.7463	0.5450	60	20
16	16	17	1.2890	1.7210	60	20
17	17	18	0.7320	0.5740	90	40
18	2	19	0.1640	0.1565	90	40
19	19	20	1.5042	1.3554	90	40
20	20	21	0.4095	0.4784	90	40
21	21	22	0.7089	0.9373	90	40
22	3	23	0.4512	0.3083	90	50
23	23	24	0.8980	0.7091	420	200
24	24	25	0.8960	0.7011	420	200
25	6	26	0.2030	0.1034	60	25
26	26	27	0.2842	0.1447	60	25
27	27	28	1.0590	0.9337	60	20
28	28	29	0.8042	0.7006	120	70
29	29	30	0.5075	0.2585	200	600
30	30	31	0.9774	0.9630	150	70
31	31	32	0.3105	0.3619	210	100
32	32	33	0.3410	0.5302	60	40

B.2 69-BUS RDN

The single line diagram of 12.66 kV, 69-bus RDN, which is also used as test system in this thesis is illustrated in Figure B.2. The relevant bus and branch data for this test system given in Table B.2 (Baran and Wu, 1989*a*).

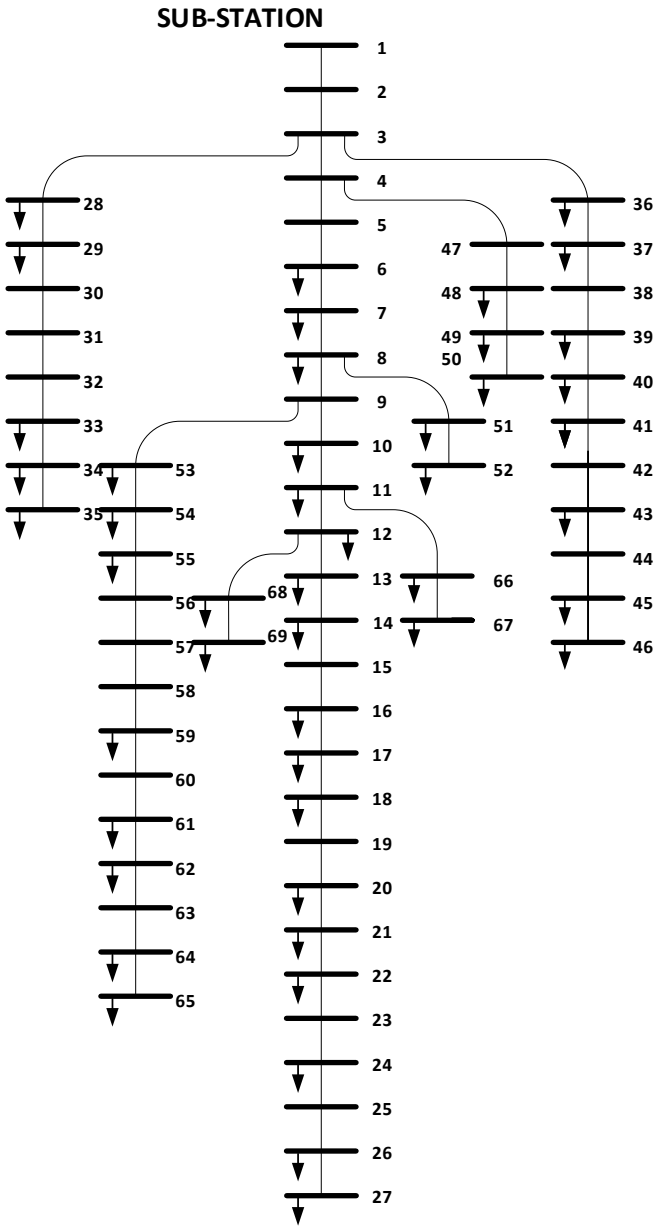

Fig. B.2: Single Line Diagram of 69-Bus RDN

Table B.2: Branch and Bus Data for 69-bus RDN

Branch Number	Bus Number		Branch Parameters		Load at Receiving End Bus	
	Sending End	Receiving End	Resistance (Ω)	Reactance (Ω)	Active power (kW)	Reactive power (kVAr)
1	1	2	0.0005	0.0012	0	0
2	2	3	0.0005	0.0012	0	0
3	3	4	0.0015	0.0036	0	0
4	4	5	0.0251	0.0294	0	0
5	5	6	0.3660	0.1864	2.6	2.2
6	6	7	0.3811	0.1941	40	30
7	7	8	0.0922	0.0470	75	54
8	8	9	0.0493	0.0251	30	22
9	9	10	0.8190	0.2707	28	19
10	10	11	0.1872	0.0619	145	104
11	11	12	0.7114	0.2351	145	104
12	12	13	1.0300	0.3400	8	5
13	13	14	1.0440	0.3450	8	5
14	14	15	1.0580	0.3496	0	0
15	15	16	0.1966	0.0650	45	30
16	16	17	0.3744	0.1238	60	35
17	17	18	0.0047	0.0016	60	35
18	18	19	0.3276	0.1083	0	0
19	19	20	0.2106	0.0696	1	0.6
20	20	21	0.3416	0.1129	114	81
21	21	22	0.0140	0.0046	5.3	3.5
22	22	23	0.1591	0.0526	0	0
23	23	24	0.3463	0.1145	28	20
24	24	25	0.7488	0.2475	0	0
25	25	26	0.3089	0.1021	14	10
26	26	27	0.1732	0.0572	14	10
27	3	28	0.0044	0.0108	26	18.6
28	28	29	0.0640	0.1565	26	18.6
29	29	30	0.3978	0.1315	0	0
30	30	31	0.0702	0.0232	0	0
31	31	32	0.3510	0.1160	0	0
32	32	33	0.8390	0.2816	14	10
33	33	34	1.7080	0.5646	19.5	14
34	34	35	1.4740	0.4873	6	4
35	4	36	0.0034	0.0084	26	18.55

Table B.2 continued .....

Table B.2 – Continued from previous page

Branch Number	Bus Number		Branch Parameters		Load at Receiving End Bus	
	Sending End	Receiving End	Resistance (Ω)	Reactance (Ω)	Active power (kW)	Reactive power (kVAr)
36	36	37	0.0851	0.2083	26	18.55
37	37	38	0.2898	0.7091	0	0
38	38	39	0.0822	0.2011	24	17
39	39	40	0.0928	0.0473	24	17
40	40	41	0.3319	1.1114	1.2	1
41	9	42	0.1740	0.0886	0	0
42	42	43	0.2030	0.1034	6	4.3
43	43	44	0.2842	0.1447	0	0
44	44	45	0.2813	0.1433	39.22	26.3
45	45	46	1.5900	0.5337	39.22	26.3
46	46	47	0.7837	0.2630	0	0
47	47	48	0.3042	0.1006	79	56.4
48	48	49	0.3861	0.1172	384.7	274.5
49	49	50	0.5075	0.2585	384.7	274.5
50	50	51	0.0974	0.0496	40.5	28.3
51	51	52	0.1450	0.0738	3.6	2.7
52	52	53	0.7105	0.3619	4.35	3.5
53	53	54	1.0410	0.5302	26.40	19
54	11	55	0.2012	0.0611	26	17
55	55	56	0.0047	0.0014	0	0
56	12	57	0.7394	0.2444	0	0
57	57	58	0.0047	0.0016	0	0
58	3	59	0.0044	0.0108	100	72
59	59	60	0.0640	0.1565	0	0
60	60	61	0.1053	0.1230	1244	888
61	61	62	0.0304	0.0355	32	23
62	62	63	0.0018	0.0021	0	0
63	63	64	0.7283	0.8509	227	162
64	64	65	0.3100	0.3623	59	42
65	65	66	0.0410	0.0478	18	13
66	66	67	0.0092	0.0116	18	13
67	67	68	0.1089	0.1373	28	20
68	68	69	0.0009	0.0012	28	20

Appendix–C

Load Sample Statistics

The mean and standard deviation of load sampled by MCS and LHS is tabulated in Table C.1. The sample size for MCS is 1000 and for LHS it is 100.

Table C.1: Mean and Standard Deviation of Active and Reactive Power Load of 33-bus RDN

Bus Number	**Active Power (kW)**				**Reactive Power (kVAr)**			
	MCS		**LHS**		**MCS**		**LHS**	
	μ	σ	μ	σ	μ	σ	μ	σ
1	0	0	0	0	0	0	0	0
2	100.195	9.880	99.999	0.101	59.650	6.108	59.999	0.100
3	90.355	8.976	90.000	0.100	40.031	3.878	34.000	0.102
4	120.298	12.188	119.999	0.100	80.460	7.956	80.001	0.103
5	60.160	6.128	60.001	0.101	29.946	2.893	30.001	0.100
6	59.735	5.844	60.001	0.102	20.094	2.058	20.000	0.101
7	199.002	20.174	200.000	0.101	99.908	10.355	99.999	0.100
8	200.811	20.131	200.000	0.100	100.105	10.520	99.999	0.103
9	60.257	6.116	60.001	0.102	20.011	1.996	20.000	0.099
10	59.744	6.008	60.000	0.100	19.983	1.990	19.999	0.102
11	45.176	4.694	44.999	0.101	30.032	3.080	30.000	0.099
12	60.206	6.131	60.001	0.100	35.143	3.423	35.000	0.100
13	59.867	6.124	59.999	0.102	34.916	3.389	34.999	0.099
14	119.677	12.107	120.000	0.099	79.715	8.130	80.000	0.099
15	60.139	5.987	60.001	0.100	9.983	1.011	10.001	0.100
16	59.925	6.083	59.999	0.100	19.990	1.998	20.000	0.105
17	59.795	5.806	59.999	0.100	20.005	2.002	20.000	0.099
18	89.341	9.222	90.000	0.099	39.917	3.815	40.000	0.100
19	89.969	8.900	89.999	0.101	39.833	3.989	40.000	0.101
20	90.056	9.236	89.999	0.101	40.047	4.023	40.000	0.099
21	90.174	8.769	89.999	0.101	40.027	4.085	40.000	0.099
22	90.905	9.403	90.000	0.101	39.952	3.964	40.000	0.100
23	90.206	8.947	90.000	0.100	49.906	4.873	49.999	0.100
24	420.037	42.877	419.999	0.101	200.444	19.890	200.000	0.102
25	421.011	42.800	419.999	0.099	200.213	19.856	199.999	0.100

Table C.1 continued .....

Table C.1 – Continued from previous page

Bus Number	Active Power (kW)				Reactive Power (kVAr)			
	MCS		LHS		MCS		LHS	
	μ	σ	μ	σ	μ	σ	μ	σ
26	59.647	5.741	59.999	0.100	25.019	2.413	25.000	0.100
27	59.971	6.152	60.000	0.100	24.931	2.520	24.999	0.102
28	60.369	6.105	59.999	0.103	20.036	2.035	20.000	0.100
29	120.839	12.165	119.999	0.102	70.121	6.850	70.000	0.099
30	200.763	19.664	199.999	0.101	598.091	62.081	600.000	0.101
31	150.136	15.194	149.999	0.101	70.079	6.955	70.000	0.101
32	209.589	21.270	210.001	0.102	99.991	10.145	99.999	0.102
33	60.229	6.180	60.000	0.099	40.045	3.892	40.000	0.099